JOHANNES KEPLER
UNIVERSITÄT LINZ
Netzwerk für Forschung, Lehre und Praxis

Spectroscopic Studies on Novel Donor-Acceptor and Low Band-gap Polymeric Semiconductors

Dissertation

zur Erlangung des akademischen Grades

Doktor der Naturwissenschaften

Angefertigt am *Institut für Chemie, Abteilung Physikalische Chemie*

Betreuung:

o. Univ. Prof. Mag. Dr. Rer. Nat. Niyazi Serdar Sariciftci
o. Univ. Prof. Dipl. Ing. Dr. Tech. Wolfgang Buchberger

Eingereicht von:

Mag. Rer. Nat. Antonio Cravino

Mitbetreuung:

Ass. Prof. Mag. Dr. Rer. Nat. Helmut Neugebauer

Linz, November 2002

To the memory of my mother

Sidun

U mæ ninin u mæ
u mæ
lerfe grasse au su
d'amë d'amë
tûmù duçe benignu
de teu muaè
spremmûu 'nta maccaia
de staë de staë
e oua grûmmu de sangue ouëge
e denti de laete
e i euggi di surdatti chen arraggë
cu'a scciûmma a a bucca cacciuéi de baë
a scurrï a gente cumme selvaggin-a
finch'u sangue sarvaegu nu gh'à smurtau a qué
e doppu u feru in gua i feri d'ä prixún
e 'nte ferie a semensa velenusa d'ä depurtaziún
perchè de nostru da a cianûa a u meü
nu peua ciû cresce ni ærbu ni spica ni figgeü
ciao mæ 'nin l'eredítaë
l'è ascusa
'nte sta çittaë
ch'a brûxa ch'a brûxa
inta seia che chin-a
e in stu gran ciaeu de feugu
pe a teu morte piccin-a.

(Fabrizio De André, song in Genoese dialect)

I want to thank:

- my supervisor Niyazi Serdar Sariciftci and his collaborators Christoph Brabec and Helmut Neugebauer, for their very clear advice and great, friendly support;

- the former and present members of our Institute: Andrei Andrev, Elif Arici, Eugen Baumgartner, Patrick Denk, Thomas Fromherz, Desta Gebeheyu, Serap Gunes, Harald Hoppe, Enrik Johansson, Markus Koppe, Carita Kvarnström, Manfred Lipp, Maria Antonietta Loi, Gebhard "Gebi" Matt, Dieter Meissner, Attila Mozer, David Mühlbacher, Birgit Paulik, Gabriele Prager, Roman Rittberger, Markus Scharber, Daniela Stonescu, Christoph Winder, Elisabeth Wirtl, Teketel Yohannes, Gerald Zerza;

- our collaborators, for providing the materials and participating in valuable experiments and discussions: Mats R. Andersson, Marinella Catellani, Lothar Dunsch, Eitan Ehrenfreund, Raphael Goméz, Jan C. "Kees" Hummelen, Reneé Janssen, Silvia Luzzati, Michele Maggini, Nazario Martín, Ruth Müllner, José Segura, Peter Skabara, Mattias Svensson, Fred Wudl;

- all my friends and relatives for their long-running, continuos personal support. Especially, my friend Galit for her loving support and company;

- my mother, my father and my sister, for their inestimable help.

Unfortunately, my mother cannot see this work finished. This work is dedicated to her. *Ciao ma'*.

Abstract

Novel low band-gap conjugated polymeric semiconductors as well as conjugated electron donor chains carrying electron acceptor substituents were electrochemically prepared and investigated by means of different spectroscopic techniques. Using *in situ* FTIR and ESR spectroelectrochemistry, the spectroscopic features of injected positive charges are found to be different as opposed to the negative charge carriers on the same conjugated polymer. These results, for which the theoretical models so far developed do not account, demonstrate the different structure and delocalisation of charge carriers with opposite signs. In addition, vibrational spectroscopy results proof the enhanced "quinoid" character of low band-gap conjugated chains. Excited state spectroscopy was applied to study photoexcitations in conjugated polymers carrying tetracyanoanthraquinone type or fullerene moieties. This novel class of materials, hereafter called *double-cable* polymers, was found promising as alternative to the conjugated polymer:fullerene mixtures currently used for the preparation of "bulk-heterojunction" polymeric solar cells.

Zusammenfassung

Neuartige konjugierte Polymer Halbleiter mit kleiner Bandlücke und konjugierte Elektron Donor Ketten mit kovalent gebundenen Elektron Akzeptor Substituenten wurden elektrochemisch erzeugt und mit verschiedenen spektroskopischen Methoden untersucht. Mit *in situ* FTIR und ESR Spektroelektrochemie wurden verschiedene spektroskopische Signaturen für positive und negative Ladungsträger beobachtet. Diese Resultate, für die es bis jetzt keine theoretische Erklärung gibt, demonstrieren die unterschiedliche Struktur und lokale Verteilung der positiven und negativen Ladungsträger. Zusätzlich zeigen Vibrationsspektroskopie Untersuchungen den verstärkten chinoiden Charakter der konjugierten Ketten mit kleiner Bandlücke. Die Photoanregungen in konjugierten Polymeren mit kovalent gebundenen tetracyanoanthraquinon-ähnlichen Molekülen bzw. Fullerenen als Seitenketten, wurden mit Anregungsspektroskopie untersucht. Diese neue Materialklasse wird auch als *Doppelkabel* Polymer bezeichnet. Wie Resultate zeigen, könnten diese *Doppelkabel* Materialien eine vielversprechende Alternative zur "Bulk-Heterojunktion" Polymersolarzelle darstellen.

Contents

***Chapter 3*. Spectroscopic studies of low band-gap polydithienothiophenes**

***Chapter 4*. Advanced materials for non-composite donor-acceptor systems**

CHAPTER 1. INTRODUCTION

During the last two decades, research has been increasing in the field of synthesis and characterization of molecules with extended π-electron delocalisation. Among the development of new applications using organic materials like conjugated polymers[1-3] and fullerenes,[4-9] polymeric light emitting diodes and displays are today entering the market.[10-16] Furthermore, the discovery of a photoinduced electron transfer from non-degenerate ground-state conjugated polymers to fullerenes[17] enabled the fabrication of inexpensive and flexible large-area solar cells and photodetectors.[18-19] For many of the above applications, a balanced transport of holes and electrons is important. In particular, for photovoltaic applications, the exploitation of low band-gap conjugated polymers would be of great benefit for the solar energy harvesting. In this work we have prepared and studied both conjugated polymers with low band-gap and conjugated chain bearing electron acceptor moieties. The main targets of our investigations were:

a) to compare positive and negative charge carriers, their nature and delocalization, in one-and-the-same material;

b) to explore the suitability of novel intrinsic donor-acceptor conjugated polymers (*double-cable* polymers) as ambipolar materials for photovoltaic and optoelectronic applications.

1.1. POSITIVE AND NEGATIVE CHARGE CARRIERS IN CONJUGATED POLYMERS - RAMAN AND IR COMPARATIVE STUDIES

Due to the strong lattice relaxation in one dimensional systems with electron-phonon coupling,[2] chemical as well as electrochemical oxidation and reduction of non degenerate ground-state conjugated polymers usually lead to the formation of charge carriers with spin 1/2, denoted as positive/negative polarons (radical-cations/-anions), delocalized along the polymer chain and which exhibit peculiar electronic, vibrational and charge transport properties.[2,3] Also photoexcitation may lead to charge separation and to the formation of such charge carriers (photodoping).[2,21,22] The lattice relaxation

induces new electronic levels within the polymer π-π* energy gap (band-gap) and usually lead to an insulator-to-metal transition at a critical doping level. The oxidation and reduction processes involving the formation of positive and negative charge carriers in conjugated polymers are described, in analogy to inorganic semiconductors, as *p*-, and *n*- doping, respectively.

Due to the strong electron-phonon coupling in conjugated polymers, Raman spectroscopy and infrared absorption are powerful techniques for the investigation of the doping induced lattice relaxation around the charge carriers. Consequently, the vibrational behaviour of relatively simple conjugated polymers in their pristine and doped states (mostly of the *p*-type) has been the subject of much theoretical and experimental work during the last two decades.[23-31] On the other hand, detailed studies of more complicated or *n-doped* conjugated polymers have been limited by theoretical difficulties and by their frequent instability, respectively.

The infrared spectra of conjugated polymers in their conductive (chemically- electrochemically- or photodoped) states are characterized by intense infrared absorption bands (infrared active vibrations, IRAV bands), typically ranging from 1600 cm^{-1} to 700 cm^{-1}.[23] These bands originate from the strong electron-phonon coupling mentioned above and thus provide not only structural but also electronic information. In addition, broad IR absorption bands at higher energy usually accompany IRAVs. These bands correspond to the transitions involving the electronic levels induced in the gap, *via* lattice relaxation, by the doping process.

Several theoretical models have been developed in order to explain the spectroscopic signatures of charge carriers in conjugated polymers. For the description of the electronic and vibrational properties of neutral and doped *trans*-polyacetylene, Horovitz *et al*. and Ehrenfreund *et al*. have considered the change in the charge density wave associated to the vibrational motion of the polymer backbone.[25,26] As quantification of the localisation of charge a "pinning parameter" was introduced. Zerbi *et al*. explained the IRAV bands by the IR activation of the Raman active A_g modes in the pristine form of the polymer due to the local breaking of the symmetry around the

charge carrier.[23,27,28] In this model, the high intensity of the IRAV bands is motivated by the large variation of the electric dipole moment associated to the oscillation of the charged defect. An "*effective conjugation coordinate*" (ECC) describes the changes in geometry going from the ground- to the excited-state of the polymer as an alternating stretching-shrinking of carbon-carbon bonds. The higher the contribution of a given mode to the ECC, the higher is the intensity of the corresponding IRAV band. This origin of the IRAV bands shows that both Raman spectroscopy and IR spectroscopy as complementary techniques are necessary for understanding the vibrational spectra of pristine and doped conjugated polymers. Recently, Ehrenfreund and Vardeny used a model introduced by Girlando *et al*. (GPS model)[29] to establish a link between the electronic absorption bands and the IRAV bands of doping induced spectra.[30] All of the models correlate intensity, width and position of the IRAV bands to the delocalisation of charge carriers along the polymer chain.

These theories, developed for relatively simple systems like *trans*-polyacetylene and extended to few polyheteroaromates, do not account for possible differences in the IRAV signatures of positive and negative charge carriers. In addition, since the "pinning" in absence of counterions should be lower, photoinduced IRAV bands should appear at lower wavenumbers than chemically induced bands.[32] Experimental work has confirmed that these models rationalize the spectroscopic behaviour of conjugated polymers, providing a self-consistent description of the vibrational properties of many and relatively simple systems like, for instance, poly(alkylthiophene)s.[23,31] However, some complex conjugated polymers show a more complex behaviour. These materials are often promising candidates for applications since they may combine low band gap, outstanding optical properties and high stability in either the *p*- and *n*-doped states. A detailed description of the electronic and vibrational properties of such materials is necessary for the basic understanding of their behaviour. In particular, spectroscopic studies of conjugated polymers with stable *n*-doped state might be useful to achieve better experimental and theoretical descriptions of the so far rarely observed negative charge carriers in conjugated polymers.

We have selected, due to their low band-gap and both the *p*- and *n*-dopability, the polydithienothiophenes (PDTTs) poly(dithieno[3,4-b:3',4'-d]thiophene) (PDTT1), poly-(dithieno[3,4-b:3',2'-d]thiophene) (PDTT2) and poly-(dithieno[3,4-b:2',3'-d]thiophene) (PDTT3)[33] as materials for comparative spectroscopic studies of positive and negative doping induced defects. The results, reported in Chapter 3, demonstrate the different nature and delocalisation of positive and negative charge carriers in such conjugated polymers.

1.2. TOWARDS CONTROLLED DONOR-ACCEPTOR INTERACTIONS AND AMBIPOLAR TRANSPORT IN NON-COMPOSITE POLYMERIC MATERIALS: THE *DOUBLE-CABLE* APPROACH

The most efficient polymeric solar cells today fabricated are *bulk-heterojunctions*,[34,35] where the active layer is a blend of a conjugated polymer as electron donor (hole transporter, *p*-type material) and a soluble fullerene derivative as electron acceptor (electron transporter, *n*-type material). Beyond photoinduced charge separation, positive carriers are transported to electrodes by the donor polymer phase and electrons by hopping between contacting fullerene domains. It has been shown that the power conversion efficiency of *bulk heterojunction* solar cells can be improved dramatically by manipulating the morphology of the blend.[34] Improving the blend morphology by shrinking each of the interpenetrating two phases' dimensions below 500 nm leads to: a) a larger donor-acceptor interfacial contact area; b) less spatial separation between fullerene domains.[34,36]

The covalent linking of tethered electron accepting and conducting moieties to an electron donating and hole transporting conjugated polymer backbone appears a viable way for the preparation of ambipolar conducting *double-cable* polymers (*p*-*n* type). Their primary structure should prevent the occurrence of phase separation since the material is basically one macromolecule with two different pathways (*cables*) for different signs of charges, thus forcing the formation of continuous, interconnected network for the transport of both holes and electrons. In addition, the interaction

between the donor conjugated backbone and the acceptor moiety may be tuned by varying the chemical structure (nature and length) of their connecting spacer.[37]

Poly(3-octylthiophene), mixed with C_{60}, or a soluble fullerene derivative, has been already utilised for the preparation of prototype "bulk-heterojunction" solar cells,[38-40] suggesting the investigation of *double-cables* consisting of a polythiophene backbone with tethered fullerene units. Benincori and coworkers[41] and Ferraris *et al*.[42] showed that such fullerene substituted polythiophenes substantially retain the favorable ground state properties of the individual donor backbone and acceptor moieties. However, the occurrence of photoinduced electron transfer, which is essential for photovoltaic applications, was not investigated. The electrochemical and photophysical properties of novel *double-cable* polymers (see Chapter 5), studied by means of cyclic voltammetry (CV) and spectroscopic techniques (UV-Vis absorption, photoinduced absorption (PIA), *in situ* Fourier transform (FTIR) spectroelectrochemistry and light induced electron spin resonance (LESR) show evidence of photoinduced charge separation. A soluble *double-cable* polymer has been implemented in prototype photovoltaic devices. These results demonstrate the potential of *double-cable* polymers as non-composite active materials for electronic and photovoltaic devices.

1.3. REFERENCES

1. *Handbook of Conductive Molecules and Polymers*; Nalwa H. S. Ed.; Wiley: Chichester, 1997; Voll. 1-4.

2. *Handbook of Conducting Polymers*, 2nd edition; Skotheim, T. A.; Elsenbaumer, R. L.; Reynolds, J. R. Eds.; Marcel Dekker, New York, 1998.

3. *Semiconducting Polymers, Chemistry Physics and Engineering*; Hadziioannu G.; van Hutten P. F.; Eds.; Wiley, Weinheim, 2000.

4. M. S. Dresselhaus, G. Dresselhaus, P. C. Eklund, *Science of Fullerenes and Carbon Nanotubes, Academic Press*, San Diego (1996).

5. Diederich, F.; Thilgen, C. *Science* **1996**, *271*, 317.

6. Hirsch, A. In *Fullerenes and Related Structures, Topics in Current Chemistry*, Springer-Verlag: Berlin, 1999; Vol. 199.

7. *Fullerenes: Chemistry, Physics and Technology*; Kadish, K.; Ruoff, R.; Ed.s; Wiley Interscience, 2000.

8. Prato, M. *J. Mater. Chem.* **1997**, *7*, 1097, and references therein.

9. Segura, J. L.; Martín, N. *J. Mater. Chem*. **2000**, 2403, and references therein.

10. Burroughs, J. H.; Bradley, D. D. C.; Brown, A. B.; Marks, R. N.; Mackay, K.; Friend, R. H.; Burn, P. L.; Holmes, A. B. *Nature* (London) **1990**, *347*, 539.

11. Gustafsson, G.; Cao, Y.; Treacy, G. M.; Klavetter, F.; Colaneri, N.; Heeger, A. J. *Nature* (London) **1992**, *357*, 477.

12. Grem, G.; Leditzky, G.; Ulrich, B., Leising, G. *Adv. Mater*. **1992**, *4*, 36.

13. Kraft, A.; Grimsdale, A. C.; Holmes, A. B. *Angew. Chem. Int. Ed. Engl*. **1998**, *37*, 402.

14. Segura, J. L. *Acta Polym*. **1998**, *49*, 319.

15. Yu, W.-L.; Cao, Y.; Pei, J.; Huang, W.; Heeger, A. J. J. *Appl. Phys. Lett*. **1999**, *75*, 3270.

16. *C&EN* **2001**, April 16, 7.

17. Sariciftci, N. S.; Smilowitz, L.; Heeger, A. J.; Wudl, F. *Science* **1992**, *258*, 1474.

18. Sariciftci, N. S.; Braun, D.; Zhang, C.; Srdanov, V. I.; Heeger, A. J.; Stucky, G.; Wudl, F. *Appl. Phys. Lett*. **1993**, *62*, 585.

19. Yu, G.; Wang, J.; McElvain, J.; Heeger, A. J. *Adv. Mater*. **1998**, *10*, 1431.

20. Yokonuma, N.; Furukawa, Y.; Tasumi, M.; Kuroda, M.; Nakayama, J. *Chem. Phys. Lett*. **1996**, *255*, 431.

21. *Primary Photoexcitations in Conjugated Polymers: Molecular Exciton versus Semiconductor Band Model*, Sariciftci, N. S., Ed.; World Scientific: Singapore, 1997.

22. Sariciftci, N. S.; Smilowitz, L.; Heeger, A. J.; Wudl, F. *Science*, **1995**, *270*, 1474.

23. See for instance Del Zoppo, M.; Castiglioni, C.; Zuliani, P.; Zerbi, G. In *Handbook of Conducting Polymers*, 2nd ed.; Skotheim, T. A.; Elsenbaumer, R. L.; Reynolds, J. R., Eds.; Marcel Dekker: New York: 1988; Chapter 28, and references therein.

24. See for instance Zagorska, M.; Pron, A.; Lefrant, S. In *Handbook of Conductive Molecules and Polymers*, 2nd ed.; Nalwa, H. S., Ed.; Wiley: Chichester, 1997; Vol. 3, Chapter 4, and references therein.

825 Horovitz, B. *Solid State Commun*. **1982**, *41*, 729.

26. Ehrenfreund, E.; Vardeny, Z. V.; Brafman, O.; Horowitz, B. *Phys.Rev. B* **1987**, *36*, 1535.

27. Castiglioni, C.; Gussoni, M.; Lopez Navarrete, J. T.; Zerbi, G. *Solid State Comm*. **1988**, *36*, 1535.

28. Zerbi, G.; Gussoni, M.; Castiglioni, C. In *Conjugated Polymers*; Brédas, J. L.; Silbey, R., Eds.; Kluwer: Dordrecht, 1991; p 435.

29. Girlando, A.; Painelli, A.; Soos, Z. G. *J. Chem. Phys*. **1993**, *98*, 7459.

30. Ehrenfreund, E.; Vardeny, Z. V. *Proc. SPIE* **1997**, *3145*, 324.

31. Agosti, E.; Rivola, M.; Hernandez, V.; Del Zoppo, M.; Zerbi, G. *Synth. Met*. **1999**, *100*, 101.

32. Gussoni, M.; Castiglioni, C.; Zerbi, G. In *Spectroscopy of Advanced Materials*; Clark, R. J. H.; Hester, R. E., Eds.; Wiley: New York, 1991; p 251.

33. Arbizzani, C.; Catellani, M.; Mastragostino, M; Cerroni, M. G. *J. Electroanal. Chem*. **1997**, *423*, 23.

34. Shaheen, S. E.; Brabec, C. J.; Padinger, F.; Fromherz, T.; Hummelen, J. C.; Sariciftci, N. S. *Appl. Phys. Lett*. **2001**, *78*, 841.

35. Brabec, C. J.; Sariciftci, N. S.; Hummelen, J. C. *Adv. Funct. Mat*. **2001**, *11*, 15.

36. Geens, W.; Shaheen, S. E.; Brabec, C. J.; Poortmans, J.; Sariciftci, N. S. in *Electronic Properties of Novel Materials*; Kuzmany, H.; Fink, J.; Mehring, M.; Roth, S. Eds.; IOP, Bristol, in press.

37. Wang, Y.; Suna A. *J. Phys. Chem. B* **1997**, *101*, 5627.

38. Gebeheyu, D.; Padinger, F.; Fromherz, T.; Hummelen, J. C.; Sariciftci, N. S. *Int. J. Photoenergy* **1999**, *1*, 95.

39. Gebeheyu, D.; Padinger, F.; Fromherz, T.; Hummelen, J. C.; Sariciftci, N. S. *Bull. Chem. Soc. Ethiop*. **2000**, *14*, 57.

40. Yoshino, K.; Yin, X. H.; Morita, S.; Kawai, T.; Zakhidov, A. A. *Solid State Commun*. **1993**, *85*, 85.

41. Benincori, T.; Brenna, E.; Sannicoló, F.; Trimarco, L.; Zotti, G. *Angew. Chem*. **1996**, *108*, 718.

42. Ferraris, J. P.; Yassar, A.; Loveday, D. C.; Hmyene, M. *Opt. Mater*. (Amsterdam) **1998**, *9*, 34

CHAPTER 2. EXPERIMENTAL

In this Chapter we describe the materials subject of our work as well as the techniques used for their investigation. In addition, notes on chemicals, samples preparation and the structure of specialities are also included.

2.1. INVESTIGATED MATERIALS AND CHEMICALS

In this section, the materials that were investigated in these works as well as the chemicals used for spectroelectrochemistry experiments and device preparation are described. Some of the materials were designed with specific commitment to photovoltaic applications, and were synthesized by our coworkers within international collaborations. For these novel molecules and polymers, the synthetic scheme is also presented.

2.1.1 Polydithienothiophenes (PDTTs)

Polydithienothiophenes (PDTTs) poly(dithieno[3,4-b:3',4'-d]thiophene) (PDTT1), poly-(dithieno[3,4-b:3',2'-d]thiophene) (PDTT2) and poly-(dithieno[3,4-b:2',3'-d]thiophene) (PDTT3)[1-4] were polymerized electrochemically starting from dithienothiophene monomers sinthesized following the methods reported in 1971 by De Jong and Janssen.[5,6] The synthesis of these monomers have been carried out by Marinella Catellani and coworkers in Milano. The polymer structures are shown in Figure 2.1 along with their band-gap values.[1] According to Bolognesi and coworkers[7] and Bredas *et al*.,[8] PDTT1, PDTT2 and PDTT3 can be regarded as polythiophene-like chains in which a thienothiophene aromatic moiety,[9,10] evidenced by bold bonds in Figure 2.1, is fused to each thiophene ring. PDTTs have been prepared following the idea that an aromatic system fused to the thiophene ring lying in the polythiophene-like chain increases the quinoidal character of the latter and, therefore, the π-electron inter-ring delocalization along the whole polymer (see inset in Fig. 2.1, where PDTT3 is

sketched as example).[11-13] Indeed, according to this synthetic principle, PDTT1, PDTT2 and PDTT3 show low band-gap values. The higher the aromaticity of the fused thienothiophene moiety, which increases in the sequence PDTT1, PDTT2, PDTT3,[10] the lower the polymer band-gap. A detailed description of the electrochemical properties of these polymers is given by Reference 1.

In our work, PDTTs were investigated spectroscopically and spectroelectrochemically in order to elucidate the spectroscopic behavior of both positive as well as the negative charge carriers. In addition, the relationship between the quinoidal character of a polyconjugated chain and the size of the band-gap was also addressed.

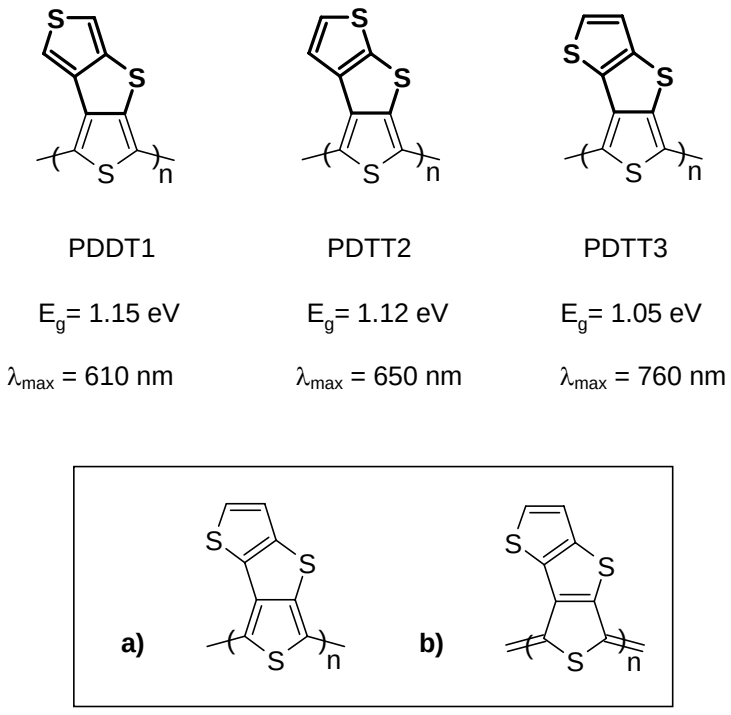

Fig. 2.1: Chemical structures, band-gap values (E_g) and maximun absorption wavelengths (λ_{max}) of PDTTs. E_g and λ_{max} data from Ref. 1. The inset show the relevant canonical forms: **a**) aromatic; **b**) quinoid.

2.1.2. Oligo(*p*-phenylene vinylene)-fulleropyrrolidine dyads (OPVn-C_{60})

The chemical structures of OPVn-C_{60} are depicted in Fig. 2.2. This series of oligo(*p*-phenylene vinylene)-fulleropyrrolidine dyads was recently prepared and investigated by E. Peeters et al.[14] Although OPV1-C_{60} is the smallest term of the series of dyads, it lacks a vinylene group and, formally, is not an oligo(*p*-phenylene vinylene) derivative. OPV1-C_{60} stands for *N*-Methyl-2-{4-(4-methyl-2,5-bis[(*S*)-2-methylbutoxy]phenyl}-3,4-fulleropyrrolidine; OPV2-C_{60} for *N*-Methyl-2-{4-(4-methyl-2,5-bis[(*S*)-2-methylbutoxy]styryl]-2,5-bis[(*S*)-2-methylbutoxy]phenyl}-3,4-fulleropyrrolidine; OPV3-C_{60} for *N*-Methyl-2-{4-[4-(4-methyl-2,5-bis[(*S*)-2-methylbutoxy]-styryl)-2,5-bis[(*S*)-2-methylbutoxy]styryl]-2,5-bis[(*S*)-2-methylbutoxy]phenyl}-3,4-fulleropyrrolidine, and OPV4-C_{60} for *N*-Methyl-2-(4-{4-[4-(4-methyl-2,5-bis[(*S*)-2-methylbutoxy]-styryl)-2,5-bis[(*S*)-2-methylbutoxy]styryl]-2,5-bis[(*S*)-2-methylbutoxy]-styryl}-2,5-bis[(*S*)-2-methylbutoxy]phenyl)-3,4-fulleropyrrolidine.

The goal of this part of our work was to manipulate the morphology within the photoactive films of bulk-heterojunction solar cells, using the dyads as alternative to the commonly used PCBM (see Section 2.1.7.).

2.1.3. Polythiophene bearing tetracyanoanthraquinodimethane moieities (PUCM6)

Starting from UCM6, synthesized by Nazario Martín and his co-workers in Madrid (Fig. 2.3) in collaboration with Mats Andersson and Mattias Svensson in Göteborg, the corresponding *double-cable* polymer PUCM6 was prepared by electrochemical oxidation (see Chapter 5). This systems, as well as the monomer and polymer described in the next section, was developed to investigate the electrochemical and photophisical properties of a single material with both electron donating and accepting properties. Moreover, PUCM6 offers the possibility to investigate an acceptor moiety alternative to fullerenes.

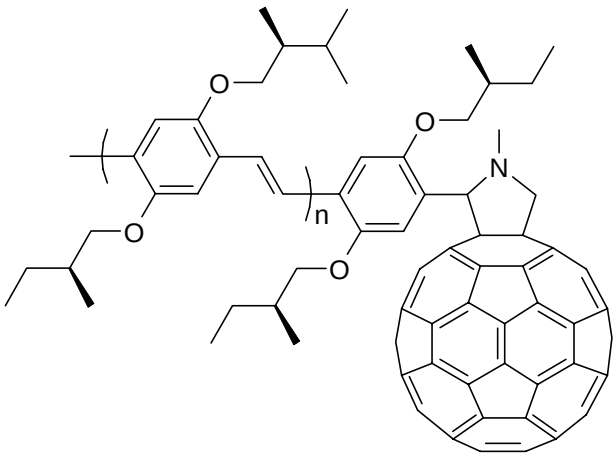

Fig. 2.2: Chemical structure of OPV*n*C_{60}

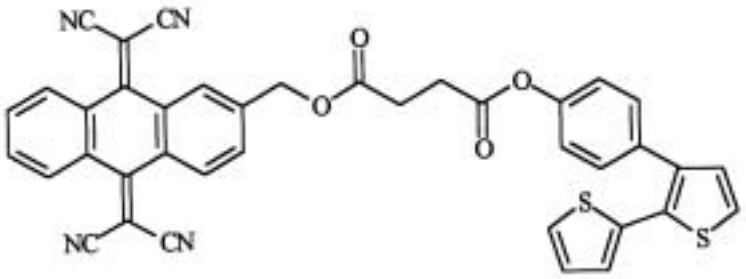

Fig. 2.3: Chemical structure of monomer UCM6

2.1.4. Electrochemically synthesized polythiophenes bearing fulleropyrrolidine moieties

The route to the bithiophene-fulleropyrrolidine **1**, used as monomer for electrochemical polymerisation, is outlined in Scheme 2.1. The synthesis was carried out by Mats Andersson (Göteborg), Michele Maggini (Padova) and coworkers. The route to **1** starts with commercially available 4-hydroxybenzaldehyde and 1-iodo-2-[2-(2-iodo-ethoxy)-ethoxy]-ethane. Reaction between 4-hydroxybenzaldehyde and the bis-iododerivative in the presence of K_2CO_3 in acetone at reflux temperature afforded the product of monosubstitution **2** in 20% isolated yield. Palladium-catalysed coupling of 4-bromophenol with 3-thiophene-boronic acid[9] followed by NBS-bromination gave the highly reactive derivative **3** that was coupled directly with 2-thiophene-boronic acid to afford **4**. Reaction of **2** with the potassium salt of bis-thiophene phenol **4** gave functionalised bithiophene **5** in 50% yield. Condensation of **5** with sarcosine in the presence of C_{60}[31] provided **1** in 49% isolated yield. All spectroscopic and analytical data were consistent with the proposed molecular structures.

The electropolymerisation of **1** affords a *double-cable* polymer that allowed the first observation of a photoinduced electron transfer in this class of materials.

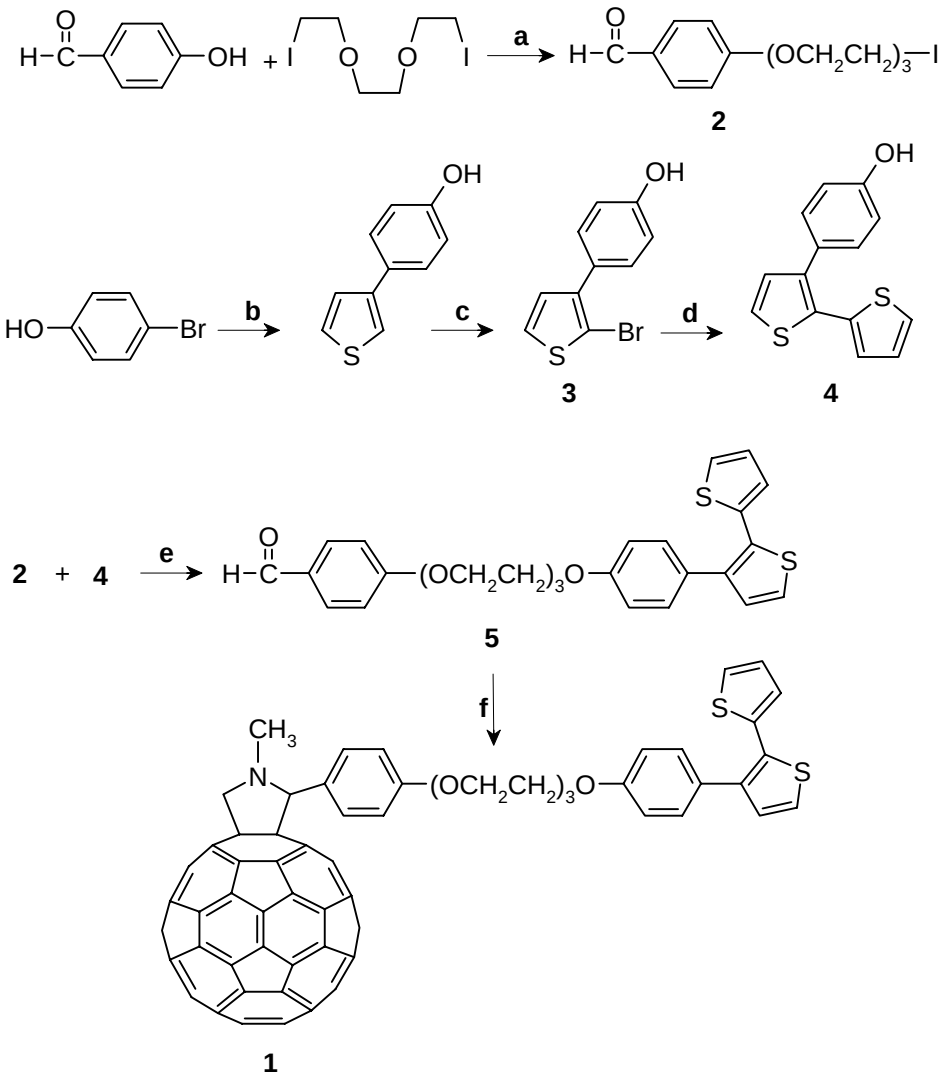

Reagents and conditions: a, K_2CO_3, acetone, reflux, 8h, 20%; b, 3-thiophene-boronic acid, *tetrakis*(triphenylphosphine)palladium(0), DME, $NaHCO_3$ (1M), 12h, 76%; c, NBS, DMF, 12h, 87% (crude); d, 2-thiophene-boronic acid, *tetrakis*(triphenylphosphine)palladium(0), DME, $NaHCO_3$ (1M), 12h, 48%; e, K_2CO_3, acetone, reflux, 8h, 50%; f, N-methylglycine, C_{60}, chlorobenzene, reflux, 2h, 49%.

Scheme 2.1

2.1.5. Chemically synthesized and soluble polythiophene bearing fullerene moieties

Polymer **6** (Fig. 2.4) is a random copolymer with repeating units of 3-(4'-(1'',4'',7''-trioxaoctyl)phenyl)thiophene **7** and of a thiophene-substituted fulleropyrrolidine **12**. The synthesis was carried out by Mats Andersson (Göteborg), Michele Maggini (Padova) and coworkers. Scheme 2.2 outlines the synthetic strategy towards *double-cable* **6**. Fulleropyrrolidine **12** was synthesised in five steps starting from commercially available 4-octylphenol and 1,8-dibromo octane that in 2-butanol and K_2CO_3 at reflux temperature afforded bromoderivative **8** in 66% isolated yield. Compound **8** was brominated with NBS in DMF for 24 h at room temperature to obtain **9** directly used, without further purification, in a palladium-catalysed coupling[16] with 3-thiophene boronic acid[17] affording **10** in 40% isolated yield. Reaction of **10** and 4-hydroxybenzaldehyde in the presence of K_2CO_3 and acetone at reflux temperature gave thiophene-aldehyde **11** in 80% yield. Aldehyde **11** was then condensed with sarcosine in the presence of C_{60} affording **12** in 52% isolated yield.[18] All spectroscopic and analytical data were consistent with the proposed molecular structures. Polymer **6** was prepared by mixing monomers **12** and **7 (**in a 1:9 ratio**)** in $CHCl_3$ followed by addition of $FeCl_3$ over a period of 5 hours. The resulting material was carefully dedoped and Soxhlet-extracted with diethyl ether to remove unreacted monomers and low molecular weight oligomers. The molecular weight of the copolymer, isolated in 12% yield, was M_n = 28000, M_w = 48000; determined by size exclusion chromatograpy using polystyrene standards. The ^{1}H NMR spectrum of **6** showed that approximately 7% of **12** was incorporated in the copolymer. Monomer **7**, as well as the corresponding polythiophene **PEOPT** (α-α' liknkages) used as reference (see Chapter 4), were prepared as described in the literature.[19]

2.1.6. Poly((2-methoxy-5-(3,7-dimethyloctyloxy)-*p*-phenylene)-vinylene) (MDMO-PPV)

MDMO-PPV (see Chart) was purchased from COVION. This well studied conjugated polymer was developed to improve the efficiency of organic LEDs and has successfuly been utilized as electron donor in bulk-heterojunction solar cells. Here in Linz, solar cells with efficiency above 2.5% in AM1.5 illumination conditions are prepared by mixing MDMO-PPV and PCBM (see next section).

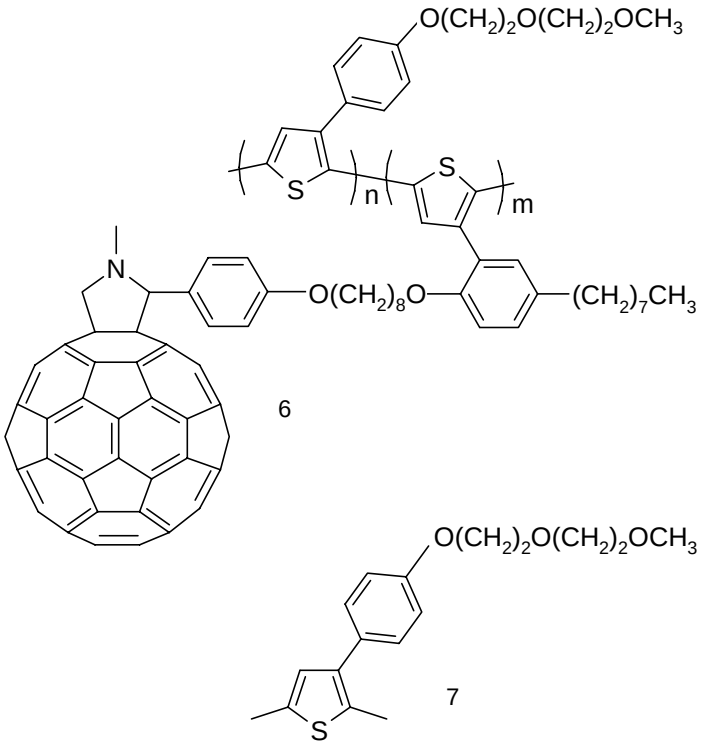

Fig. 2.4: Chemical structure of polymer **6** and monomer **7**.

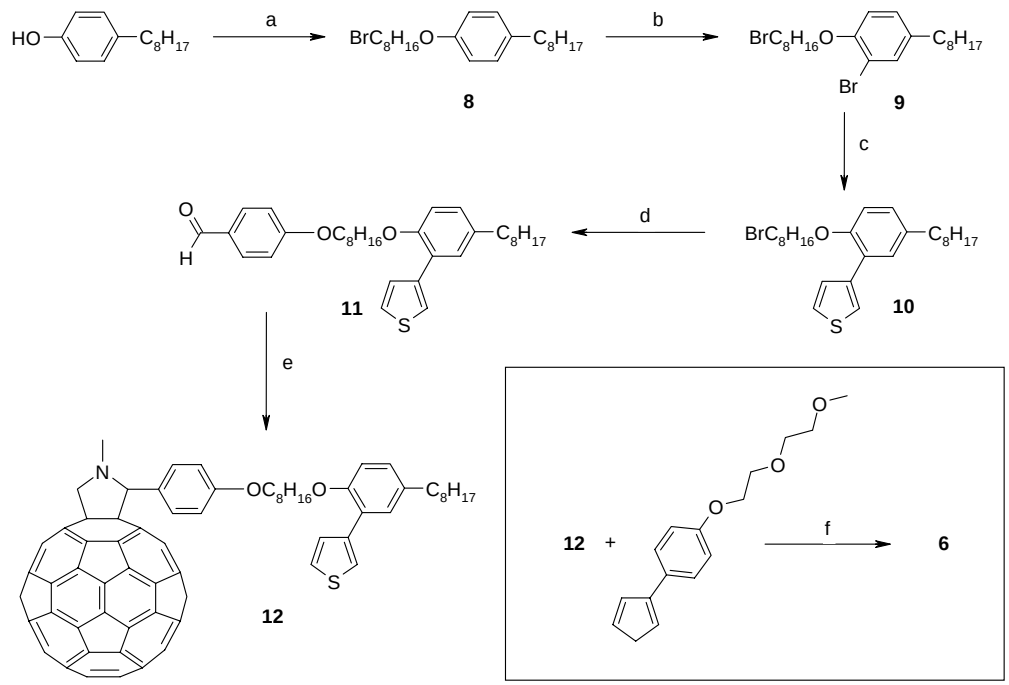

Reagents and conditions: a, 1,8-dibromooctane, K_2CO_3, 2-butanol, reflux, 24 h, 66%; b, NBS, DMF, RT, 20 h, 94%; c, 3-thiophene boronic acid, tetrakis(triphenylphosphine)palladium(0), $NaHCO_3$ (1 M), DME, reflux, 10 h, 40%; d, 4-hydroxybenzaldehyde, K_2CO_3, acetone, reflux, 36 h, 80%; e, N methylglycine, C_{60}, chlorobenzene, reflux, 5 h, 52%; f, $CHCl_3$, $FeCl_3$ (1:6) - (0.05 M), 5 h, 57%.

Scheme 2.2

2.1.7. 1-(3-Methoxycarbonyl)-propyl-1-1-phenyl-(6,6)C_{61} (PCBM)

PCBM (see Chart) is a soluble methanofullerene synthesized to combine the outstanding electronic properties of C_{60} and solubility. Its synthesis was reported in 1993 by Hummelen et al.[20] Since that early time, many soluble fullerene derivatives were synthesized. However, as mentioned just above, PCBM remains the first choice

fullerene electron acceptor for the preparation of bulk-heterojunction solar cells. In this work, we have used PCBM as standard electron acceptor for spectroscopic studies as well as for the fabrication of reference devices.

2.1.8. Poly(ethylenedioxythiophene):polystirene sulphonate (PEDOT:PSS)

PEDOT:PSS (see Chart) was purchased from Bayer, as Baytron P, and diluted with 3 volumes of 2-propanol. This *p*-doped conductive conjugated polymer is widely used as thin film (50-100 nm) on the transparent conductive electrode to prevent short circuits in thin film organic optoelectronic devices.

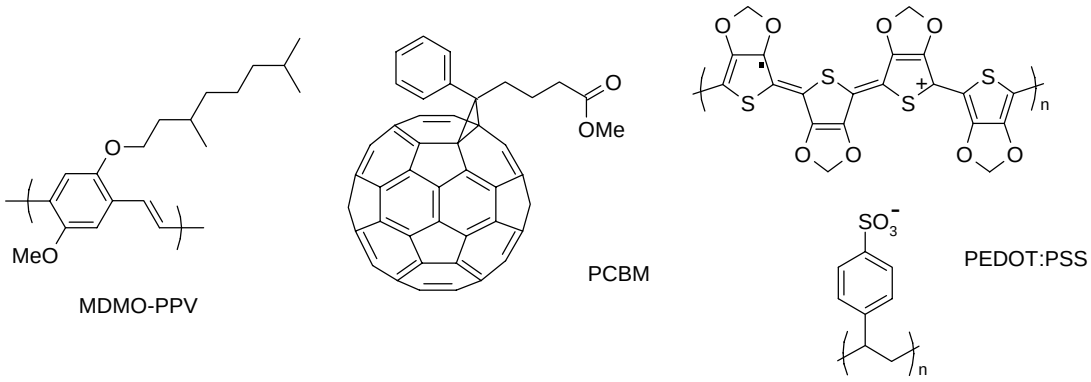

Chart

2.2. SAMPLES PREPARATION

In most cases, samples for spectroscopic measurements were thin-films drop- or spun-cast from solution onto appropriate substrates. For IR spectroscopy, KBr disks or pellets as well as ZnSe disks were used. For measurements in the Vis-NIR spectral range, sample were cast on glass. When samples were electrochemically deposited,

electrodes were transparent in the spectral region of interest. For IR spectroscopy, ZnSe reflection elements with an evaporated Pt grid or slightly doped Ge reflection elements were used. For Vis-NIR spectroscopy, ITO coated glasses or plastic foils were used.
Usually, solvents were of analytical grade from Aldrich, Fluka, J. T. Bakers and were used as received. For spectroelectrochemical experiments, toluene was distilled and kept over sodium while acetonitrile was stored over activated molecular sieves (4 Å).
The supporting electrolyte used for electrochemical and spectroelectrochemical measurements was tetrabutylammonium hexafluorophosphate (98 %, Fluka), dried in vacuum at 180 °C just prior of the experiments.
Drying of the samples was done in a oven under vacuum or by means of a nitrogen laminar flow box.

2.3. EXPERIMENTAL TECHNIQUES

2.3.1. Electrochemical polymerization and cyclic voltammetry

For electrochemical polymerization and cyclic voltammetry (CV) a conventional three-electrode cell was used. The working and the counter electrodes were Pt foils. An Ag/AgCl wire (calibrated with ferrocene just after the experiment) was used as quasi-reference electrode. The supporting electrolyte solution was typically 0.1 M tetrabutylammonium hexafluorophosphate in anhydrous toluene, CH_2Cl_2 or toluene/CH_3CN 7:3 v/v. Experiments in monomer-free conditions were carried out using the same electrolyte dissolved in CH_3CN. The electrochemical apparatus consisted of a Jaissle 1002T-NC potentiostat, a Prodis 1/14 I sweep generator and a Rikadenki RY-PIA x-y recorder. All the experiments were done at room temperature and under Argon.

2.3.2. Electron transfer studies and *in-situ* FTIR spectroelectrochemistry

For spectroscopy in the Vis-NIR range, the polymer films were electrodeposited or drop cast onto ITO coated glass and plastic foils. The UV-Vis absorption spectra of the films were taken at room temperature on a Cary-3 spectrophotometer. The photoinduced absorption (PIA) studies in the Vis-NIR were done using the Ar^+ ion laser lines at 351 and 476 nm as pump source (40 mW on a 4 mm diameter spot). The pump beam was modulated mechanically at a chopper frequency of 210 Hz. The change in the probe beam (120 W, tungsten lamp) transmission ($-\Delta T$) were detected, after dispersion with a 0.3 m monochromator, in the range 0.55-2.15 eV by a Si-InGaAsSb sandwich detector. The detector signals were recorded phase-sensitively with a dual-phase lock-in amplifier. The probe light transmission (T) was recorded separately using the same chopper frequency, then the PIA spectra were calculated as $-\Delta T/T$. Experiments were done at 100 K (the set-up is shown schematically in Fig. 2.5). Polymer films deposited on ZnSe (see below) were used for photoinduced FTIR absorption measurements (PIA-FTIR). The samples were placed in a liquid N_2 cryostat and illuminated in the 45° geometry (λ = 476 or 488 nm, 30 mW/cm^2, see Fig. 2.6). 10 single beam spectra were recorded in dark and then under illumination, repeating this sequence 300 times. From the resulting "light-off" and "light-on" spectra, the PIA was calculated as $-\Delta T/T$. All of the FTIR spectra were recorded with a resolution of 4 cm^{-1}, using a Bruker IFS 66/S equipped with a liquid N_2 cooled MCT detector. Attenuated total reflection (ATR) FTIR measurements during the electrochemical oxidation and reduction of the polymers were done in situ using the cell depicted schematically in Fig 2.6 Details and the set-up for in situ spectroelectrochemistry have been published.[22-24] The working electrode was a Pt grid evaporated onto a ZnSe reflection element or a Ge reflection element (when not differently stated, the other electrochemical parameters and conditions were as those described in the previous section). During potential scanning at a rate of 5 mV/s, single beam IR spectra were recorded consecutively. Each spectrum covers about 90 mV in the corresponding CV. By selecting a spectrum taken just prior of the investigated redox process as reference and relating the subsequent spectra to this chosen reference, specific electrochemically induced spectral changes were observed (the difference spectra were calculated as $\Delta(-\log T_{ATR})$, where T_{ATR} is the transmittance in the ATR

geometry). For LESR spectroscopy the polymer films on ITO coated plastic, cut in stripes of approximately 2 mm x 10 mm, were sandwiched and placed into a ESR quartz tube which was evacuated and then sealed in Ar atmosphere. The sample was placed in the high-Q-cavity of a X-band ESR spectrometer and cooled down to 100 K. For the "light-on" spectrum, illumination was made at 476 nm. To take into account residual spins due to the oxidative polymerization process as well as persistent light induced changes, "dark spectra" and "light-off" spectra were recorded just prior and after illumination, respectively. The LESR spectrum was then calculated by subtracting the "dark" signal from the "light-on" signal.

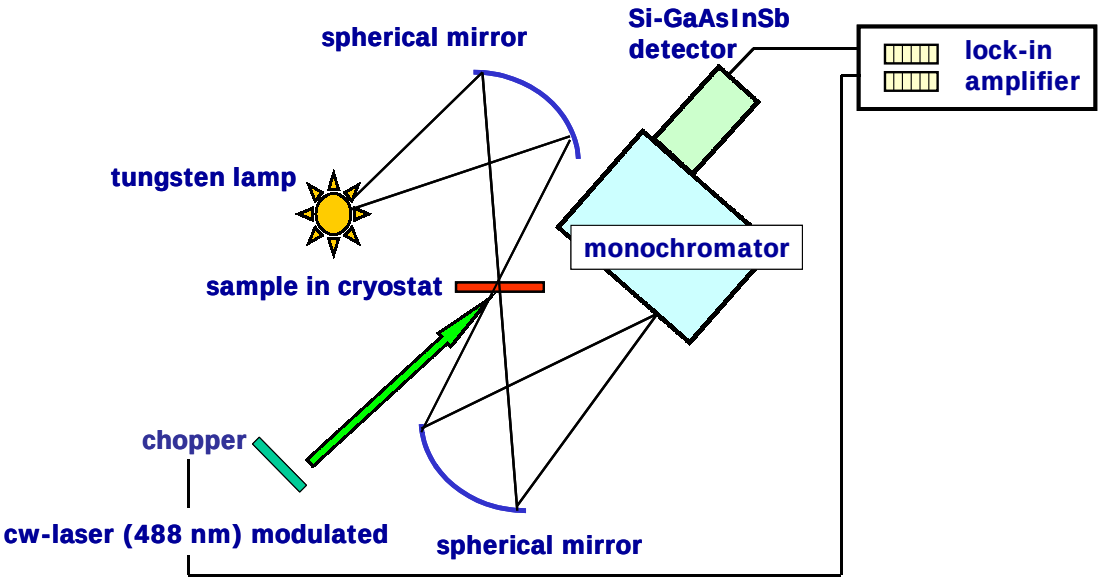

Fig. 2.5: Set-up for photoinduced Vis-NIR absorption.

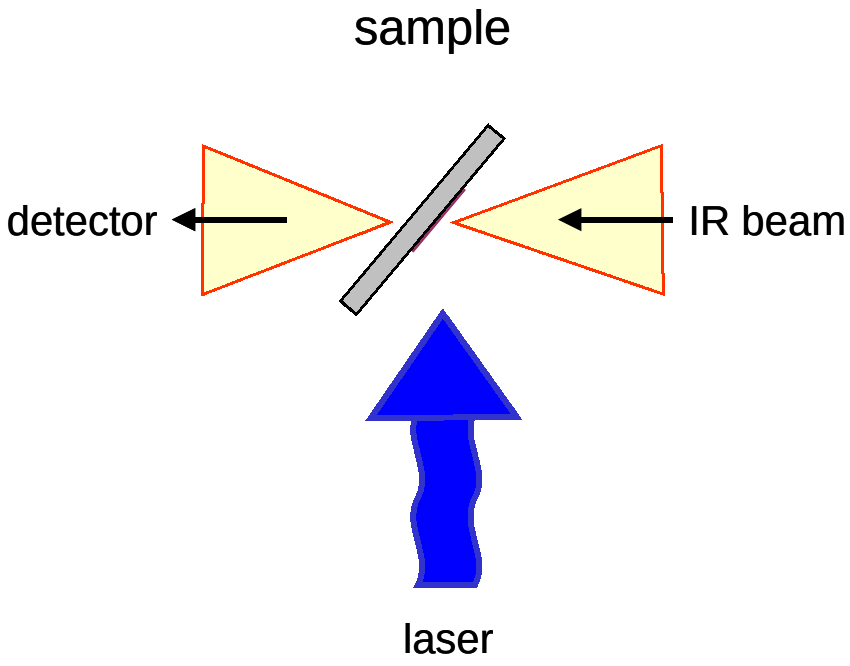

Fig. 2.6: Schematical set-up for photoinduced FTIR absorption

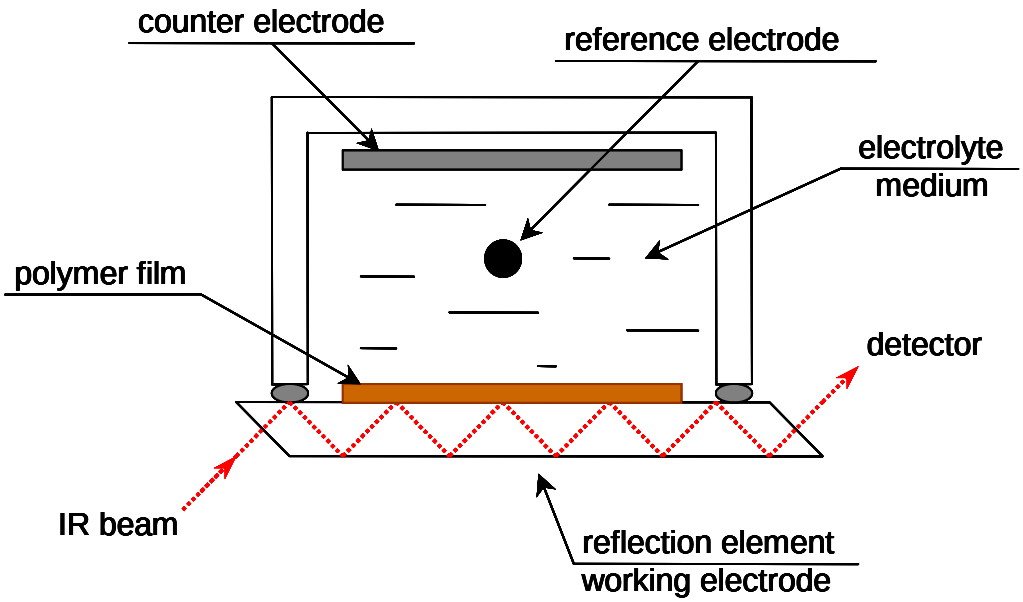

Fig. 2.7: Cell for *in situ* attenuated total reflection FTIR spectroelectrochemistry

2.4. REFERENCES

1. Arbizzani, C.; Catellani, M.; Mastragostino, M; Cerroni, M. G. *J. Electroanal. Chem.* **1997**, *423*, 23.

2. Arbizzani, C.; Catellani, M.; Cerroni, M. G.; Mastragostino, M. *Synth. Met*. **1997**, *84*, 249.

3. Bolognesi, A.; Catellani, M.; Destri, S.; Porzio, W. *Mol. Cryst. Liq. Cryst*. **1990**, *187*, 259.

4. Taliani, C.; Ruani, G.; Zamboni, R.; Bolognesi, A.; Catellani, M.; Destri, S.; Porzio, W.; Ostoja, P. *Synth. Met*. **1989**, *28*, C507.

5. De Jong, F.; Janssen, M. J. *J. Org. Chem*. **1971**, *36*, 1945.

6. De Jong, F.; Janssen, M. J. *J. Org. Chem*. **1971**, *36*, 1998.

7. Bolognesi, A.; Catellani, M.; Destri, S.; Ferro, D. R.; Porzio, W. *Synth. Met*. **1989**, 28, C527.

8 Catellani, M.; Lazzaroni, R.; Luzzati, S.; Brédas, J. L. *Synth. Met*. **1999**, *101*, 175.

9. Cava, M. P.; Latshmikantam, M. V. In *Compherensive Heterocyclic Chemistry, the Structure, Reactions, Synthesis and Uses of Heterocyclic Compounds*, 1st ed.; Bird, C. W.; Cheeseman, G. W. H.; Eds.; Pergamon Press: Oxford, 1984; Vol. 4, p. 1040.

10 Gutman, I.; Milun, M.; Trinajstić, N. *J. Am. Chem. Soc*. **1977**, *99*, 692.

11. Brédas, J. L. *Mol. Cryst. Liq. Cryst*. **1985**, *49*, 118.

12 Patil, O.; Heeger, A. J.; Wudl, F. *Chem. Rev*. **1988**, *88*, 183.

13 Kertesz, M. In *Handbook of Conductive Molecules and Polymers*; Nalwa H. S. Ed.; Wiley: Chichester, 1997; Vol. 4, Chapter 3.

14 E. Peters E., P. A. van Hal, J. Knol, C. J. Brabec, N. S. Sariciftci, J. C. Hummelen, R. A. J. Janssen, *J. Phys. Chem. B*, **2000**, *104*, 10174.

15. Maggini, M.; Scorrano, G.; Prato, M. *J. Am. Chem. Soc*. **1993**, *115*, 9798.

16. Martin, A. R., Yang Y. *Acta Chem. Scand.* **1993**, *47,* 221

17. Prato M., Maggini M, *Acc. Chem. Res*. **1998**, *31*, 519

18. Theander M., Inganäs O., Mammo W., Olinga T., Svensson M., Andersson M. R. *J. Phys. Chem. B* **1999**, *103,* 7771.

19. Brabec C. J, Winder C., Scharber M. C., Sariciftci N. S., Andersson M. R., Hummelen J.C., Svensson M., Andersson M. R. *J. Chem. Phys.* **2001**,115, 7235

20. Hummelen, J. C.; Knight, B. W.; Lepec, F.; Wudl, F.; Yao, J.; Wilkins, C. L. *J. Org. Chem.* **1995***, 60,* 532.

21. Neugebauer, H.; Nauer, G.; Neckel, A.; Tourillon, G.; Garnier, F.; Lang, P. *J. Phys. Chem*. **1984**, *88*, 652.

22. Neugebauer, H.; Ping, Z. *Mikrochim. Acta* **1997**, [Suppl.] *14*, 125.

23. Neugebauer, H.; Sariciftci, N. S. In *Lower Dimensional Systems and Molecular Electronics*, Nato ASI series, Series B: Physics, Vol. 248; Metzger, R. M.; Day, P.; Papavassiliou, G. C., Eds.; Plenum Press; New York, 1991; p 401.

CHAPTER 3. SPECTROSCOPIC STUDIES OF LOW BAND-GAP POLYDITHIENOTHIOPHENES

In Chapter 1 we have mentioned the theories developed in order to explain the doping- or photoinduced infrared spectroscopic features (IRAV) of conjugated polymers. These models, developed for relatively simple systems like *trans*-polyacetylene - in which both positive and negative charge carriers are topologically equivalent - have been extended to few polyheteroaromates. So far, these theoretical descriptions do not account for possible differences in the IRAV signatures of positive and negative charge carriers. A detailed description of the electronic and vibrational properties of conjugated polymer with low band-gap and stable in either the *p*- and *n*-doped states is necessary for the basic understanding of their behaviour. In particular, spectroscopic studies of conjugated polymers whit stable *n*-doped state might be useful to achieve better experimental and theoretical descriptions of the so far rarely observed negative charge carriers in conjugated polymers.

Due to the electron-phonon coupling in conjugated polymers, we expected that the different moieties fused to the same polythiophene-like chain influence also the vibrational behavior of PDTT1, PDTT2 and PDTT3. By means of Raman spectroscopy, *in situ* attenuated total reflection FTIR spectroelectrochemistry and photoinduced FTIR absorption spectroscopy, we have indeed observed that these members of the same polymer family exhibit a variety of spectroscopic behaviors. In particular, PDTT1 and PDTT2 in their *p*- and *n*-doped states show two different IRAV patterns. Conversely, no substantial differences are found between the spectra of *p*- and *n*-doped PDTT3. In all cases, the photoinduced IR absorption spectra resemble those of the *p*-doped polymer and do not show softening of modes, indicating that a kind of pinning occurs even in absence of electrolyte counterions. Moreover, a vibrational signature for an increased quinoidal character of the chain is observed.

Electron spin resonance (ESR) combined with electrochemistry has been applied successfully in the elucidation of the doping mechanisms of several conjugated

polymers and can directly proof the formation of paramagnetic charge carriers such as polarons.[1-2] In situ ESR spectroelectrochemistry measurements performed during *p*- and *n*-doping of PDTT1, PDTT2 and PDTT3 revealed that the charge carriers of polaronic nature exhibit unusually high *g*-factors. In addition, negative polarons have systematically higher *g*-factors as compared to their positive counterparts.

3.1 VIBRATIONAL SPECTROSCOPY

3.1.1. Raman spectroscopy

We used Raman scattering spectroscopy to obtain some insight on how the different thienothiophene moieties are affecting the π-electron delocalization of the polythiophene-like conjugated backbone. The resonant Raman spectra obtained at various excitation wavelengths are displayed in Fig. 3.1, 3.2 and 3.3. In the following discussion, α, β and γ refer to PDTT1, PDTT2 and PDTT3, respectively. Upon tuning the excitation wavelength within the polymer π→π* absorption bands (for absorption spectra see Ref. 16), the selective excitation of chain segments with different π-electron delocalization leads to a frequency dispersion and to an intensity redistribution of the Raman modes. At lower excitation wavelengths, i.e. in resonance with the shortest conjugation lengths, PDTTs exhibit two intense Raman bands, indexed 1 and 2 (Fig. 3.1(a-d), Fig. 3.2(a-c) and Fig. 3.3(a-d). See also Table 3.1). With the NIR excitation (λ= 1064 nm) near the onset of the absorption band of PDTTs[5] and thus in resonance with the chain segments with the more extended π-electron delocalization, the Raman spectra display a much more complicated pattern. The PDTT1 Raman spectrum (Fig. 3.1(d)) shows four relevant bands at 1466 (α_1), 1422 (α_2), 1287 (α_3), 1237 cm^{-1} (α_4); a broad and weaker feature is seen at about 850 cm^{-1}. The Raman spectrum of PDTT2 (Fig. 3.2(c)) is rather similar to that of PDTT1. Although red-shifted, the intense bands seen at 1431 (β_1) and 1395 (β_2) cm^{-1} compare well with α_1 and α_2. Again, two bands are at 1287 (β_3) and 1237 cm^{-1} (β_4). The most striking difference is the presence of several medium or weak bands below 1000 cm^{-1} (β_5-β_9, listed in Table 3.2). The PDTT3 (NIR excitation) spectrum (Fig. 3.3(d)) shows a quite complicated pattern, in which five main

bands are observed at 1475 (γ_0), 1422 (γ_1), 1344 (γ_3), 1318 (γ_4) and 639 (γ_7) cm^{-1} along with several weaker features.

These spectral features evidence that the Raman behavior of PDTTs is significantly different from that of simpler polythiophenes. In general, Raman spectra of the polythiophene family show three main lines coupled to the electronic transition. Two dominant lines are around 1500 cm^{-1} and 1450 cm^{-1} (C=C stretching region)[6,7] while a weaker feature is seen within the range 1080-1050 cm^{-1} (C-C stretching + C-H wagging component).[8,9] The modes that posses the largest ECC character correspond to the bands near 1500 cm^{-1}, which show a weak dispersion with different chain lengths (as well as with different excitation wavelengths in polydispersed samples). This behavior is the vibrational signature proving that in polythiophenes π-electrons are mostly confined within each thiophene ring or within a very restricted domain of the chain.[8,9] For PDTTs, significant differences to the simpler polythiophene Raman spectra are found:

- more complicated spectra are observed for PDTTs (more Raman lines are seen going from PDTT1 to PDTT2 and PDTT3);

- most of the PDTTs Raman bands show both intensity redistribution and frequency dispersion with the excitation wavelength. The intense bands indexed 1 and 2 (see Fig. 3.1(a-d), Fig. 3.2(a-c), Fig. 3.3(a-d) and Table 3.1) are identified as the modes with the largest ECC contribution which, as opposed to simple polythiophenes, exhibit a more relevant dispersion. Moreover, lines indexed 1 and 2 appear at significantly lower wavenumbers than the two lines near 1500 cm^{-1} in the simple polythiophenes' spectra;

- in PDTTs no relevant Raman lines are observed around 1100 cm^{-1};

- in the region around 1300 cm^{-1} no dominant lines are observed for polythiophenes while two intense lines are seen for the PDTTs (band index 3 and 4).

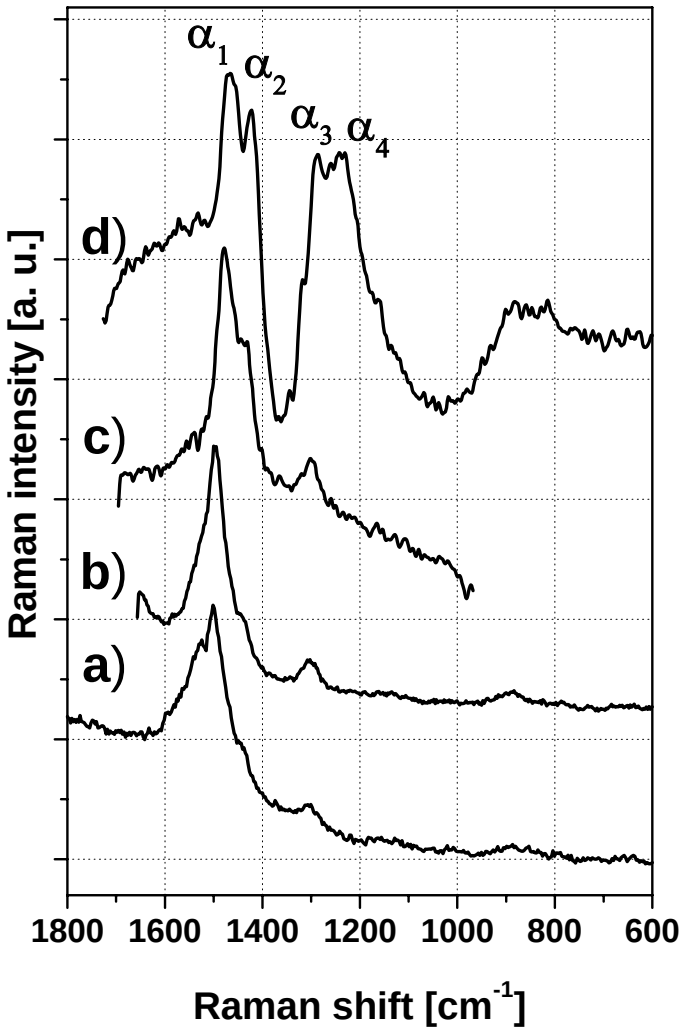

Fig. 3.1: Raman spectra of pristine PDTT1. Excitation at 457 (a), 488 (b) 633 (c) and 1064 nm (d).

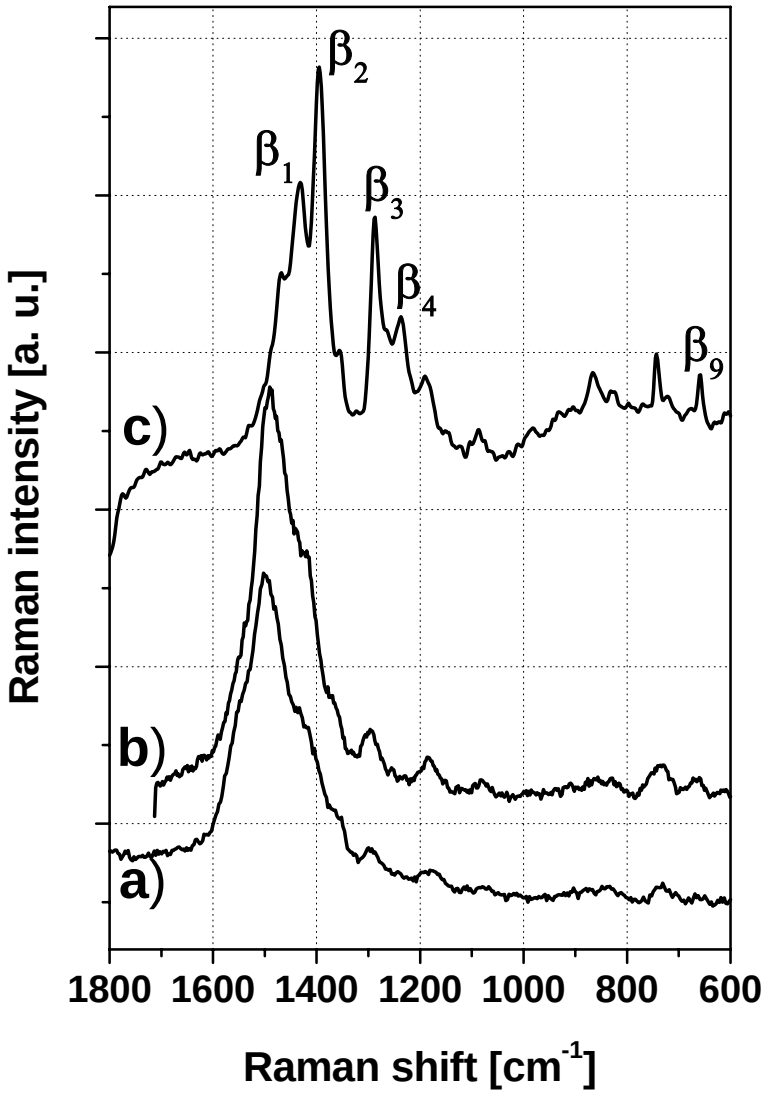

Fig. 3.3:Raman spectra of pristine PDTT2. Excitation at 457 (a), 514 (b) and 1064 nm (c).

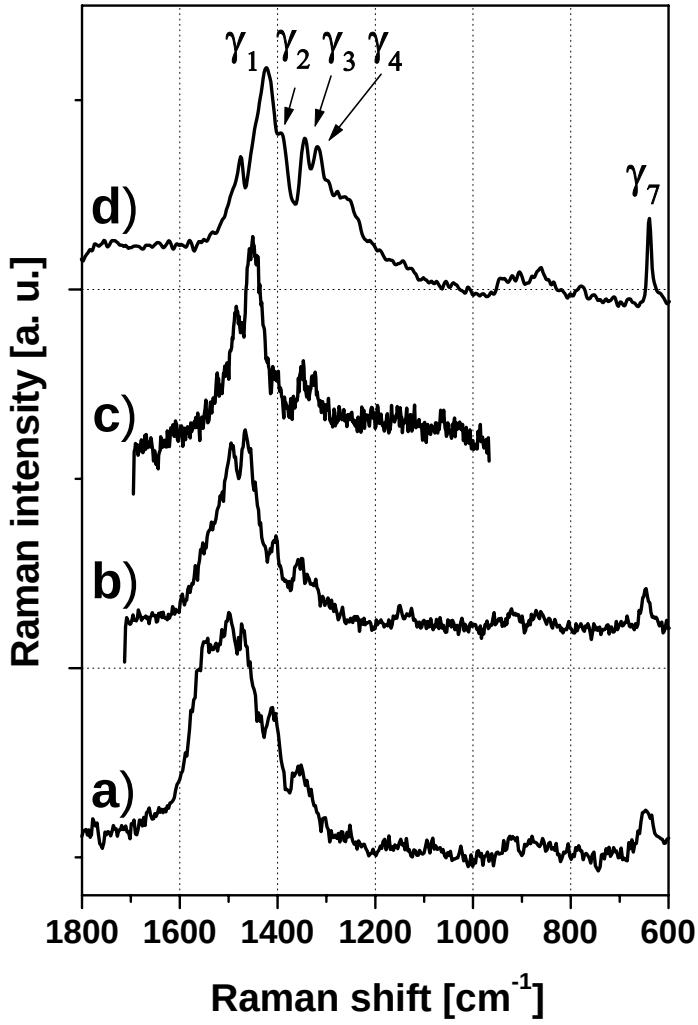

Fig. 3.4: Raman spectra of pristine PDTT3. Excitation at 457 (a), 514 (b), 633 (c) and 1064 nm (d).

Most of the above differences can be explained considering the enhanced weight of the quinoidal canonical form in the definition of the PDTTs electronic ground-state and hence the increased inter-ring electronic delocalization:

- this effect is overcoming the π-electron confinement found in polythiophenes (as well as it is reducing the band-gap size). Therefore, the modes containing the strongest ECC contribution do exhibit the predicted frequency dispersion;

- apart from the relative differences in the weight of the canonical forms (crucial for the size of the band-gap) it is known that in both polythiophenes and PDTTs the ground-state is aromatic (the canonical structure a) in the inset of Fig. 3.1 has the major weight in its definition).[10] Therefore, the C=C stretching vibration mostly contributing to the ECC mode must be that between the nuclei C_α-C_β of the thiophene ring lying in the polythiophene-like chain. As such, the red-shift of lines 1 and 2 in PDTTs compared to the corresponding ECC modes in polythiophenes is motivated by the decrease of the C_α-C_β force constant that must accompany the increased quinoidal character of the chain. As further corroboration, these lines shift to lower wavenumbers as the polymer band-gap decreases ($\nu(\alpha_1) > \nu(\beta_1) > \nu(\gamma_1)$ and $\nu(\alpha_2) > \nu(\beta_2), \nu(\gamma_2)$);

- conversely, the C_α-$C_{\alpha'}$ (inter-ring bond) force constant should increase with increasing quinoid character of the chain and, therefore, some bands should appear at higher wavenumber in the PDTTs spectra than in those of polythiophenes. For the latter polymers, a medium band near 1200 cm^{-1} has been assigned to C_α-$C_{\alpha'}$ symmetric stretching.[6,7] Thus, it is noteworthy that PDTT spectra show intense lines, well above 1200 cm^{-1}, that shift to higher wavenumbers as the band-gap decreases ($\nu(\alpha_3) < \nu(\beta_3) < \nu(\gamma_3)$ and $\nu(\alpha_4) < \nu(\beta_4), \nu(\gamma_4)$).

In conclusion, the Raman spectra of PDTTs display the spectral signatures of an increased quinoidal character of the polythiophene-like chain compared to polythiophenes and of the involvement of the thienothiophene moieties to the polymer

backbone π-electron delocalization. These effects are increasing from PDTT1 to PDTT2 to PDTT3.

3.1.2. In situ FTIR spectroelectrochemistry

As mentioned above, PDTT1, PDTT2 and PDTT3 are among the few conjugated polymers so far described that undergo both reversible *p*- and *n*-doping. By combining cyclic voltammetry and ATR-FTIR spectroscopy we have recorded, in situ, the IR spectral changes during the doping processes of PDTT1, PDTT2 and PDTT3. The cyclic voltammograms (scan rate 5 mV/s) taken during the in situ IR spectroelectrochemical experiments are shown in Fig. 3.5.

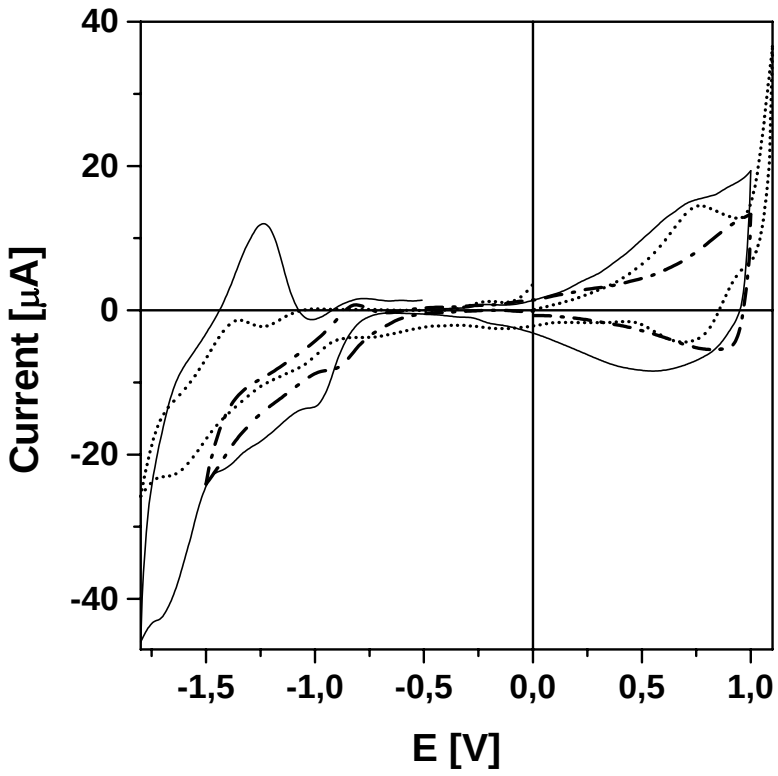

Fig. 3.5: Cyclic voltammogramms of PDTT1 (dash-dotted line), PDTT2 (dotted line) and PDTT3 (solid line), recorded during the in situ ATR-FTIR experiments.

The IR spectral changes developing during *p*- and *n*-doping of PDTT1 are depicted in Fig. 3.6. With both *p*- and *n*-doping the spectra show a broad electronic absorption band, with maximum around 3600 cm^{-1}, and IRAV bands in the vibrational range (the latter is represented in detail in Figure 3.7).

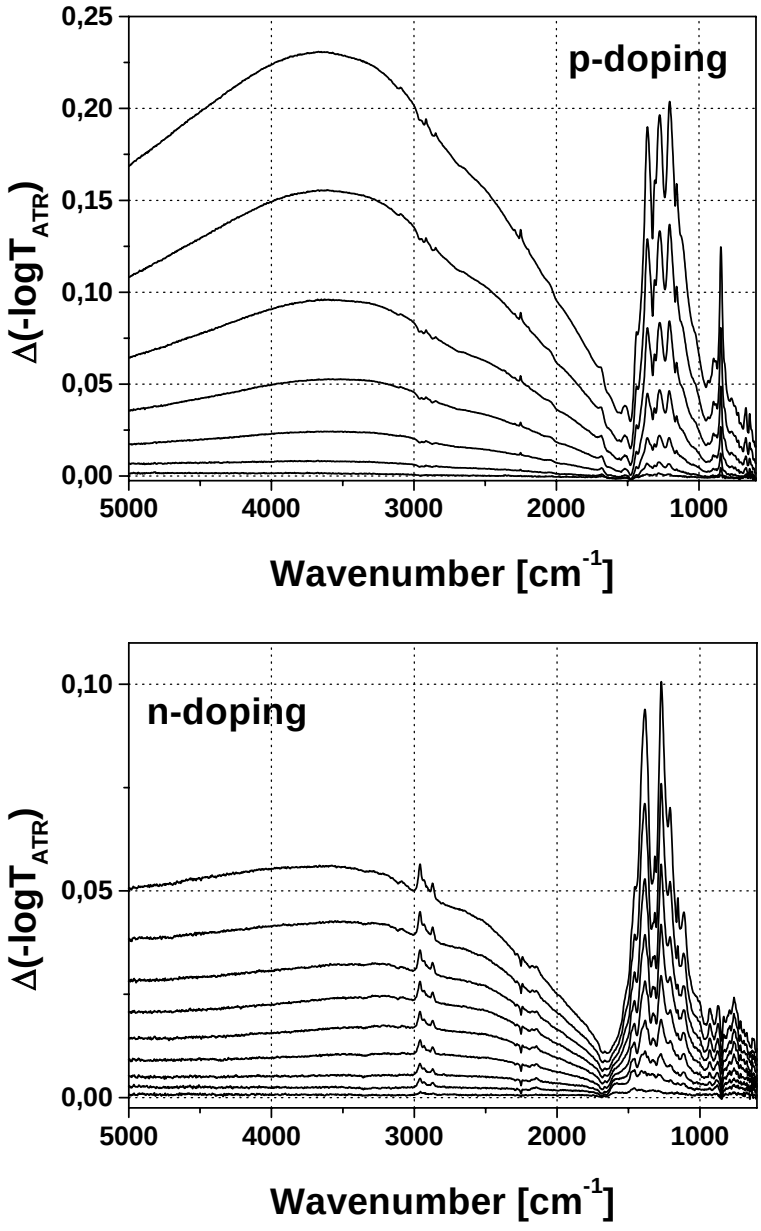

Fig. 3.6: FTIR difference spectra during *p*- and *n*-doping of PDTT1. Sequence: bottom to top.

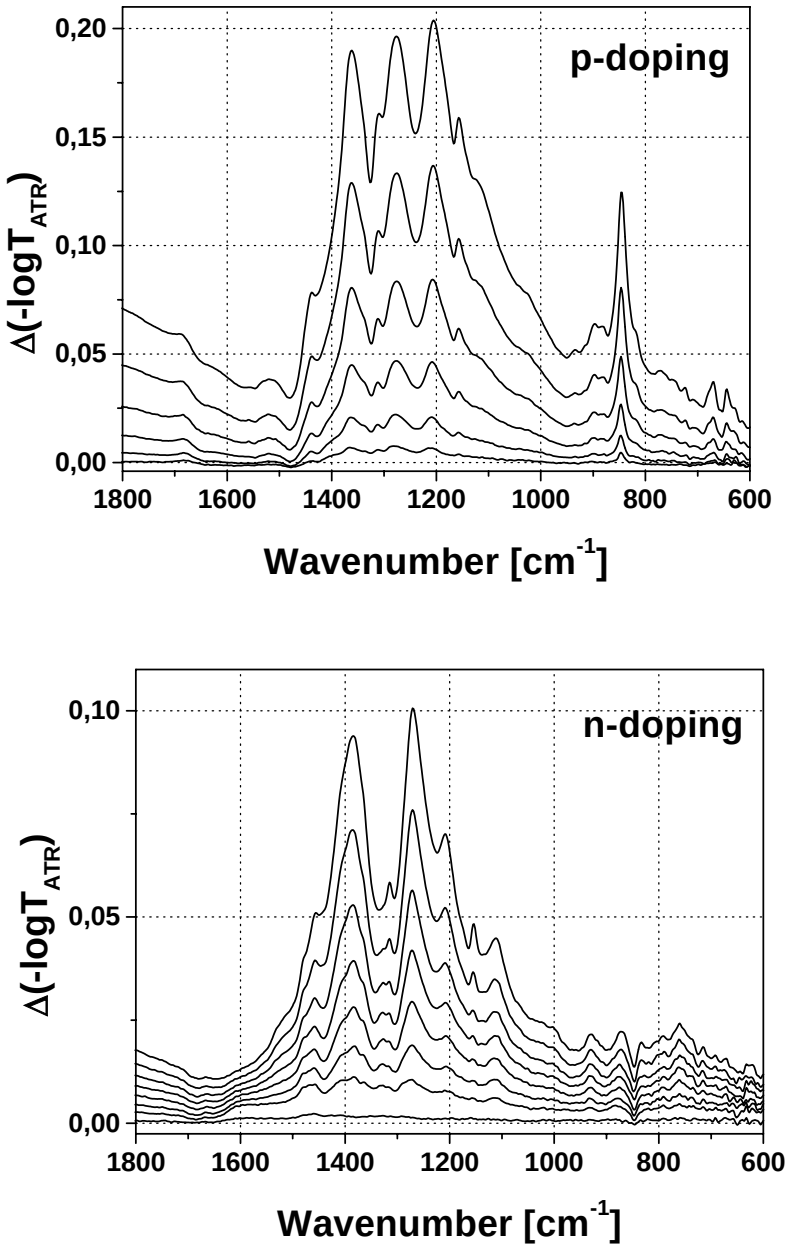

Fig. 3.7: FTIR difference spectra during *p*- and *n*-doping of PDDT1. IRAV range. Sequence: bottom to top.

The frequencies and the characteristics of the IRAV bands are reported, along with those observed upon doping of PDTT2 and PDTT3, in Table 3.2 (Table 3.2 collects also frequencies from the PIA-IR absorption spectra that will be discussed later). The sharp peak at 842 cm^{-1}, growing during the *p*-doping of all polymers, is due to the incorporation of the hexafluorophosphate ions balancing the charge formed on the polymer by the oxidation process. As can be seen, the following differences between *p*- and *n*-doped PDTT1 spectra are observed:

- the *p*-doped polymer spectrum shows three dominant IRAV bands while only two intense IRAV bands emerge upon *n*-doping (Fig. 3.7);

- in the *n*-doped polymer spectrum, the intensity of all features is about 50% lower of that observed in the *p*-doped polymer spectrum (Fig. 3.6);

- the relative intensities of bands are different in the two differently doped polymer forms. In particular, the intensity of the in-the-gap electronic absorption band relative to those of IRAV bands is drastically lower in the *n*-doped polymer spectrum (Fig. 3.6).

A quite similar behavior shows PDTT2, whose spectra during *p*- and *n*-doping are depicted in Figure 3.8. Again, the spectral patterns include a broad eletronic absorption band above 1500 cm^{-1} and IRAV bands in the vibrational range (detailed in Fig. 3.9). Although the spectra are not as dissimilar as in the previous case, differences between the *p*- and *n*-doped polymer spectra are observed:

- *p*-doped PDTT2 shows an ill-defined IRAV spectrum due to the overlap of broad bands while the *n*-doped polymer spectrum clearly shows four intense IRAV bands (Fig. 3.9);

- remarkable differences are also seen when considering the features with medium and weak intensity below 800 cm^{-1} (Fig. 3.9);

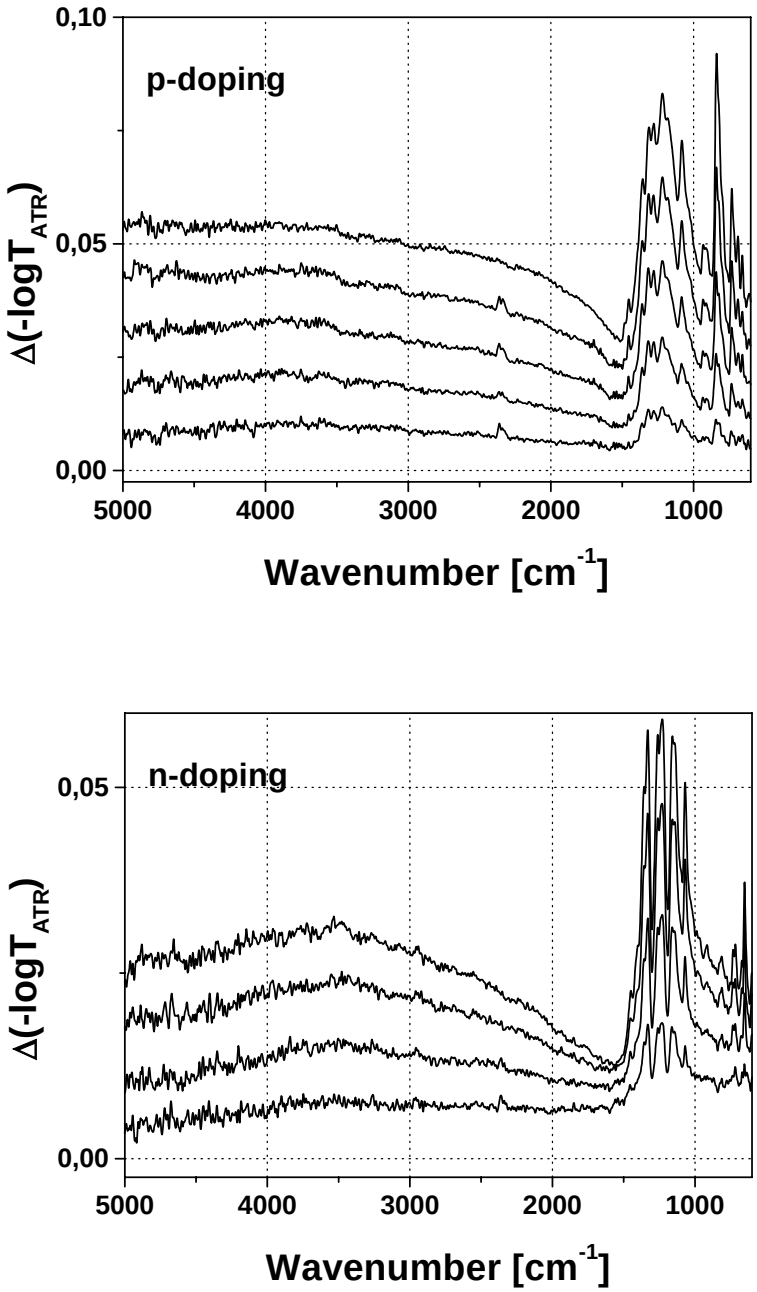

Fig. 3.8: FTIR difference spectra during *p*- and *n*-doping of PDTT2. Sequence: bottom to top.

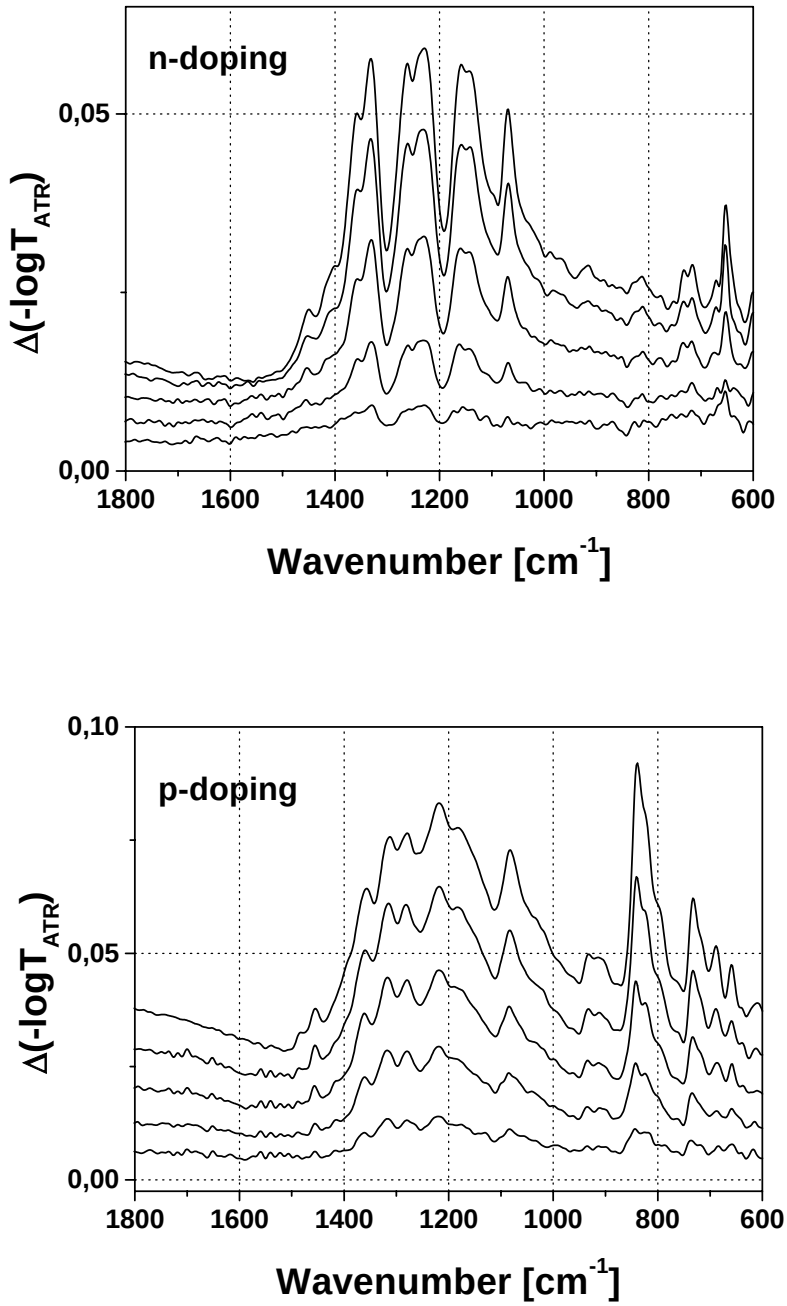

Fig. 3.9: FTIR difference spectra during *p*- and *n*-doping of PDDT2. IRAV range. Sequence: bottom to top.

- similar to PDTT1, the intensity of the *n*-doped PDTT2 bands is about 50% lower of those seen in the *p*-doped polymer spectrum.

Such differences indicate a different delocalization for the positive and negative charge carriers in PDTT1 and PDTT2, as already reported for other *p*- and *n*-dopable polymers like poly(ethylene-2,3-dioxythiophene) (PEDOT)[11-13] and poly(isothianaphthenemethine).[15] Despite the feasibility of reversible doping of both signs these polymers maintain a higher delocalization/mobility of positive charge carriers, as indicated by the higher intensity, the larger bandwidth and the lower wavenumber observed for the IRAV bands of the *p*-doped polymer forms as compared to the *n*-doped state.

For PDTT3 we have observed a different and peculiar behavior.[13,15] Its *p*-doped state show a spectrum (Fig. 3.10 and 3.11) dominated by a broad absorption at high energy, with maximum at about 2800 cm^{-1}, and a complicated IRAV band pattern. The main bands in the range 1500 - 1000 cm^{-1} are rather broad, which indicates, together with their high intensity, a rather high delocalization of the positive charges along the chain. Several sharp peaks appear in the region 950 - 600 cm^{-1}. The high energy part of the *n*-doped PDTT3 spectrum (Fig. 3.10) shows a broad bands with maximum that shifts from 3250 to 2800 cm^{-1} with increasing doping level. The IRAV bands that arise during *n*-doping process give a pattern similar to that of the *p*-doped polymer form (Fig. 3.11). Apart from slight differences in the relative intensities, especially above 1000 cm^{-1} all of the spectral features are present in both spectra of the oxidized and reduced PDTT3. Again, sharp peaks appear in the region from 950 to 600 cm^{-1}. In contrast to other polythiophene- based conjugated polymers as well as PDTT1 and PDTT2, the difference spectra of *p*- and *n*-doped PDTT3 exhibit IRAV bands with almost the same intensities. The high similarity between the spectral features of oxidized and reduced PDTT3 suggests that the nature and delocalization of the charge carriers of both signs are similar.

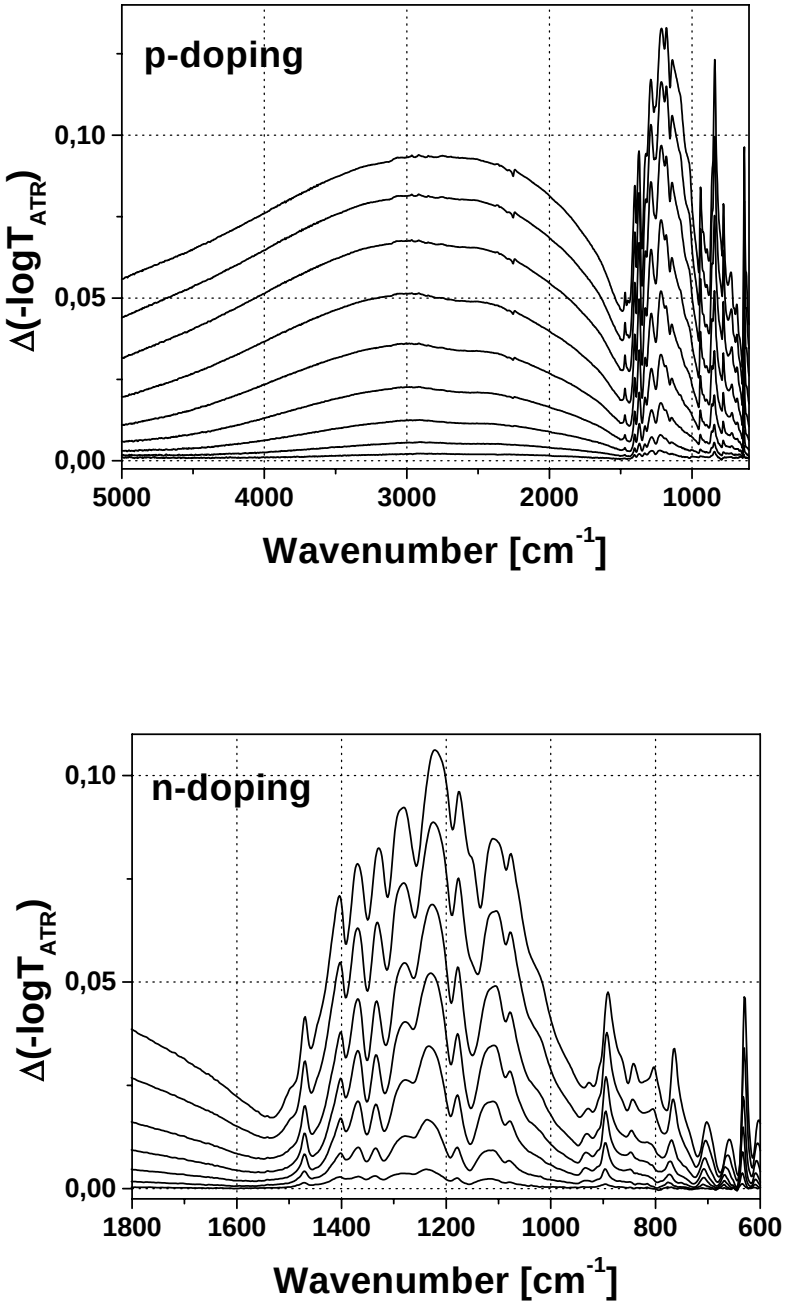

Fig. 3.10: FTIR difference spectra during *p*- and *n*-doping of PDTT3. Sequence: bottom to top.

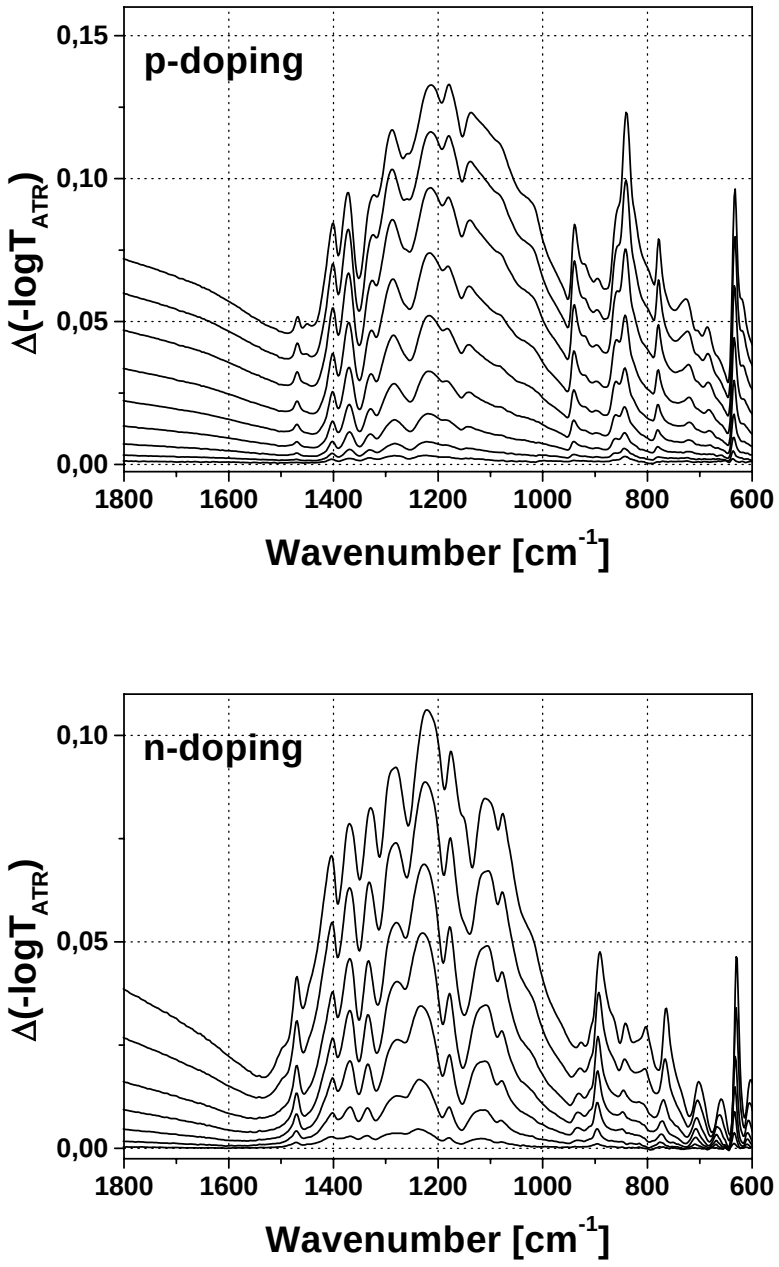

Fig. 3.11: FTIR difference spectra during *p*- and *n*-doping of PDDT3. IRAV range. Sequence: bottom to top.

Despite the polythiophene-like nature of the chain and as already observed by Raman spectroscopy, all of the p-doped PDTTs I R spectra do not compare well to those of simpler *p*-doped polythiophenes.[16,17] Such a dissimilarity should not be observed if modes located within the fused thienothiophene moiety would not contribute significantly to the ECC. Within the PDTTs series, the results confirm that the π-electrons of the fused thienothiophene moiety of PDTTs affect differently the π-electron delocalization along the polythiophene-like chain, thus determining the different electronic and vibrational properties of the polymers. In particular, the fact that the spectral complexity increases from PDTT1 to PDDT2 and PDDT3, can be explained by the increased interaction between the π-electrons within the fused moiety and the polythiophene-like chain, according to the enhanced inter-ring delocalization as the band-gap decreases.

3.1.3. Photoinduced IR absorption

The spectral signatures of charged carriers (electronic absorption and IRAV bands) are also observed in the photoinduced IR absorption (PIA) spectra, which are presented in Figure 3.12 and in Fig. 3.13 (band wavenumbers are collated in Table 3.2). The formation of both positive and negative charge carriers can be expected by dissociation of excitons after photoexcitation as well as by direct excitation.[18] However, it can be seen that all of the PDTTs PIA-IR spectra are similar to those of the corresponding *p*-doped polymer, especially concerning the IRAV bands. Such a similarity is implicit only for PDTT3, whose positive and negative charge carriers possess nearly identical IR signatures. For PDTT1 and PDTT2, which show different spectra in the *p*- and *n*-doped state, it must be inferred that mostly positive polarons are delocalized and behave as majority charge carriers in the photodoped material. Conversely, negative charges are probably trapped within certain sites of the polymer, e.g. chain defects, or localized in the repeating units themselves. These results are consistent with the higher *p*-type charge carrier delocalization in PDTT1 and PDTT2 found by the *in situ* FTIR spectroelectrochemical measurements.

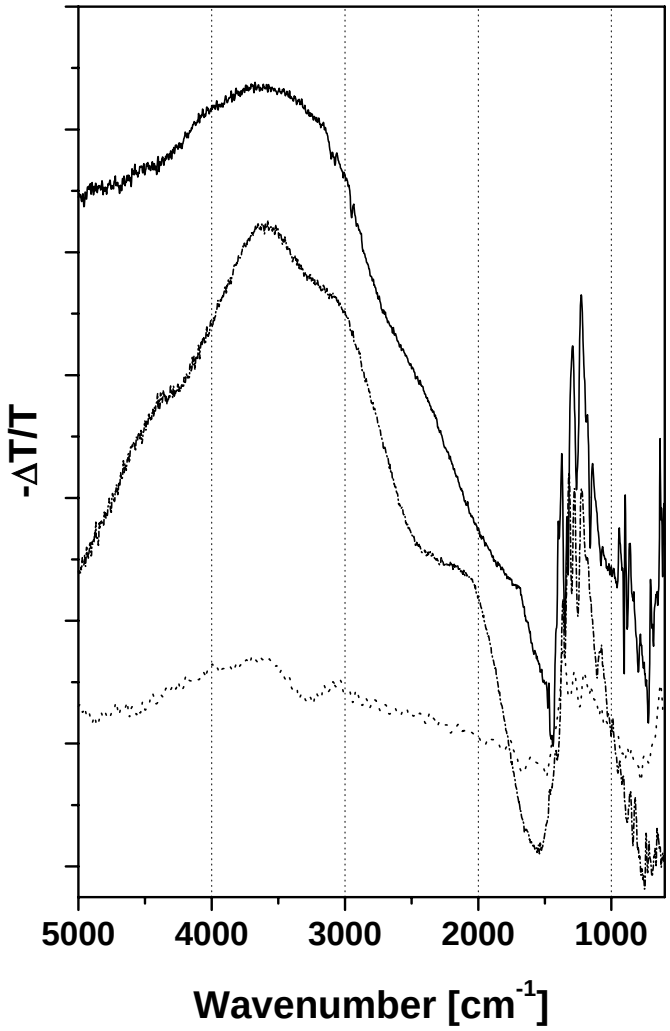

Fig. 3.12: PIA-FTIR spectra of PDTT1 (dotted line), PDTT2 (dash-dotted line) and PDTT3 (solid line).

In all cases, no softening of IRAV modes is observed in the photoexcited spectra as compared to the electrochemical doping induced spectra. On the contrary, some bands even show a small blue-shift in the photoexcited case. This observation suggests that the small number of carriers generated by photodoping have a kind of "extra-pinning", possibly arising from localized negative charges acting as pinning sites for the positive carriers. Such an effect explains the similarity of the IRAV frequencies despite the absence of electrolyte counterions in the photoexcited case.

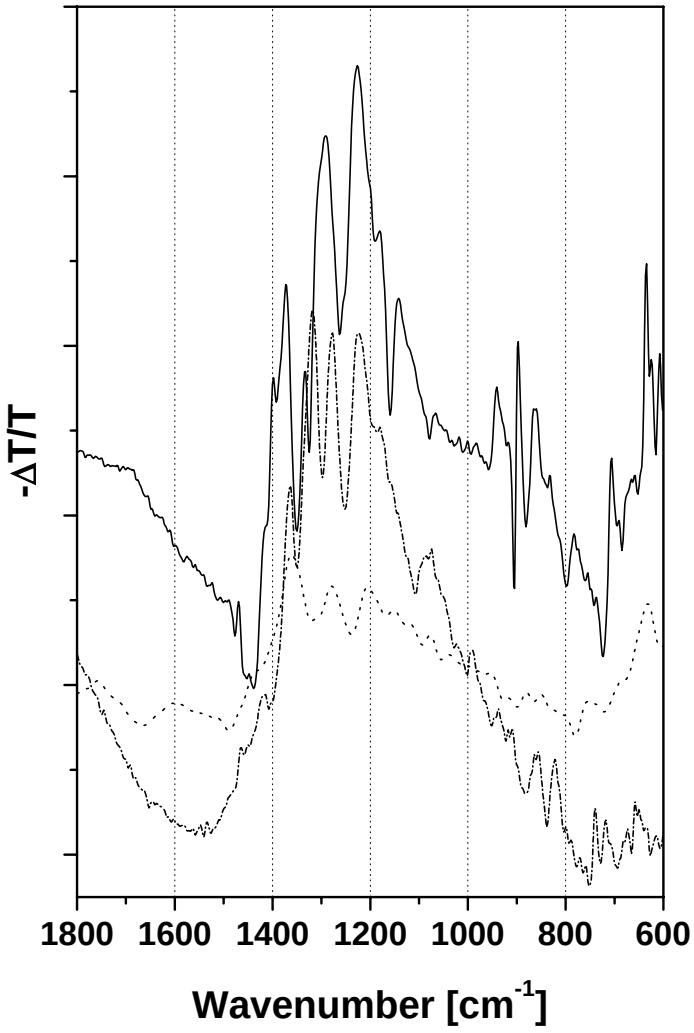

Fig. 3.13: PIA-FTIR spectra of PDTT1 (dotted line), PDTT2 (dash-dotted line) and PDTT3 (solid line). Spectra are arbitrarily rescaled.

3.2. COMPARISON OF RAMAN AND IR RESULTS

As explained in the introduction, the theories developed to elucidate the Raman and IR spectroscopic behavior of conjugated polymers predict an almost one-to-one correspondence between the Raman lines of the neutral samples and the IRAV bands activated by doping or illumination.

In detail, the NIR Raman spectrum of PDTT3 exhibits five main bands at 1475 cm^{-1} (γ_0), 1422 (γ_1), 1344 (γ_3), 1318 (γ_4) and 639 cm^{-1} (γ_7); shoulders or broad and weaker features are detected at about 1390 (γ_2), 1270 (γ_5) and around 900 cm^{-1} (several overlapping bands with low intensities, indicated as (γ_6). In contrast to the results obtained with simpler conjugated polymers, some Raman bands of PDTT3 coincide with Raman modes of the monomer. The two Raman bands observed at 1475 cm^{-1} and 1407 cm^{-1} (γ_2) in the spectrum taken with excitation at 457 nm, which is in off-resonance with the π-π^* transition of the polymer, correspond to two very strong Raman bands of the monomer. Further coincidences with weaker monomer bands are observed for the modes at 1473 (γ_1) and 1355 cm^{-1} (γ_3). As underlined in the above discussion, Raman spectra show intensity redistribution with the exciting energy. Going from 457 nm to NIR excitation, the band seen at 1475 cm^{-1} (457 nm) disappear and band γ_2 becomes a shoulder. This behavior, associated with the already discussed correspondence to two strong Raman modes of the monomer, indicates that these modes are located with the dithienothiophene moiety. Band γ_1 strongly increases in intensity with increasing excitation wavelength and becomes the dominating signal in the spectrum taken with NIR excitation. Other signals that gain in intensity, but have no correspondence to monomer Raman bands, are γ_4, γ_5, and γ_6. The last two are only clearly seen with NIR excitation. Band γ_0 loses intensity but remains noticeable even exciting with long wavelengths. As underlined in Section 3.1.1, the main bands show also changes in frequency at different excitation energies. Bands γ_0, γ_1, γ_3 and γ_4 decrease in frequency with decreasing excitation energy, i.e. according to the models by the selective enhancement of longer conjugated segments.

Correspondences between these Raman bands and IRAV bands of the electrochemically *p*-doped PDTT3 are found:

- band γ_0, which decreases and moderately shifts in Raman, shows a further shift to lower frequency in the IR spectrum;

- the set of bands γ_1, γ_3 and γ_4, which gain in intensity increasing the excitation wavelength, remains intense and shows a remarkable shift (about 30 cm^{-1}) going to the IR spectrum of oxidized PDTT3. Band γ_1 seems to split in two bands at 1401 and 1371 cm^{-1};

- the broad and weak features γ_5 and γ_6, emerging in the Raman spectrum taken with NIR excitation, appear with rather high intensity in the IR absorption and give the two extended and complicated patterns in the regions 1250-1120 cm^{-1} and 950-770 cm^{-1}. The feature γ_6 seems to be splitted in several broad components.

- A remarkable and particular behavior shows the low-frequency band at about 640 cm^{-1} (γ_7), which is quite far from the range commonly considered for IRAV modes. It does not show dispersion and it is always quite strong upon changing the excitation wavelength. Moreover, almost no changes in its relative intensity and position are detected in the IR spectrum. This fact is suggesting that this band is associated to a mode that, altough being coupled to the π-electronic system of the polymeric backbone, is localized within the fused thienothiophene moiety.
  The localization of this mode is also indicated by the sharpness of the corresponding band. In the Raman spectra of polythiophenes, very weak features in this low frequency region of the spectrum were found and identified as A_g ring deformation modes containing C-S stretching character.[19] Infrared bands of neutral and doped polythiophene in the region ranging from 900 to 600 cm^{-1} have also been assigned to thiophene ring modes by several groups.[20] In PDTT3, similar contributions from C-S stretching modes localized in the fused rings but still coupled to the π-electronic system of the polymeric backbone, can be expected and are indeed found by the rather intense band γ_7.

In PDTT2, it can be seen that the bands α_1 and α_2, which in Raman show large intensity redistribution, and softening with increasing excitation wavelength, exhibit further changes going to the IR spectra. Band α_1 weakens in the *p*-doped polymer spectrum and is observed only as shoulder in the PIA-FTIR spectrum. Conversely, α_2, observed as a shoulder in the Raman spectrum with excitation at 457 nm, becomes stronger with the

NIR excitation and is among the dominant bands in the doped and PIA-FTIR polymer spectra. In addition to the softening with increasing excitation wavelength, α_1 and α_2 show a further shift to red in the FTIR polymer spectra. For PDTT2, due to the complexity of the spectral pattern and especially to the overlapping of several bands in the *p*-doped polymer spectrum, a band-to-band correlation would be too speculative and has not been done. However, it can be noted that the sharp and medium band β_9, observed in all of the IR as well as the Raman spectra of PDDT2, seems to have the same origin as γ_7 in PDTT3.[15]

3.3. *IN SITU* ESR SPECTROSCOPY

In addition to vibrational spectroscopy, ESR spectra of PDTTs were recorded in situ during electrochemical *p*- and *n*-doping in potential scan experiments. These studies have been performed at the group of Lothar Dunsch in Dresden, Germany. In all cases, the formation of paramagnetic charge carriers (polarons) is observed. As an example, Fig. 3.14 shows the ESR signal obtained during p-doping and dedoping of PDTT3. A detailed study of the behavior of the ESR signal and its correlation to electrochemical parameters (e.g. amount of charge, electrode potential) is in progress. The maximum signal obtained during *p*- and *n*-doping was used for the determination of the g-factors. The rescaled spectra of the respective charge carriers in PDTT1, PDTT2 and PDTT3 are shown in Fig. 3.15. *P*-doped PDTTs spectra consist of a single line at g-factors around 2.004, which is higher than the values commonly observed for doped (as well as photoexcited) conjugated oligomers[21] and polymers.[22-25] The *n*-doped PDTTs spectra consist of a single line at even higher g-factors. The spin signature of negative polarons is seen by the lines at g-factor values ranging from 2.0049 (PDTT2) to 2.0054 (PDTT1). These g-factors are remarkably high. Origin of the high g-factors is assumed to be the stronger spin-orbit coupling within the PDTTs, potentially related to the sulphur atoms in the fused moieties, which again shows their strong influence to the polymer properties. In fact, g-factors are related to the participation of carbon atom and heteroatoms according to the equation

$$\Delta g = g - g_e \propto \lambda / E_g$$

where g_e is the free-electron g-factor (2.0023), λ is the spin-orbit coupling parameter (29 cm^{-1} for C_{2p}, 382 cm^{-1} for S_{3p}) and E_g is the polymer band gap.

It is also remarkable that the g-factor for the negative polaron as compared to the positive polaron on one-and-the-same polymer is systematically higher. This g-factor shift can have several origins:

- the different spin-orbit coupling terms by the different polaron distribution on the sulphur atoms in the *p*- and *n*-doped polymer;

- the differences in excited state energies for the *n*- and *p*-polarons, respectively, resulting in different g-factor shift term due to the denominator in the spin-orbit terms.[26]

- In principle, there could also be an effect due to the incorporation of different counterions during *p*- and *n*-doping.[27]

Independently of the doping sign, all ESR lines are narrow (ΔH_{P-P} of 2-3.5 G). Rather narrow ESR lines for doped conducting polymers are commonly observed and interpreted by motional as well as exchange narrowing due to a large number of carriers.[28] Positions and widths of the ESR lines are listed in Table 3.3.

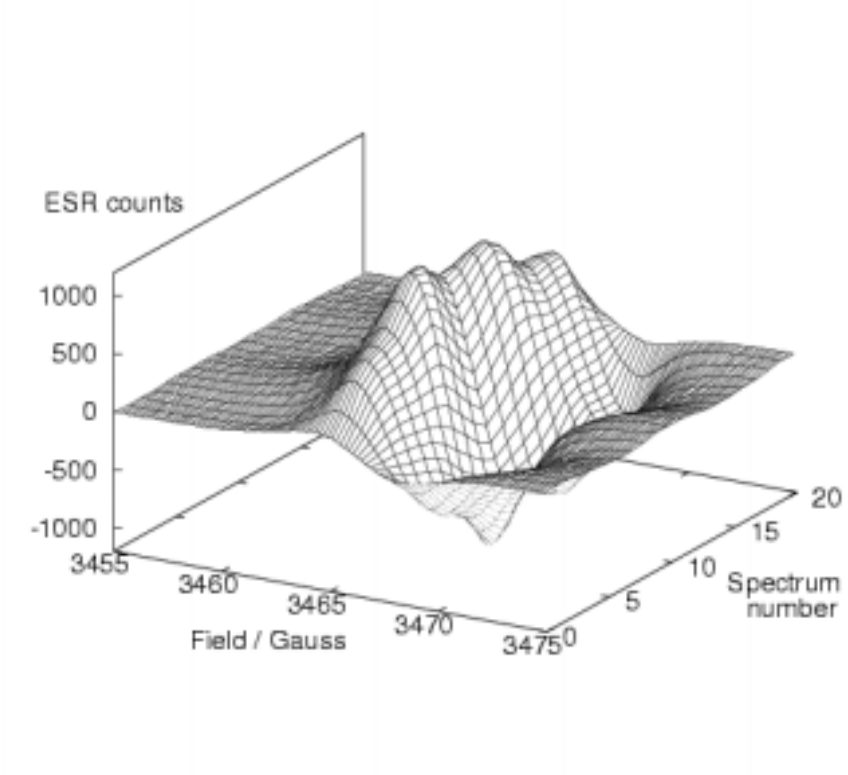

Fig. 3.14: In situ ESR spectra during p-doping (spectrum number 0-10) and dedoping (11-20) of PDTT3.

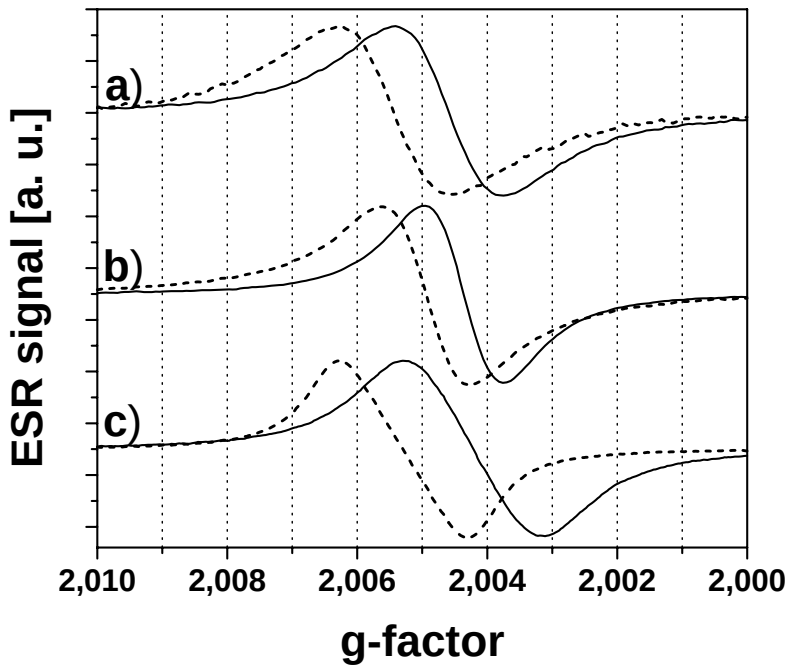

Fig. 3.15: in situ ESR spectra of *p*- (solid line) and *n*-doped (dotted line) PDTT1 (a), PDTT2 (b) and PDTT3 (c). Spectra are arbitrarily rescaled.

3.4 CONCLUSIONS

We have investigated the pristine and doped PDTTs, low band-gap polymers that undergo reversible electrochemical *p*- and *n*-doping as well as photodoping. In pristine PDTTs, the Raman modes mostly contributing to the ECC do undergo intensity redistribution as well as frequency dispersion by changing the exciting light frequency. This behavior can be taken as a vibrational signature of the enhanced quinoid character of the chain, which overcomes the π-electron confinement typical of simpler polythiophenes and lowers the polymer band-gap sizes. In doped PDTT1 and PDTT2, charge carriers of opposite signs show different spectral signatures while in doped PDTT3 no significant differences are observed. The spectral patterns are strongly affected by the different aromatic moieties fused to the thiophene rings forming the polythiophene-like chain. In particular, as their aromaticity increases and thus the polymer band-gap decreases, modes located within the fused moiety couple to the delocalized electron system along the polythiophene backbone.

With in situ ESR spectroelectrochemistry, paramagnetic charge carriers were observed upon both signs of doping. The spins of the positive carriers were found at g-factors higher than those reported for most of *p*-doped conjugated polymers. The spin of negative carriers exhibits a shift of the g-factors to even higher values as compared to the positive polarons. These results corroborate the conclusion that positively and negatively charged carriers within the same conjugated polymers may posses different structure and delocalization, as concluded from their vibrational spectroscopic signatures.

Table 3.1. Band assignment and wavenumber of Raman and IRAV modes. Wavelenghts are the Raman excitation lines; p, *p*-doping; n, *n*-doping; PIA, photodoping; w, weak; vw, very weak; sh, shoulder.

	PDTT1				
	$\nu(\alpha_1)$	$\nu(\alpha_2)$	$\nu(\alpha_3)$	$\nu(\alpha_4)$	$\nu(\alpha_5)$
457 nm	1501	sh	1303	-	vw
488 nm	1495	1440 sh	1300	-	vw
633 nm	1479	1437 sh	1298	-	/
1064 nm	1466	1422	1287	1237	≈ 850 w
p	1438 w	1361	1277	1205	-
n	1456 w	1385	1271	1207	-
PIA	sh	1361	1278	1206	-

	PDTT2								
	$\nu(\beta_1)$	$\nu(\beta_2)$	$\nu(\beta_3)$	$\nu(\beta_4)$	$\nu(\beta_5)$	$\nu(\beta_6)$	$\nu(\beta_7)$	$\nu(\beta_8)$	$\nu(\beta_9)$
457 nm	1502	1437	vw	-	vw	-	-	vw	vvw
514 nm	1490	1419	1295	-	1184	vw	vw	731	vw
1064 nm	1431	1395	1287	1237	1190	1086	866	743	658

	PDTT3							
	$\nu(\gamma_0)$	$\nu(\gamma_1)$	$\nu(\gamma_2)$	$\nu(\gamma_3)$	$\nu(\gamma_4)$	$\nu(\gamma_5)$	$\nu(\gamma_6)$	$\nu(\gamma_7)$
457 nm	1500	1473	1407	1355	-	-	-	646
514 nm	1495	1466	1402	1353	1331	-	-	646
633 nm	1485	1451	1402	1348	1325	-	-	/
1064 nm	1475	1422	1400 sh	1344	1318	1250 b	950-770	639
p (n)	1460	1401	-	1326	1287	1250-	950-	634
		1371				1120	770	

PIA	1469	1400	-	1330	1295	1250-	950-770	634
		1372				1120		

Table 3.2. IR bands of doped PDTTs. Numbers are wavenumbers, vs, very strong; s, strong; m, medium; w, weak; vw, very weak; el, electrolyte; p, *p*-doping; n, *n*-doping; PIA, photodoping.

PDTT1 p	PDTT1 n	PDTT1 PIA
1687vw		
1518w	1525	
1438 vw	1456	
1361 vs	1385 vs	1361
1309 vw	1315 w	
1277 vs	1271 vs	1278
1205 vs	1207 m	1206
1157 w	1153 w	1151
1122	1111 w	
		1078
	929 w	
899 w		
845 vs el		
	760 vw	756
669 w		
644 w		630

PDTT2 p	PDTT2 n	PDTT2 PIA
1456 w	1450 w	
1392	1402	
1356 m	1349 ms	1363
1307		1317
1279		1276
	1249 vs	
1217 vs		1225
1178 m		
	1147 vs	
1082 s	1068 s	1082
922 mv		
837 vs el		
733 s sh	723 w	
690 mw		
659 w	651 m	657

PDTT3 p	PDDT3 n	PDDT3 PIA
1460 w	1469 w	1469
1445 vw		
1401 m	1403 m	1400
1371m	1369 m	1372
1326	1329 m	1330
1287 m	1281 s	1295
1214 s	1221 vs	1226
1180 s	1176 s	1180
1139 s	1150	1140
	1110 s	
1020	1080 m	
940 w		941
	891 m	862
842 vs el		
778 w	764 m	777
721 w	700 w	
684 w	660 w	
634 s	630 s	634

Table 3.3. Position and line width of doped PDTTs ESR signals. p, *p*-doping; n, *n*-doping.

	PDTT1	PDTT2	PDTT3
g-factor p / n	2.0045 / 2.0054	2.0044 / 2.0049	2.0042 / 2.0052
$\Delta H_{P\text{-}P}$ (G) p / n	2.7 / 2.8	2.0 / 2.2	3.6 / 3.3

3.5. REFERENCES

1. Neudeck, A.; Petr, A.; Dunsch, L. *Synth. Met*. **1999**, *107*, 143.

2. Neudeck, A.; Petr, A.; Dunsch, L. *J. Phys. Chem. B.* **1999**, *103*, 912.

3. Rapta, P.; Petr, A.; Dunsch, L.; Ivaska, A. *Synth. Met*. **2001**, *119*, 409.

4. Petr, A.; Kvarnström, C.; Dunsch, L.; Ivaska, A. *Synth. Met*. **2000**, *108*, 245.

5. Arbizzani, C.; Catellani, M.; Cerroni, M. G.; Mastragostino, M. *Synth. Met*. **1997**, *84*, 249.

6. Pron, A.; Louarn, G.; Lapkowsky, M.; Zagorska, M.; Glowczyk-Zubek, J.; Lefrant, S. *Macromolecules* **1995**, *28*, 4644.

8. Agosti, E.; Rivola, M.; Hernandez, V.; Del Zoppo, M.; Zerbi, G. *Synth. Met*. **1999**, *100*, 101.

7. Louarn, G.; Trznadel, M.; Buisson, J. P.; Laska, J.; Pron, A.; Lapkowsky, M.; Lefrant, S. *J. Phys. Chem*. **1996**, *100*, 1232.

9 See ref. 16, p. 768 and pp. 799-800 (Raman lines B,C, D).

10. Catellani, M.; Lazzaroni, R.; Luzzati, S.; Brédas, J. L. *Synth. Met*. **1999**, *101*, 175.

11. Kvarnström, C.; Neugebauer, H.; Blomquist, S.; Ahonen, H. J.; Kankare, J.; Ivaska, A.; Sariciftci, N. S. *J. Mol. Struct*. **2000**, *521*, 271.

12. Kvarnström, C.; Neugebauer, H.; Blomquist, S.; Ahonen, H. J.; Kankare, J.; Ivaska, A.; Sariciftci, N. S. *Synt. Met*. **1999**, *101*, 66.

13. Neugebauer, H.; Kvarnstroem, C.; Cravino, A.; Yohannes, T.; Sariciftci, N. S. *Synth. Met*. **2001**, *116*, 115.

14. Neugebauer, H.; Kvarnström, C.; Brabec, C. J.; Sariciftci, N. S.; Kiebooms, R.; Wudl, F.; Luzzati, S. *J. Chem. Phys*. **1999**, 11039

15. Cravino, A.; Neugebauer, H.; Luzzati, S.; Catellani, M.; Sariciftci, N. S. *J. Phys. Chem. B* **2001**, *105*, 46.

16. See for instance Del Zoppo, M.; Castiglioni, C.; Zuliani, P.; Zerbi, G. In *Handbook of Conducting Polymers*, 2nd ed.; Skotheim, T. A.; Elsenbaumer, R. L.; Reynolds, J. R., Eds.; Marcel Dekker: New York: 1988; Chapter 28, and references therein.

17. Neugebauer, H.; Neckel, A.; Brinda-Konopik, N. In *Electronic Properties of Polymers and Related Compounds*; Kuzmany, H.; Mehring, M.; Roth, S.; Eds.; Solid State Sci. 63, Springer: Heidelberg, 1985; p.227.

18. Moses, D.; Dogariu, A.; Heeger, A. J. *Synth. Met*. **2001**, *11*, 19.

19. Schaffer, H. E., Heeger, A. J. *Solid State Commun*. **1986**, *59*, 415.

20. Kobayashi, M., Chen, J., Chung, T.-C., Moraes, F., Heeger, A. J., Wudl, F. *Synth. Met*. **1984**, *9*, 77.

21. Simmoneau, A.; Chauvet, O.; Molinié, P.; Froyer, G. *Synth. Met.* **1997**, *84*, 657.

22. M. Sebti, M.; Merlin, A.; Ghanbaja, J.; Billaud, D. *Synth. Met.* **1997**, *84*, 665.

23. Dyakonov, V.; Zorinyants, G.; Scharber, M. C.; Brabec, C. J.; Janssen, R. A. J.; Hummelen, J. C.; Sariciftci, N. S. *Phys. Rev. B* **1999**, *59*, 8019.

24. Chandrasekhar, P. *Conducting Polymers, Fundamentals and Applications. A Practical Approach*; Kluwer Academic: Norwell, 1999; pp. 315-322.

25. *Handbook of Conductive Molecules and Polymers*, 2nd ed.; Nalwa, H. S., Ed.; Wiley: Chichester, 1997; Vol. 3, Ch. 3.

26. Weil, J. A.; Bolton, J. R.; Wertz, J. E. Electron Paramagnetic Resonance, Elementary Theory and Practical Applications; Wiley: New York, 1994.

27. Salem, L. *The Molecular Orbital Theory of Conjugated Systems*; W. A. Benjamin: Reading, 1966; Ch. 5.

28. Mizoguchi, K.; Kuroda, S. In in *Handbook of Conductive Molecules and Polymers*, ed. Nalwa, H. S. vol. 3, p. 251, John Wiley & Sons, **1997**.

CHAPTER 4. ADVANCED MATERIALS FOR NON-COMPOSITE DONOR-ACCEPTOR SYSTEMS

4.1. INTRODUCTION

Different strategies to improve the processability of fullerenes and/or to achieve their intimate mixing with conjugated polymers have been proposed. To control the morphology within the photoactive layer and to obtain a predetermined nanoscopic phase-separated network, systems as diblock-copolymers (conjugated donor block plus fullerene-bearing block)[1] and conjugated oligomer-fullerene dyads have been prepared.[2-10] Recently, several groups have developed the so-called *double-cable* polymers approach. The work done in Linz on this novel class of functional materials is the subject of the next Section. Peeters et al. used an oligo(*p*-phenylene vinylene)-fulleropyrrolidine dyad to fabricate solar cells with efficiencies comparable to those of other previously reported "bulk-heterojunction" solar cells.[9] However, for several donor-acceptor dyads it was found that depending on a number of factors (e.g. polarity of the solvent, aggregation state, conjugation length of the donor unit, etc.) detrimental photoinduced energy transfer can compete with photoinduced electron transfer.[8-11]

In this part of the work, we investigated the conjugated oligomer-fullerene dyads oligo(*p*-phenylene vinylene)-fulleropyrrolidine OPV*n*-C_{60}[18] (*n* = 1-4, number of phenyl rings, see Fig. 4.1) as components in MDMO-PPV based solar cells. The idea of investigating OPV*n*-C_{60} as alternative to C_{60} and PCBM in MDMO-PPV *bulk-heterojunction* solar cells is based on the following considerations:

- the fullerene moiety of the dyads can act as acceptor with respect of the donor MDMO-PPV;
- the OPV*n*C_{60} chemical structure shows similarity to that of MDMO-PPV, which act as matrix. Therefore, a better compatibility and a higher miscibility between the polymer matrix and the added acceptor, leading to more glassy, more homogeneous *bulk-heterojunctions*, can be expected;

- the longer OPV*n*C_{60} (n = 3, 4) are colored, light absorbing molecules. This may results, via direct intramolecular electron transfer or energy transfer assisted process (antenna effect), in improved light-harvesting properties compared to MDMO-PPV/PCBM devices.

Moreover, pristine OPV*n*C_{60} posses different photophysical behavior. In the solid state, the longer terms of the series (n= 3, 4) undergo photoinduced electron transfer affording long-living charge separated states. On the contrary, the shorter terms (n= 1, 2) do not undergo, or undergo only to a very small extent, photoinduced electron transfer.[12] Thus, the comparison of these dyads as electron acceptor seems interesting to study the correlation between their photophysical properties and the charge generation and transport mechanism in operating photovoltaic devices.

4.2. OLIGO(*P*-PHENYLENE VINYLENE)-FULLEROPYRROLIDINE DYADS AS ELECTRON ACCEPTOR COMPONENT IN MDMO-PPV BASED PLASTIC SOLAR CELLS

Photovoltaic devices were prepared on poly(ethylene terephtalate) foils covered with patterned indium-tin oxide (ITO) as transparent electrode. First, the substrate was covered with Baytron-P to obtain a smooth surface and prevent shunts. Then, one, two or three layers of the donor-acceptor blend were deposited from toluene solution. All organic layers were cast by the doctor blade technique. Thin stripes of aluminum as counter electrodes were deposited by thermal evaporation to form active areas of 5 mm^2.

Figure 4.2 displays the AFM images of the surface of MDMO-PPV/OPV_2C_{60} (a) and MDMO-PPV/PCBM (b) blend films, cast by doctor blading from toluene. The images show clearly that the blending behaviour of OPV2C_{60} is much superior than that of PCBM. Very similar results were obtained with the other terms of the dyad series. Based on this striking surface difference, it is reasonable to assume also a more glassy,

uniform morphology (less phase separation) within the MDMO-PPV/OPV*n*C_{60} bulk-heterojunctions as compared to the MDMO-PPV/PCBM one.[13]

The I/V characteristics of the devices are collated in Table 4.1. Considering the three layer devices, in which shorts due to pin-holes are reasonably prevented, a clear trend is observed: the longer the OPV*n*- moiety, the lower is the I_{SC}. The linear plots of the typical I/V curves for the three layer devices (area of 0.05 cm^2) are shown in Fig. 4.3. The devices were characterized in dark and under white-light illumination from a halogen lamp (~ 65 mW/cm^2). The I/V curves were found reversible. In dark, the devices made with OPV1C_{60} and OPV2C_{60} (the shorter terms) show a diode behaviour. However, the rectification ratio between -2 and +2 V is limited to approximately 10. Conversely, almost no diode behaviour is observed with the longer terms OPV3C_{60} and OPV4C_{60}. Under ~ 65 mW/cm^2 white-light illumination the I_{SC} values varies from ca. 65 μA for OPV1C_{60} to ca. 6 μA for OPV1C_{60}. The V_{OC} values range from 700 up to 800 mV, slightly increasing with the length of the OPV*n* moiety. All curves show rather low filling factor (FF), defined as $(I_{max}\times V_{max})/(I_{SC}\times V_{OC})$ where I_{max} and V_{max} are corresponding to the point of maximum power output.

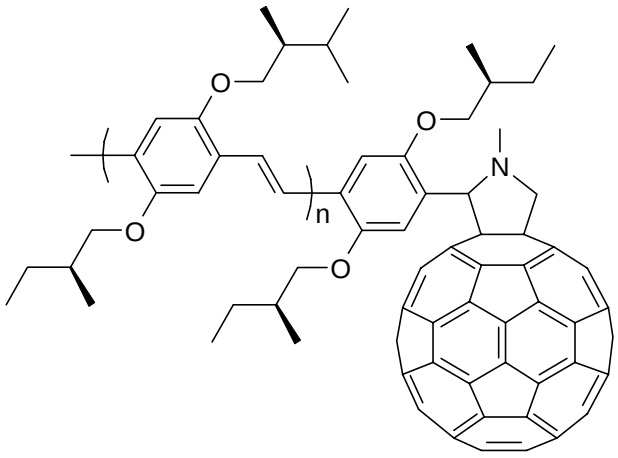

Fig. 4.1: Chemical structure of OPV*n*C_{60}

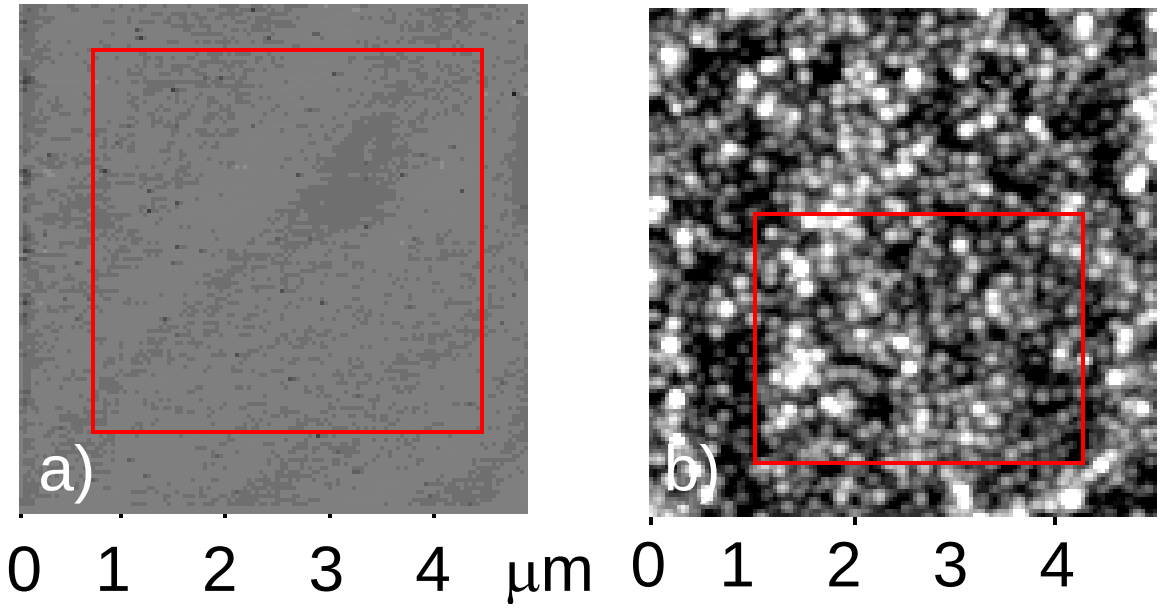

Fig. 4.2 AFM pictures of the surface of (**a**) a MDMO-PPV/OPV2C_{60} blend and, for comparison, (b) a MDMO-PPV/PCBM blend.

Table 4.1: I/V characteristics of OPV*n*C_{60} devices.

OPVnC$_{60}$	**1 layer**	**2 layers**	**3 layers**
n= 1	**600 mV** **45 μA**	**550-650 mV** **> 100 μA**	**650-750 mV** **ca. 65 μA**
n= 2	**750 mV** **40 μA**	**700 mV** **25 μA**	**760-770 mV** **28 μA**
n= 3	**700 mV** **25 μA**	**700 mV** **25 μA**	**780 mV** **11 -14 μA**
n= 4	**700-750 mV** **30 μA**	**760 mV** **15 μA**	**780-800 mV** **6 μA**

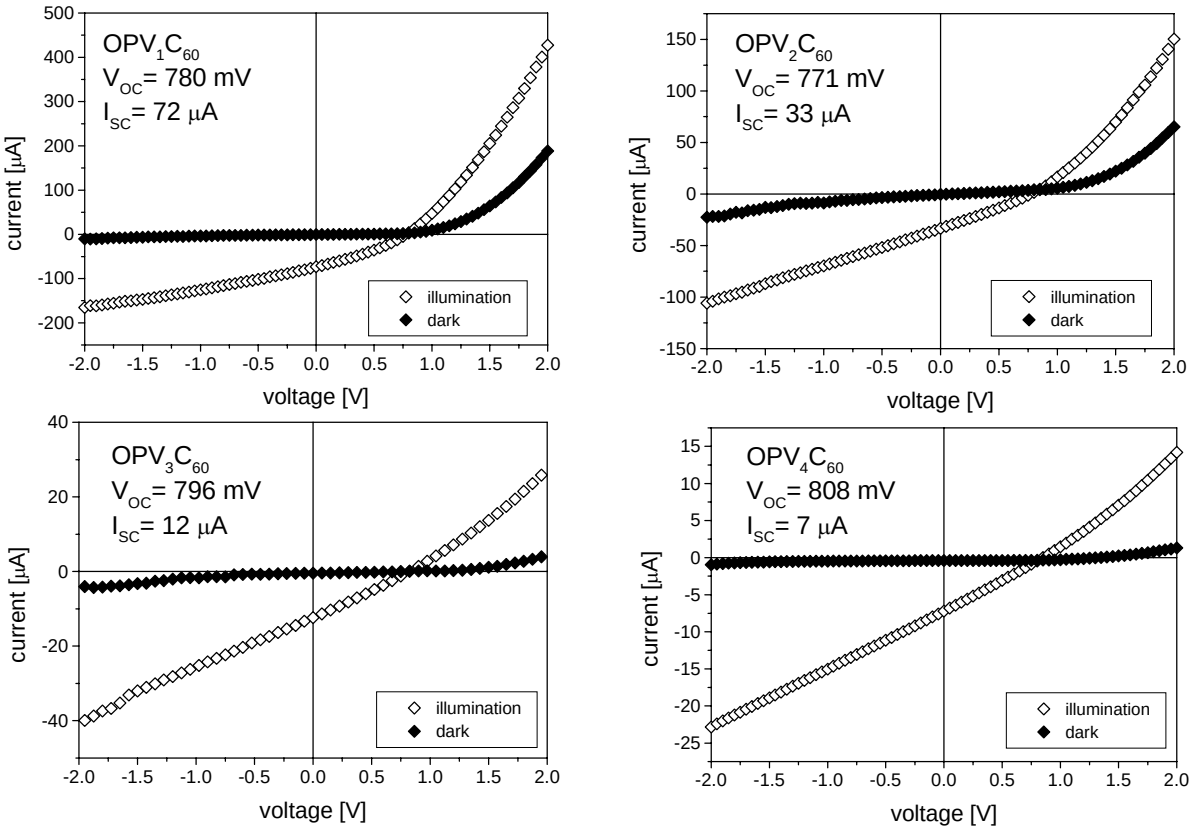

Fig. 4.7: I/V curves of MDMO-PPV/OPV*n*C_{60} devices.

Altough all OPV*n*C_{60} dyads show the same blending behaviour, the highest I_{SC} currents are obtained using OPV1C_{60}. This is suggesting that the photophysical properties of the dyad may play the major role: the performance of MDMO-PPV/OPVn-C_{60} devices may likely be influenced by the occurrence of an intramolecular photoinduced electron transfer between the donor and acceptor moieties *within* the dyad, enhancing carriers recombination. Indeed, OPV4-C_{60} gives the less efficient devices due to the low values of the I_{SC} while OPV1-C_{60}, in which intramolecular photoinduced electron transfer does not occur,[12] seems to be attractive for further investigations aimed to the

optimization of such type of devices. The solar cells prepared with this dyad showed better performance than those made as reference, using the standard MDMO-PPV/PCBM blend (typical values for these latter devices were: V_{OC} ~ 700 mV, I_{SC} ~ 60 μA, two layer devices). In conclusion, we have prepared *bulk-heterojunction* solar cells with MDMO-PPV/OPV*n*C_{60} blends as photoactive layer. It seems that the use of dyads that undergo photoinduced electron transfer (OPV4C_{60}, OPV3C_{60} and OPV2C_{60}) affect the devices performance reducing the I_{SC} values. On the contrary, OPV1C_{60}, which does not undergo photoinduced electron transfer, can be used as valid alternative to C_{60} and PCBM. As described in the next Section, these results suggest the investigation of the so-called *double-cable* polymers as material with intrinsic and well defined electron donor/acceptor properties.

4.3. TOWARDS "MOLECULAR HETEROJUNCTION": DONOR-ACCEPTOR *DOUBLE-CABLE* POLYMERS

As discussed in the previous section, although dyads may provide a simple method to achieve dimensional control over the phase separation in donor-acceptor networks, effects like photoinduced energy transfer and eventually a fast charge carriers recombination can turn out as severe limitations for real photovoltaic applications. Indeed, photoinduced energy transfer is currently a well known phenomenon in several donor-acceptor dyads. The results discussed in the previous chapter suggest that the use of dyads capable of intramolecular charge transfer enhances geminate carrier recombination, too. Since on dyads separated charges can escape recombination only by intermolecular hopping, this appears plausible. On the contrary, in systems with a long conjugated donor backbone bearing a number of acceptor moieties - the so-called *double-cable* polymers introduced before - it can be expected that holes migrate away from electrons by a very fast intrachain diffusion process[14], preventing recombination. Therefore, *double-cable* polymers appear very interesting as materials that may retain the favourable electronic and photophysical properties of conjugated polymer/fullerene composites but in which phase separation and clustering phenomena cannot occur.

A "bulk-heterojunction" (a) (where the occurrence of acceptor clustering is emphasized for clarity), an ordered ideal *double-cable* polymer chain (b), and a picture in which the continuous pathway for the transport of electrons is given by the contacts between acceptor moieties on different polymer chains (c) are schematically depicted in Fig. 5.4. Besides other aspects like the relative positioning of the polymer chain and the acceptor moieties, as well as the positioning of an acceptor moiety with respect of its neighbours (and chain to chain), a *double-cable* polymer for PV application must meet the following requirements:

- mutually independent ground-state electronic properties of the donor backbone and of the acceptor moieties ("the cables must not short");

- a photoinduced electron transfer from the electron-donating backbone onto the electron-accepting moiety, leading to metastable long-living charged states, as a prerequisite for photogeneration of free charge carriers.

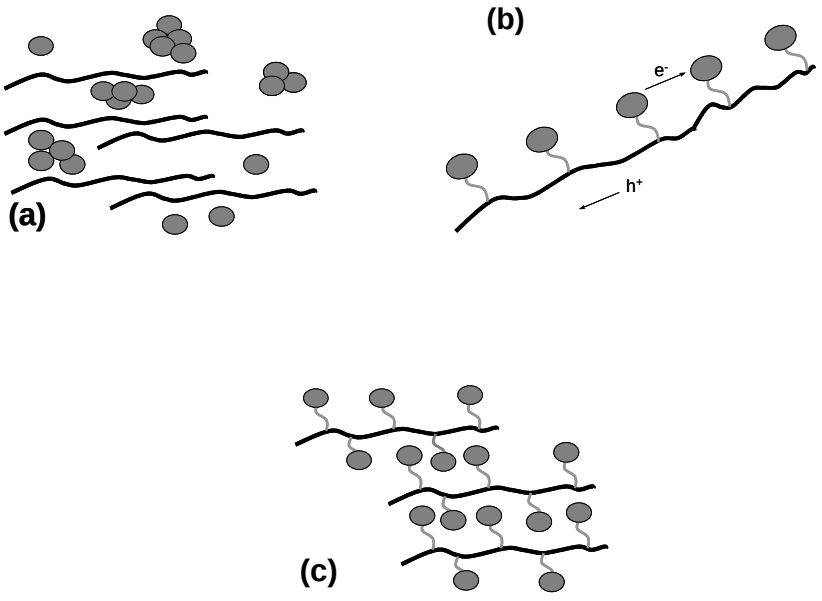

Fig. 5.4 a) Schematic representation of a "bulk-heterojunction". Clustering of the fullerene component is emphasised. **b)** An ideal, ordered *double-cable* polymer and **c)** a more realistic picture where interchain interactions are considered.

- In addition, solubility in common organic solvents is also a determinant factor, since the easy and cost-effective preparation of thin film devices involves processing from solutions.

4.3.1 Electrochemically synthesised *double-cable* polymers

A route towards the preparation of conjugated polymers is the electropolymerisation of suitable aromatic monomers.[15,16] Therefore, it is not surprising that several attempts to the preparation of novel and exotic conjugated polymers, some of them carrying electroactive moieties,[17] are made synthesising molecules specifically designed as substrates for electropolymerisation.[16] Moreover, electropolymerisation allows for the growth of polymeric thin films onto transparent electrodes suitable for most spectroscopic techniques. This is a clear advantage when solubility of a novel conjugated polymer cannot be obtained or could not be expected. As already pointed out, it has been observed that in molecular donor-acceptor dyads photoinduced energy transfer can take place competing with intramolecular charge transfer, and geminate recombination may also be enhanced. At *priori*, similar effects cannot be excluded in *double-cable* polymers. Therefore, for the design of materials and supramolecular structures for photovoltaic materials,[18] the electrochemical approach has been selected as a first step towards *double-cable* polymers as well as for the study of their electronic and photophysical behaviour.

4.3.1.1. Polythiophene bearing "TCAQ" type moieties

a) Electrosynthesys and electrochemical properties

A novel electron donor-acceptor *double-cable* polymer was prepared electrochemically starting from monomer **UCM6**, in which a TCAQ moiety is linked to a bithiophene unit through a flexible spacer (Fig. 5.5). To serve as reference for the spectroscopic investigations monomer **a** was also polymerized in the same wa as

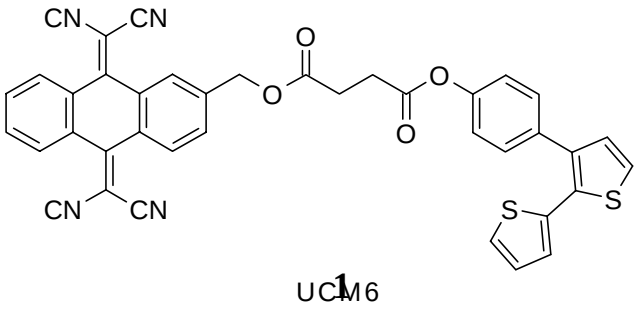

1

UCM6

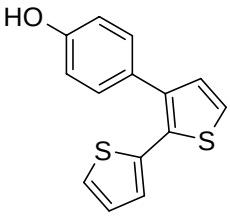

a **2**

Fig. 5.5: Chemical structures of the monomers **UCM6** and **a**.

UCM6 (Fig. 5.5). Both polymeric compounds form, on the ITO coated substrates, red colored films of excellent quality.

Fig. 5.6(a) shows the cyclic voltammogram taken during the polymerization process of **UCM6** by sweeping the potential between 0 and +1.3 V, the latter being just above the threshold for its the irreversible oxidation. The formation of the polymer can be seen by the growing redox wave centered at about 0.8 V, which corresponds to the oxidation/re-reduction of the polymeric backbone. Fig. 5.6(b) shows the cyclic voltammogram of a poly(**UCM6**) film in monomer free electrolyte solution in the potential range from –0.8 to +1.3 V. The cathodic region of the voltammogram shows only one wave, which is due to the reversible reduction of the TCAQ moiety at –0.30 V.[19] In the anodic region the voltammogram shows one reversible wave centered at +0.62 V, which corresponds to the well known oxidation/re-reduction of the polythiophene backbone.[20] The cyclic voltammogram shown in Fig. 5.6(b) is not

completely reversible: after a number of 100 potential sweeps the peak current values of all features were reduced by 50%

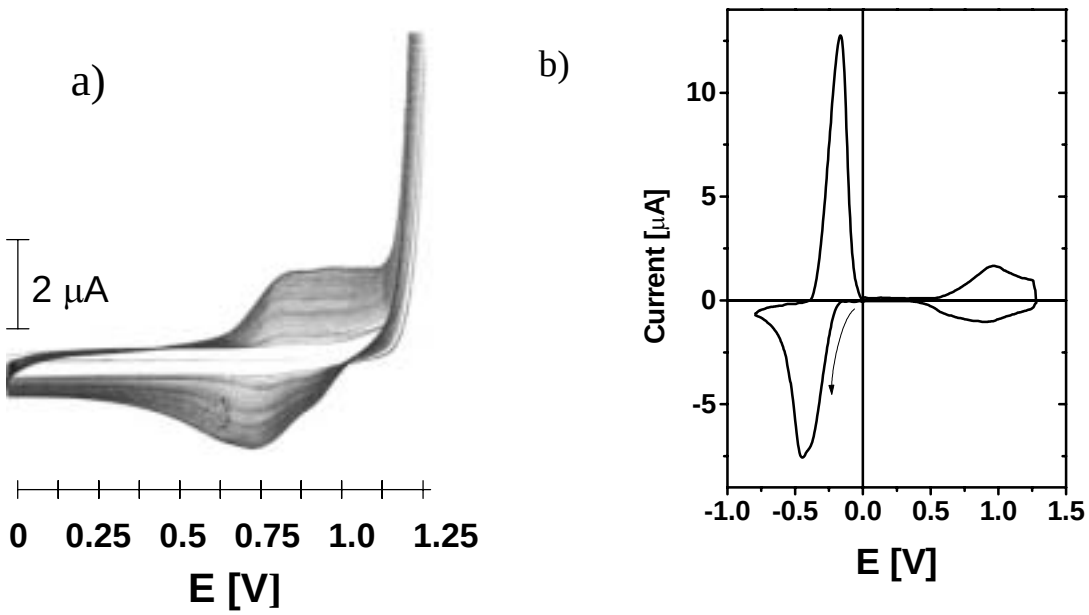

Fig. 5.6: Cyclic voltammograms taken during **a**) the electropolymerization process of **UCM6** on an ITO-coated glass electrode and **b**) the electrochemical oxidation and reduction of a film of poly(**UCM6**) on an ITO-coated glass electrode in a monomer free electrolyte solution. Potential vs. Ag/AgCl, sweep rate 0.1 V/s.

b) UV-Vis absorption spectroscopy

Fig. 5.7 shows the optical absorption spectra of a drop cast film of monomer **UCM6** along with that of an electropolymerized film of neutral poly(**UCM6**). For comparison Fig. 5.7 also shows the absorption spectrum of poly(**a**), prepared as a reference sample (see Fig. 5.5). The absorption spectrum of monomer **UCM6** has an onset around 430 nm and a maximum at 350 nm, which corresponds to the lowest electronic transition of the TCAQ unit.[19] The electropolymerized sample poly(**UCM6**) also shows the same UV absorption band at 350nm. In addition to this a rather broad band with a maximum around 490 nm and a long tail extending to 650 nm appears in the polymer spectrum, which is assigned to the π-π*-transition of the extended π-

electron system. Further confirmation for the assignment given above comes from the absorption spectra of the reference poly(**a**) (Fig. 5.7). Its spectrum consists essentially of only one rather broad band with a maximum around 530 nm, typical of polythiophenes with relatively low band-gap. As expected, the 350 nm peak attributed before to the TCAQ absorption is missing. The 40 nm blueshift of the π-π*-absorption peak of poly(**UCM6**) as compared to poly(**a**) is understood as due to a shortening of the effective conjugation length in the former. This shortening of the effective conjugation length in poly(**UCM6)** may be explained by steric hindrance caused by the TCAQ side groups or by the lower solubility of **UCM6** (and its oligomer intermediates involved in the electrochemical polymerization process) compared to **a**, leading to a lower molecular weight for electrochemically prepared poly(**UCM6**). In principle, the difference in the absorption spectra of poly(**UCM6**) and poly(**a**) can also be due to the *para*-hydroxyphenyl groups in the latter, which may donate more electrons into the conjugated backbone, reducing the band-gap.

Fig. 5.8 shows the UV-Vis absorption spectra of films of poly(**UCM6**) in the electrochemically oxidized and reduced states. Electrochemical oxidation at a potential of 1.0 V effects only the polythiophene backbone of this *double-cable*. A new absorption band between 700 and 900 nm grows on the expense of the 490 nm π-π* absorption, which is reduced relative to the TCAQ absorption at 350 nm. Oscillator strength is transferred from the neutral polymer to the polymer in-the-gap absorption, probably of polaronic origin, in the near-IR spectral range. On the other hand, the electrochemical reduction effects only the TCAQ moiety of the *double- cable.* This can be seen by the decrease of the intensity of the 350 nm absorption band of neutral TCAQ

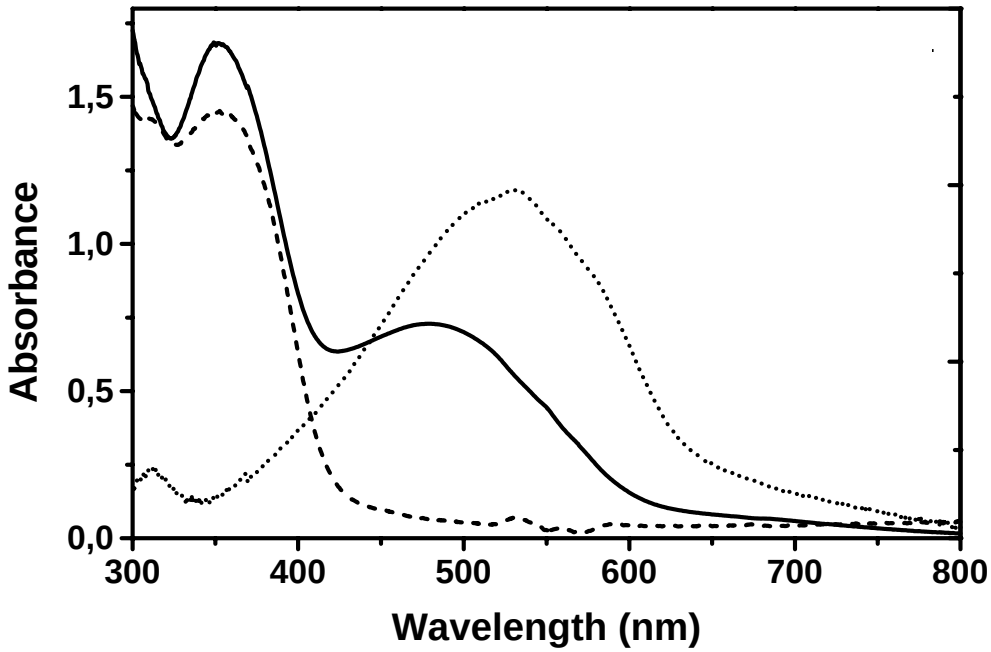

Fig. 5.7:UV-Vis absorption spectra of films of monomer **UCM6** (dashed line), poly(**UCM6**) (solid line) and poly(**a**) (dotted line).

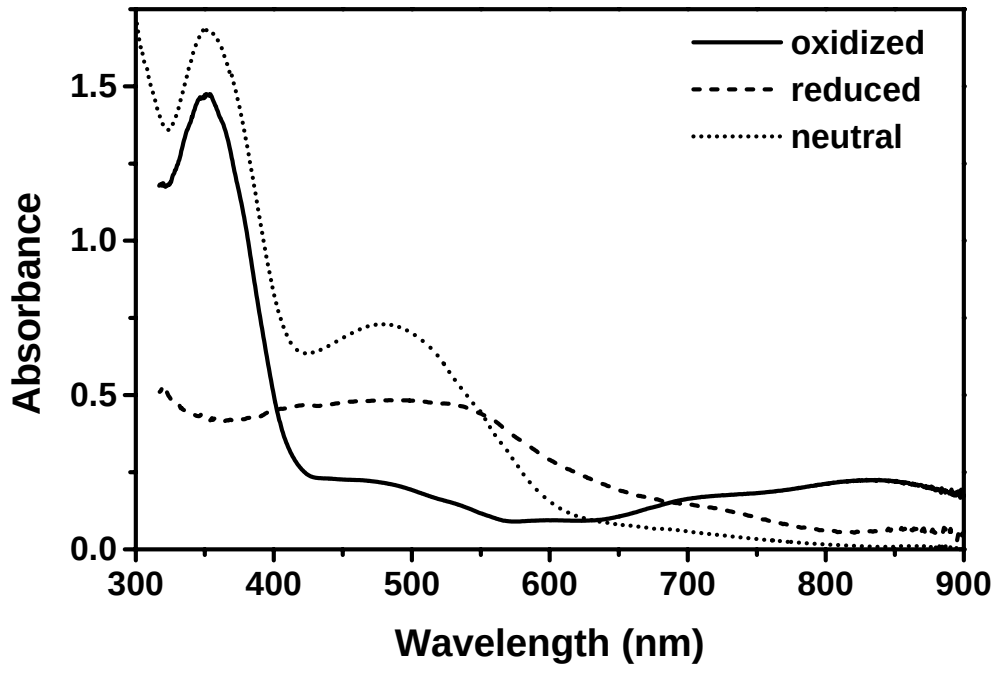

Fig. 5.8: UV-Vis absorption spectra of thin films of poly(**UCM6**) in different oxidation states: neutral polymer (dotted line), oxidized polymer (solid line), reduced polymer (dashed line).

and the enhancement of the absorption in the 550-600 nm range due to the formation of TCAQ radical-anions and dianions.[19]

c) Photoinduced electron transfer

Fig. 5.9(a) shows a comparison of the photoinduced absorption (PIA) spectra of films of monomer **UCM6** and of poly(**UCM6)**. The PIA spectrum of the monomer excited in the UV at 351 nm shows mainly one peak at 1.15 eV and a shoulder rising against 2.0 eV. Both photoinduced features may be assigned to radical anions of the TCAQ unit.[19] The PIA spectrum of poly(**UCM6**) consists of some new bands in addition to the TCAQ radical anion features observed already for the monomer: one at around 1.5 eV as a plateau and another one peaking below 0.6 eV. Both of these absorption features are assigned to charged excitations on a thiophene based conjugated backbone as observed in polythiophene before.[21] The high and low energy absorption bands of polarons of long oligothiophenes ($n \geq 9$) are around 1.5 eV and below 0.5 eV, respectively.[22] Also shown in Fig. 5.9(a) is the absorption spectrum of the electrochemically oxidized poly(**UCM6**) in the Vis-NIR spectral range, which further supports the assignment we made for the PIA spectrum of the neutral poly(**UCM6**). Electrochemical oxidation (*p*-doping) results mainly in two broad absorption peaks at 1.5 eV and below 0.6 eV and gives further evidence that the peaks in the photoinduced absorption spectra have charged excitations - of polaronic nature - as origin.

For additional clarification of the assignment given above a fit of a sum of four Gaussian curves to the PIA spectrum of poly(**UCM6**) is shown in Fig. 5.9(b). The two Gaussian curves with maxima at 1.15 eV and above 2 eV represent the TCAQ anion radical absorption and the other two curves peaking at 1.5 eV and below 0.6 eV correspond to the polaronic absorption of the polymer. The sum of these four Gaussians yields a rather good agreement with the PIA spectrum of poly(**UCM6**) in Fig. 5.9(a).

Excitation intensity and modulation frequency dependencies[23,24] of the PIA signals of poly(**UCM6**) are shown in Fig. 5.10. All PIA features exhibit a square root excitation intensity dependence suggesting a bimolecular recombination kinetics. As already

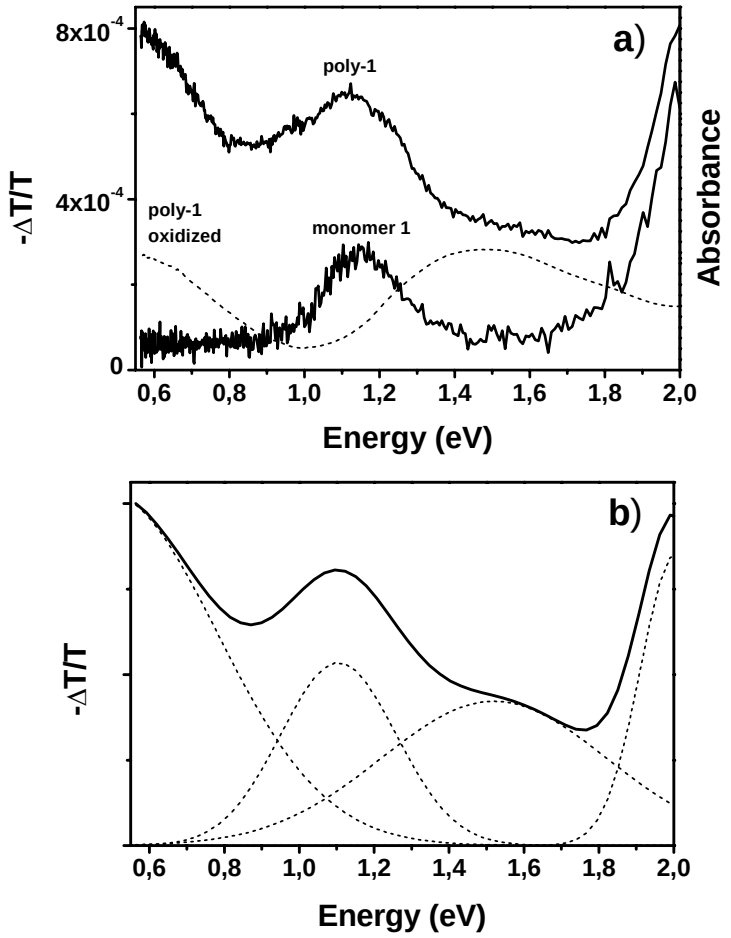

Fig. 5.9: **a**) spectra of monomer **UCM6** excited at 351 nm (lower trace, left hand axis) and poly-**1** excited at 476 nm (upper trace, left hand axis) compared to absorption spectrum of a electrochemically oxidized poly(**UCM6**) (dashed line, right hand axis). **b**) Fit to the PIA spectrum of poly(**UCM6**) by sum of four Gaussians. Sum of Gaussian peaks (solid line), single Gaussian peaks (dashed lines).

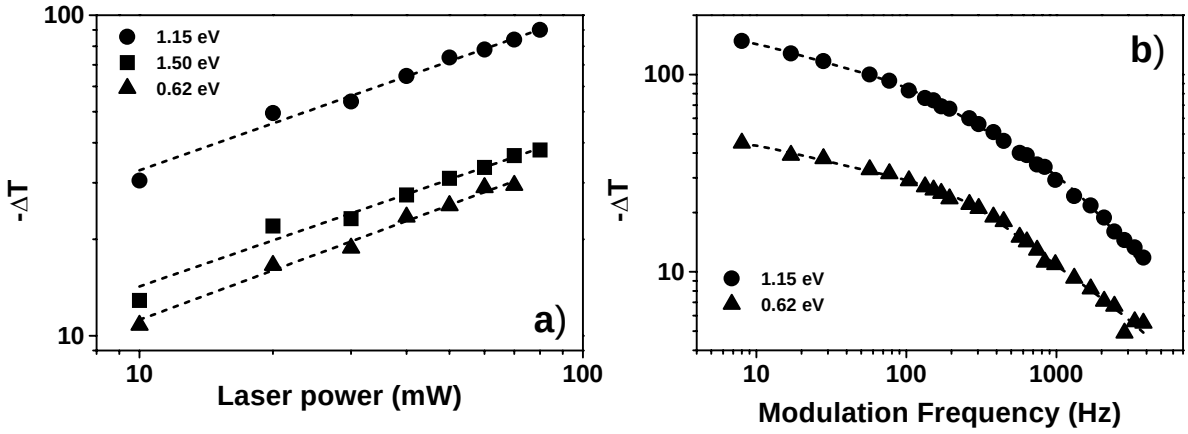

Fig. 5.10: PIA spectrum of poly(**UCM6**): **a**) excitation intensity dependence, **b**) modulation frequency dependence of PIA signal at 0.62 eV (triangles), 1.15 eV (circles), 1.5 eV (squares).

shown for the modulation frequency dependence of polaronic absorption peaks on different kinds of conjugated polymers, a broad distribution of lifetimes of the charged states is observed. A series of three time constants between some 100 microseconds up to tens of milliseconds has to be assumed for best fitting the measured relaxation kinetics.[25]

Electron spin resonance spectra of poly(**UCM6**) are shown in Fig. 5.11. The polymer films already show a very strong dark ESR signal, consisting of broad lines with *g*-values of around 2.0026 . Those lines could origin from a residual doping on the polymer backbone due to the electropolymerization process. Light induced ESR gives rise to a single broad line centered at a *g*-value of 2.0029, but with only 15% of the intensity of the dark signal. The LESR signal may be assigned to an overlap of the two close lying lines from the TCAQ anion and polymer cation radicals produced by the photoinduced charge transfer. Both TCAQ anions and oligothiophene cations are known

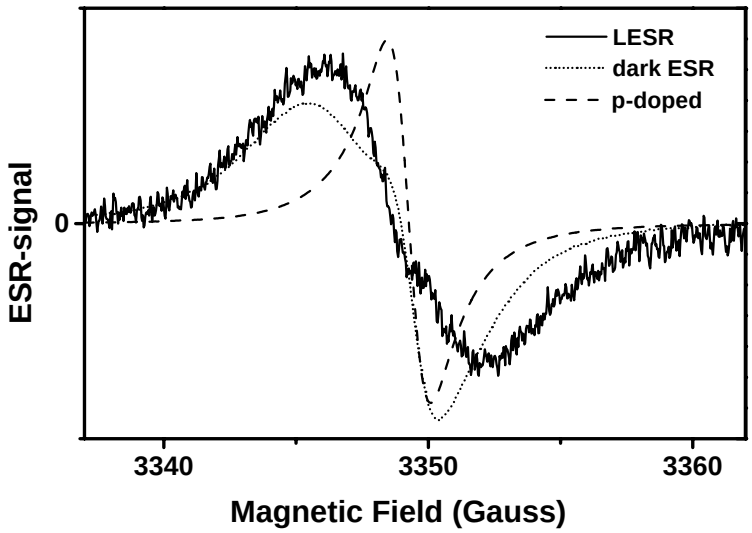

Fig. 5.11: ESR spectra of poly(**UCM6**) at 100 K. Dark ESR spectrum (dotted line), light induced ESR (LESR) spectrum (solid line), ESR of electrochemically p-doped polymer (dashed line).

to have g-factors in the range between 2.0023 and 2.0028.[19,22] A single line ESR spectrum is observed for an electrochemically oxidized poly(**UCM6**) sample. The *g*-factor is 2.0026, close to that observed commonly for radical cations of conjugated

polymers and the linewidth is narrower by a factor of 2 as compared to the light induced signal.[25,26] This narrowing of ESR line for heavily oxidized conducting polymers has been studied and interpreted as due to motional as well as exchange narrowing of a large number of mobile polarons.[27]

4.3.1.2. Polythiophene bearing fullerene moieties

a) Electrosynthesis and electrochemical properties

Even though the search for electron accepting components alternative to fullerenes is of chemical and technological interested, the results so far obtained indicates fullerenes as specially interesting functional materials.[28] Moreover, polythiophene/fullerene mixtures have been already employed for the preparation of prototype *bulk heterojunction* solar cells,[29-31] suggesting the investigation of *double-cables* consisting of a polythiophene backbone with covalently linked fullerene units. Benincori and coworkers and Ferraris and coworkers showed that such fullerene substituted polythiophenes mostly retain the favourable ground state properties of the individual polymer and fullerene moieties.[32,33] However, the occurrence of photoinduced electron transfer in this fullerene functionalized polymers was not reported. Therefore, we designed the novel bithiophene-fulleropyrrolidine dyad **1** (Fig. 5.12) as monomer for the electrochemical preparation of a polythiophene/fullerene *double-cable*. Compound **1** combines solubility and the superior electropolymerisability of bithiophenes[20] and gives a *double-cable* polymer that is heavily loaded with fullerene

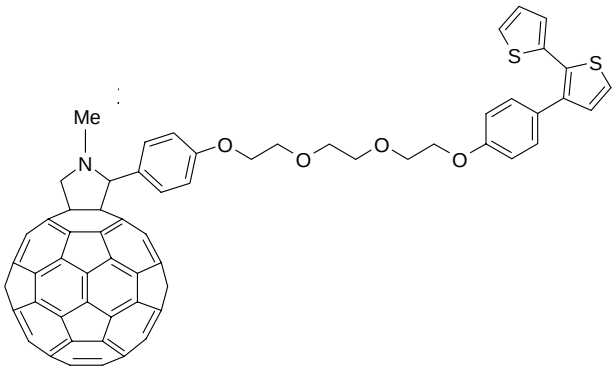

Fig. 5.12: Chemical structure of the bithiophene-fulleropyrrolidine **1**

electron conducting moieties. The cyclic voltammogram of **1**, recorded during potential cycling between 0 and 1.6 V, is illustrated in figure 5.13 (Pt as working electrode, CH_2Cl_2). The first scan shows one irreversible wave peaking at ca. +1.3 V, corresponding to the oxidation of the monomer. Recurrent potential scanning leads to the growth of a new redox wave around +0.8 V, related to the oxidation/rereduction (*p*-doping/dedoping) of a freshly formed polymeric film. Similar results were obtained using different solvents (CH_3CN/toluene mixtures) and ITO coated electrodes. Poly(**a**) (see Section 4.2.1.1.) was again used as a reference.

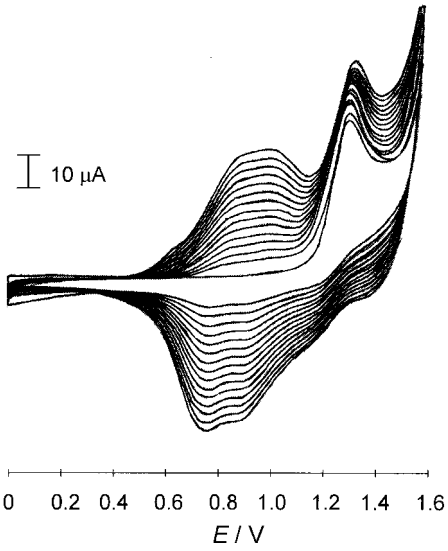

Fig. 5.13: CV of **1** (0.1 M Bu_4NPF_6 in CH_2Cl_2). Working electrode: Pt foil; reference electrode: quasi Ag/AgCl wire (-0.44 vs. Ferrocene). Scan rate 100 mV/s.

Figure 5.14 displays the cyclic voltammogram of poly(**1**) in monomer-free electrolyte solution. In the positive region, one wave, which corresponds to the *p*-doping/dedoping of the polythiophene backbone, is seen at about +0.75 V. The linear relationship between the maximum current peak and the scan rate (varied from 25 to 200 mV/s) can be seen in figure 5.15. This linear relationship is typical of a redox-active polymer attached to the electrode and also exemplifies the stability of poly(**1**) films towards p-doping.[15] Scanning the cathodic region up to -2.0 V shows several redox waves mainly related to the multiple reduction of the fullerene moiety.[34] The irreversible peak at -0.74 V, of unknown origin, is seen only during the first scan. These

results indicate that both the polythiophene backbone and the pendant fullerene moieties basically retain their individual electrochemical properties ("the cables do not short"). In contrast to the results found for *p*-doping, the reduction of the fullerene moieties leads to changes of the cyclic voltammogram and loss of electroactivity (Fig. 5.16). This loss of electroactivity upon scanning negative potentials also affects a subsequent *p*-doping process. Considering that the polymers is heavily loaded with acceptor moieties, the dissolution of the highly negatively charged material by the polar electrolyte medium, associated to morphological changes in the film structure, cannot be excluded.

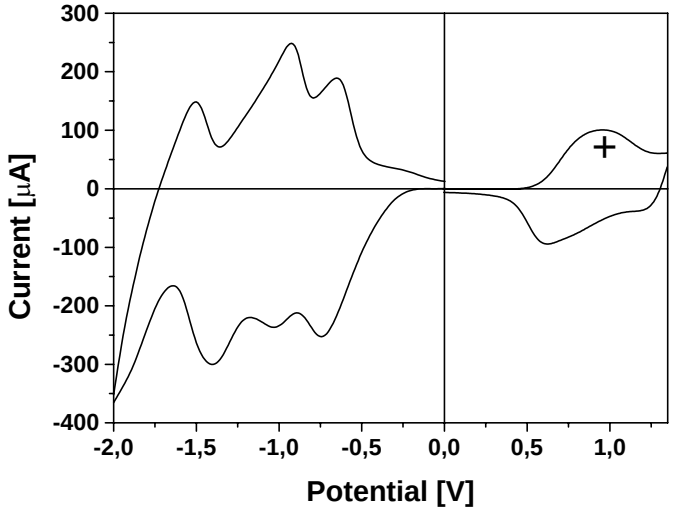

Fig. 5.14: CV of poly(**1**) on Pt foils (0.1 M Bu_4NPF_6 in CH_3CN). Reference electrode and scan rate as in Fig. 5.13.

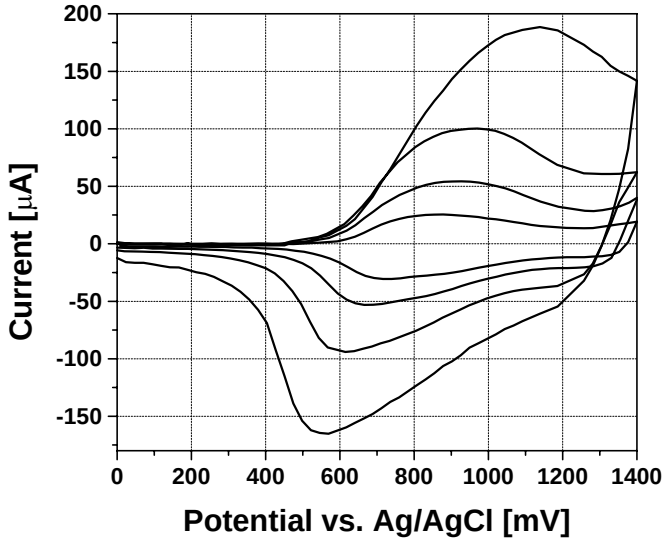

Fig. 5.15: CV (*p*-doping) of poly(**1**) at a scan rate of 25, 50, 100 and 200 mV/s.

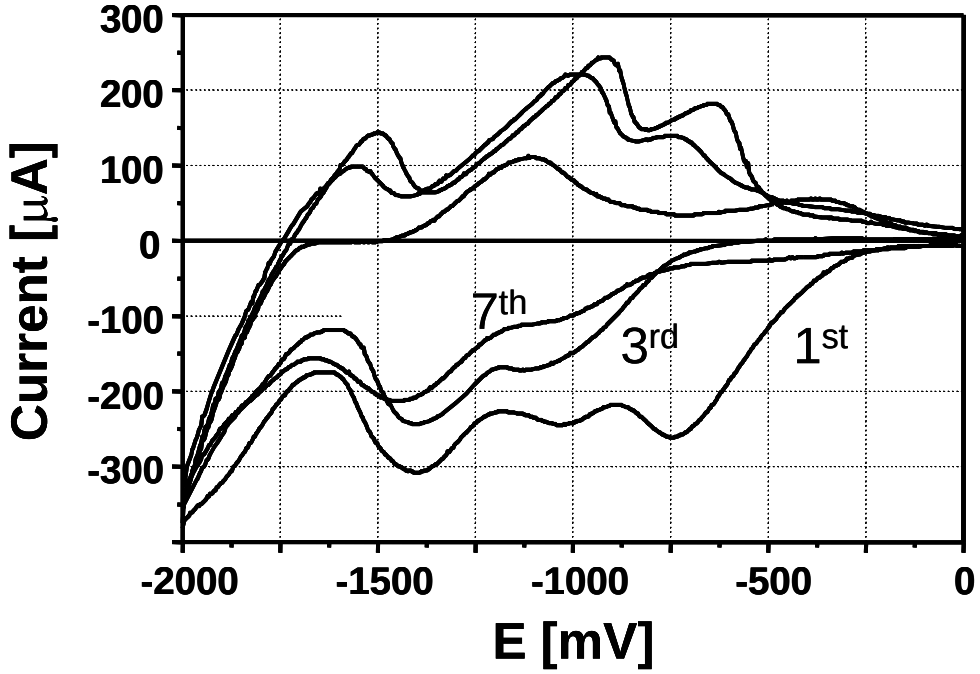

Fig. 5.16: CV (reduction) of poly(**1**). Scan rate 100 mV/s. First, third and seventh scan.

b) UV-Vis absorption spectroscopy

After dedoping by keeping the potential at 0 V, yellow-brownish and non-luminescent films were obtained. Their typical UV-Vis absorption spectrum is shown in figure 5.17 For comparison, figure 5.17 shows also the absorption spectrum of the reference poly(**a**). The build-up of a conjugated system in poly(**1**) is confirmed by the broad absorption feature ranging from about 600 nm to the ITO-glass cut-off at around 300 nm, in which the π-π* transition is seen by the shoulder at about 460 nm. As already observed for poly(**UCM6**), this value is considerably blue shifted as compared to reference polymer poly(**a**). Such a blue-shift, observed also in another electrochemically prepared double-cable polymer,[32] is proposed to originate from the shortening of the effective conjugation length in poly(**1**). As in the previous case, this effect may be explained by steric hindrance due to the bulkyness of the fullerene substituents or again by the lower solubility of monomer **1** (and its oligomer intermediates involved in the electrochemical polymerization process), leading to a lower molecular weight for electrochemically prepared poly(**1**). As will be discussed in

the following, the latter explanation is corroborated by IR measurements. According to the electrochemical characterization, no hints for ground-state donor-acceptor interactions are observed.

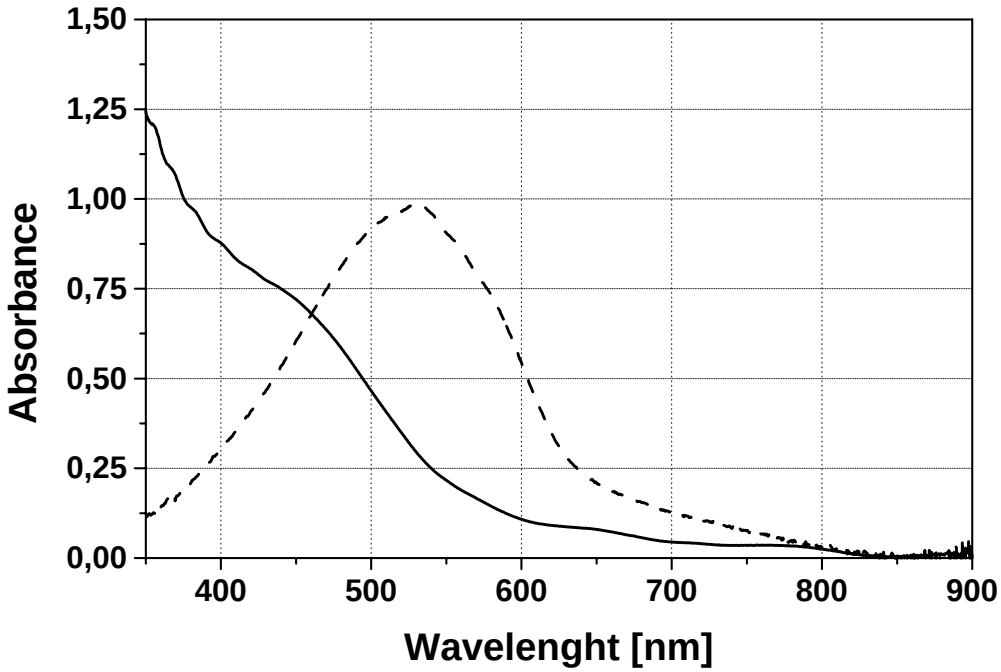

Fig. 5.17: UV-Vis absorption spectra of poly(**1**) (solid line) and poly(**a**) (dashed line).

c) Photoinduced electron transfer

The nature of the photoexcitation in poly(**1**) was investigated by means of photoinduced absorption in the Vis-NIR. The PIA spectrum, taken with excitation at 476 nm, is shown in figure 5.18. Two bands are observed, one with maxima at 1.48 eV and one peaking below 0.6 eV. Both these absorption features might be assigned to positively charged excitations, widely accepted to be polarons, of a thiophene based conjugated backbone.[21,22] In order to shed light into the relaxation kinetics of the photoexcitations, we have performed intensity and modulation frequency dependence measurements (Fig. 5.19).[23,24] Both PIA features, evaluated by the signal at 1.38 and 0.62 eV, show a square root excitation intensity dependence, thus indicating bimolecular recombination kinetics as commonly observed for charge carriers in

conjugated polymer/fullerene blends.[25] From the modulation frequency dependence, a broad distribution of charged state lifetimes is observed. The best fit has been obtained using three τ values, in the range from 0.8 to 10 ms.

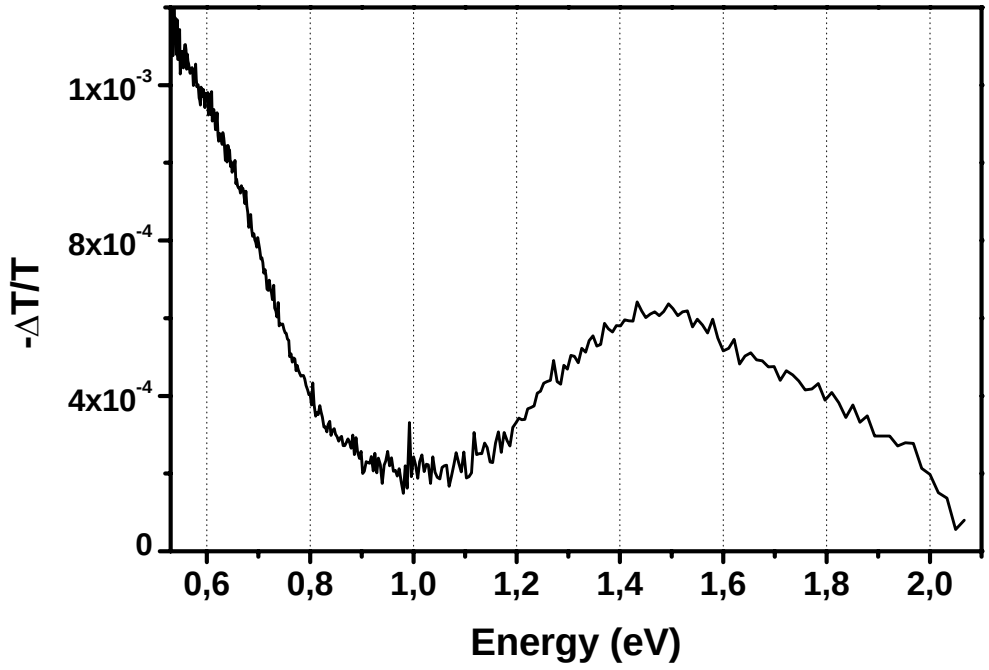

Fig. 5.18: Photoinduced Vis-NIR absorption spectrum of poly(**1**). Excitation at 476 nm (40 mW on a 4 mm diameter spot). T = 100 K.

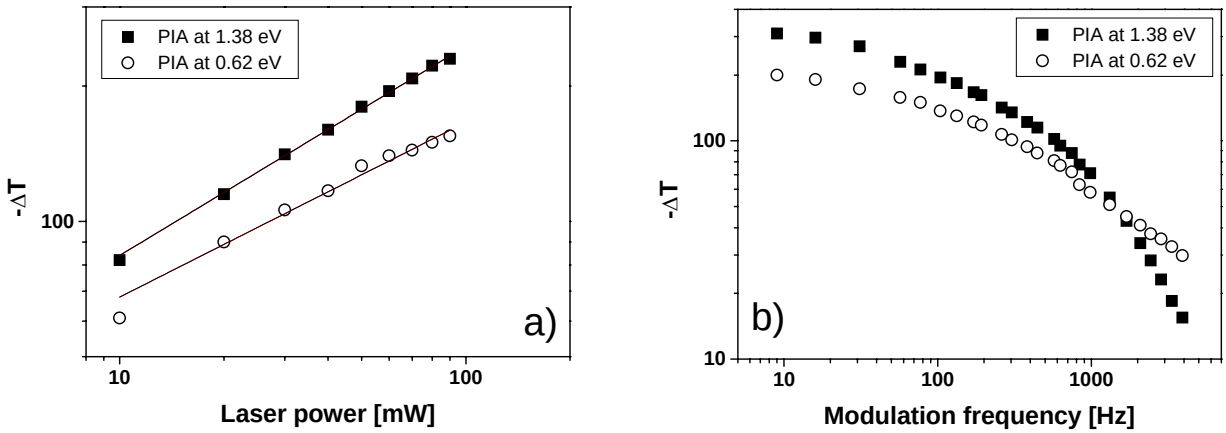

Fig. 5.19: **a**) Excitation intensity and **b**) frequency dependence of the poly(**1**) PIA signal.

The strong electron-phonon coupling in conjugated polymers allows the detection of doping- or photoinduced changes in the electronic structure also by means of vibrational spectroscopy.[35,36] Once in the doped or photoexcited state, even rather complicated conjugated polymers show relatively simple IR spectra with few intense infrared-active vibration (IRAV) bands.[37] These bands, which show correspondence to Raman-active modes of the neutral polymer, become IR-active due to the breaking of local symmetry associated with the charged backbone distorsion (see also Chapters 1 and 3).[37,38] As such, the photoinduced charge generation in poly(**1**) is corroborated also by the PIA-FTIR spectrum depicted in figure 5.20 (excitation at 476 nm). As observed in the PIA-Vis-NIR spectrum, broad electronic absorption bands, with maxima at about 4000 cm^{-1} (0.49 eV) and above 7000 cm^{-1} (> 0.87 eV), out of the detection range, are observed. In addition, three bands are seen in the vibrational range, at 1315, 1128 and 1039 cm^{-1}, respectively. In agreement with the bithiophene nature of the repeating unit and with a charged nature of the photoexcitations in poly(**1**), such a pattern displays marked similarity to that of *p*-doped and photoexcited polythiophenes.[37,39]

The difference spectra recorded *in-situ* during electrochemical oxidation (*p*-doping) of poly(**1**) are shown in Fig. 5.21. Above 2000 cm^{-1} (ca. 0.25 eV), the spectra are dominated by a very broad electronic absorption band. The vibrational part of the spectrum, detailed in figure 5.22, shows three dominant bands centered at about 1323, 1130 and 1055 cm^{-1}, which correspond to those observed in the PIA-FTIR spectrum. The weak bands at 1600 and 1480 cm^{-1} might be assigned to end-rings vibrations, thus suggesting, as already mentioned, the possibility of a relatively low molecular weight (short chain length, and therefore short effective conjugation length).[40] The discussed instability of poly(**1**) films towards reduction of the fullerene moieties does not allow the observation of clear *in situ* FTIR spectra upon scanning negative potentials.

While these results prove the photoinduced generation of metastable, positively charged states on the polythiophene backbone, a definitive evidence of a photoinduced electron transfer from the latter to the pendant fullerene moieties is obtained only by ESR. The ESR spectra of poly(**1**) films are displayed in Fig. 5.23. The dark ESR spectra

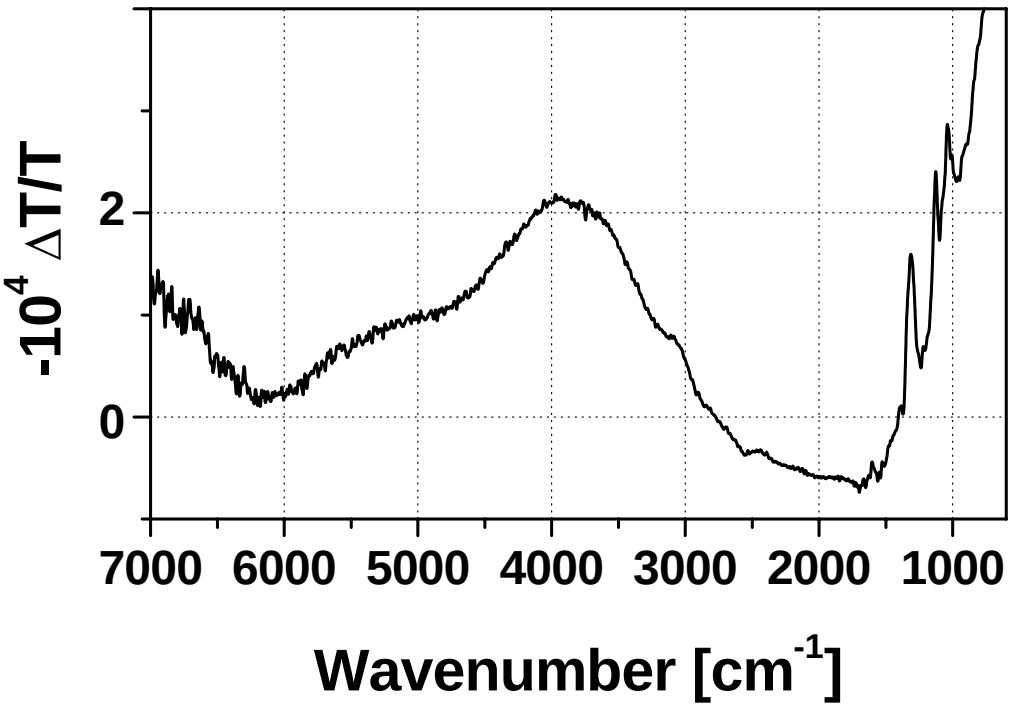

Fig 5.20: Photoinduced IR absorption of poly(**1**). Excitation at 476 nm (20 mW/cm^2). T = 100 K.

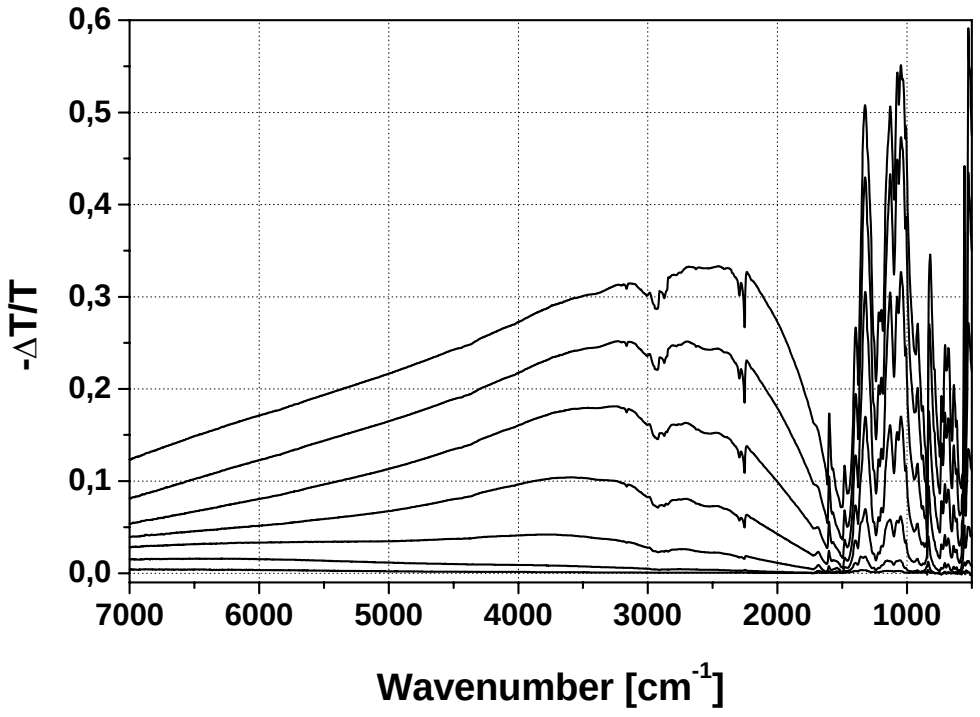

Fig. 5.21: IR difference spectra of poly(**1**) during *p*-doping. Sequence: bottom to top.

shows only one line at a *g*-factor of 2.0022, which we assigned to residual radical-cations remaining from to the oxidative electropolymerization. The light induced ESR spectrum, obtained by subtracting the "dark" signal from the "light-on" signal, shows the photogeneration of two paramagnetic species. The positive polaron on the conjugated backbone have a *g*-factor of 2.0022, while the signal at lower g-factor, 2.0004, is typical of fullerene radical-anions.[41] These results clearly indicate the occurrence of a photoinduced electron transfer from the polythiophene backbone to the pendant fullerene moieties. Also, the steady state LESR studies clearly show the long living charge separation in this non-composite material as observed earlier in conjugated polymers/fullerenes composites.[26]

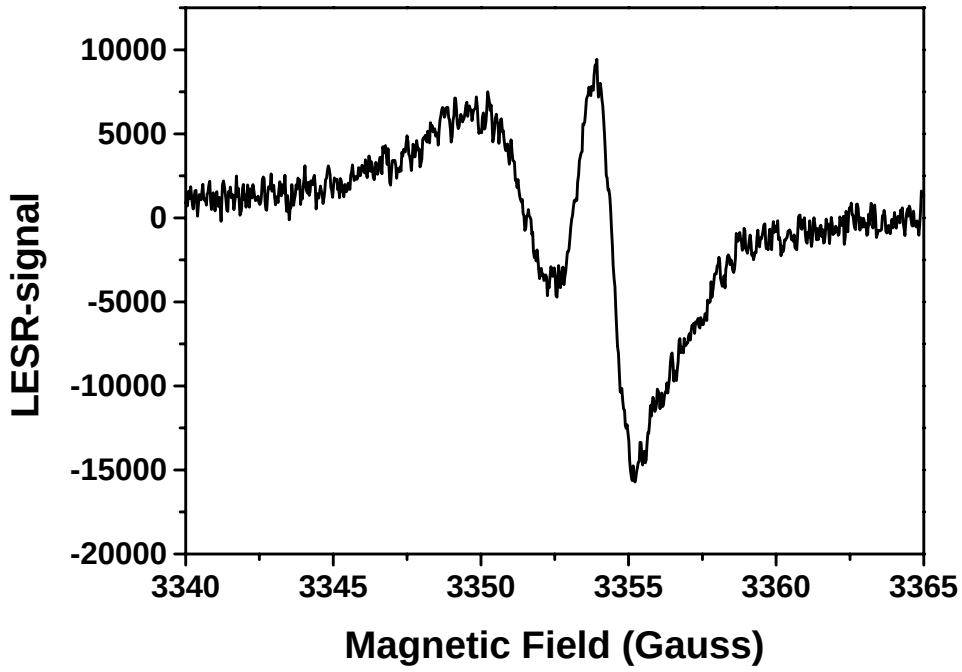

Fig 5.22: Light induced ESR spectrum of poly(**1**). Excitation at 476 nm. T = 100 K.

4.3.2. Conclusions

We have prepared novel bithiophenes, with tethered “TCAQ” type and fulleropyrrolidine moieties, suitable as monomers for electropolymerization. The

polymer films were investigated for their electrochemical and photophysical properties. The donor backbone and the acceptor moieties do not interact in the ground-state while a photoinduced electron transfer occurs in the excited state of these *double-cable* polymers, as revealed by spectroscopic measurements. The results showed that, in addition to the potential as intrinsic *p-n* transporting materials in organic devices, the class of *double-cable* polymers is of high interest for organic photovoltaics and other optoelectronic devices.

As explained in the introduction of this Section, solubility is a desired requirement for practical applications. Based on the positive results obtained with insoluble electropolymerised *double-cable* polymers, the chemical preparation and the charecterization of soluble *double-cables* are proceeding worldwide.

4.4. CHEMICALLY SYNTHESISED *DOUBLE-CABLE* POLYMER

The structure of the first soluble *double-cable* polymer **6** investigated in Linz is sketched in Fig. 5.23. Polymer **6** is a random copolymer with repeating units of 3-(4'-(1'',4'',7''-trioxaoctyl)phenyl)thiophene **7** and of a thiophene-substituted fulleropyrrolidine **12** (Scheme 2.2). Poly(3-(4'-(1'',4'',7''-trioxaoctyl)phenyl)thiophene) (PEOPT) **7** (Scheme 2.2) served as reference for PIA measurements and photovoltaic devices.

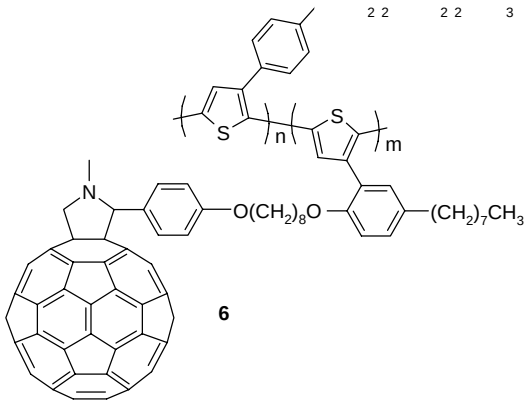

6

Fig. 5.23: Chemical structure of polymer **6**.

a) Photoinduced electron transfer

Thin films of polymers **6** and **7** were prepared by spin casting from a chloroform solution. Both **6** and **7** form orange films that could be converted upon heating to a blue, ordered form.[12,13] For the experiments presented here only the orange, disordered forms of *double-cable* **6** and reference polymer **7** were used. Fig. 5.24 shows the PIA spectra of films of **6** and reference **7**. Polymer **7** may be identified through a single peak in the PIA spectrum at 1.28 eV. As this feature shows a monomolecular recombination behaviour and no accompanying (polaronic) peak at lower energies is observed, it can be attributed to a neutral long lived excitation, i. e. a triplet state. The PIA spectrum of the *double-cable* **6** on the other hand shows two features, one at 1.42 eV and the second one below 0.6 eV, typical for charged excitations in conjugated polymers. Both features may be assigned to absorption of radical cations (polarons) on the polythiophene backbone produced by photoinduced electron transfer from the latter onto the pendant fullerenes. The observed square root excitation intensity dependence of the PIA signals is due to the bimolecular recombination of these charged species. Very similar PIA spectra have been observed for blends of the phenyl substituted polythiophene **7** mixed with fullerene derivatives.[25] The PIA spectrum of the *double-cable* **6** also resembles that one of the electropolymerised *double-cable* poly(**1**). These results prove the photoinduced electron transfer from the polymer backbone to the pendant fullerenes in this new soluble *double-cable* material.

b) Photovoltaic devices

The detailed production of the photovoltaic devices, which consisted of an indium tin oxide coated glass / poly-(3,4-ethylenedioxythiophene) poly(styrenesulfonate) (PEDOT) / active material / LiF / Al layered structure, is described elsewhere. Current/voltage characterisation of the devices was performed under illumination from a solar simulator at 800 W/m^2. Fig. 5.22 compares the I/V curves for devices from the *double-cable* **6** to devices made from reference polymer **7**. A drop of the V_{oc} from ~ 1 V for the reference polymer **7** to a V_{oc} of ~ 0.5 V for the *double-cable* **6** is observed. Additionally, the short circuit current (I_{sc}) as well as the photocurrent is increased by a

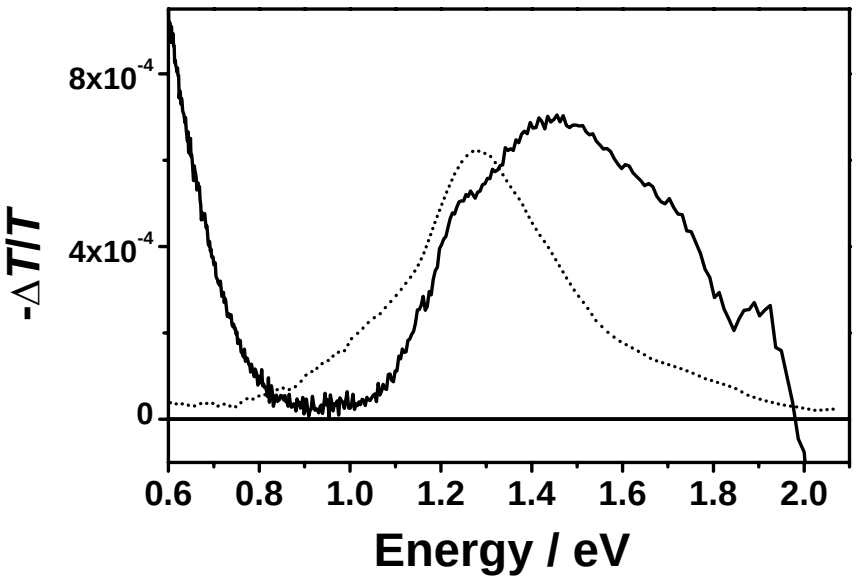

Fig. 5.21: Photoinduced absorption spectra of *double-cable* **6** (solid line) and reference polymer **7** (dashed line) excited at 476 nm, T = 100 K.

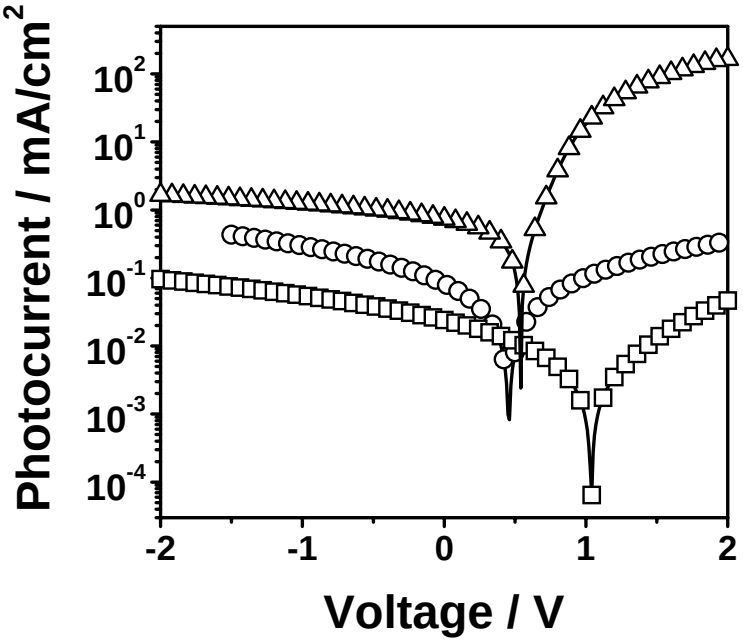

Fig. 5.22: I/V curves of photovoltaic devices with double-cable **4** (circles), double-cable **4** with additional fullerene (weight ratio 1 : 3) (triangles) and the reference polymer **7** (squares) as active materials.

factor of ~ 3, indicating the more efficient charge generation as well as the enhanced electron transport properties. However, the absolute I_{sc} values and the low rectification of the *double-cable* device reveals that the fullerene concentration of one fullerene unit for ten repeating polymer units is below the percolation threshold for electron transport in bulk heterojunction solar cells, which was recently found to follow the theoretically predicted value of 17 vol %.[42] Attaching a higher percentage of fullerenes to the backbone has been difficult up to now due to solubility problems. For that reason we additionally mixed the fullerene derivative [6,6]-Phenyl C_{61} - butyric acid methyl ester (PCBM)[3] into the *double-cable* polymer and investigated the performance of this device (Fig.5.25). The results show the potential of these materials to match the efficiency of the composites with the added functionality that these non-composite double-cables can be processed into other hosts, stretch oriented and may further functionalised for self-assembly.

4.4.1. Conclusions

In summary, a soluble electron donor/acceptor *double-cable* copolymer based on phenol-substituted-thiophene/phenol-substituted-thiophene-fulleropyrrolidine units was synthesised. The photoinduced charge transfer from the polythiophene backbone to pendant fullerenes was observed in PIA spectra and further proven in photovoltaic devices produced from this *double-cable* polymer. The relative low photocurrent shows that the fullerene concentration of this donor/acceptor *double-cable* polymer is below the percolation threshold for electron transport. Increase in fullerene concentration of the *double-cable* is predicted to enhance the photovoltaic performance.

4.5. REFERENCES

1. U. Stalmach, B. de Boer, C. Videlot, P. F. van Hutten, G. Hadziioannou, *J. Am. Chem. Soc.*, 2000, **122**, 5464.

2. N. Martín, L. Sanchez, B. Mescas, I. Pérez, *Chem. Rev*., 1998, **98**, 2527.

3. S.-G. Liu, L. Shu, J. Rivera, H. Liu, J.-M. Raimundo, J. Roncali, A. Gorgues, L. Echegoyen, *J. Org. Chem.*, 1999, **64**, 4884.

4. S. Knorr, A. Grupp, M. Mehring, G. Grube, F. Effenberger, *J. Chem. Phys. A*, 1999, **110**, 3502.

5. T. Yamashiro, Y. Aso, T. Otsubo, H. Tang, Y. Harima, K. Yamashita, *Chem. Lett*., 1999, 443.

6. J.-F. Nierengarten, J.-F. Eckert, J.-F. Nicoud, L. Ouali, V. V. Krasnikov, G. Hadziioannou, *J. Chem. Soc., Chem. Commun*., 1999, 617.

7. P. A. van Hal, J. Knol, B. M. W. Langeveld-Voss, S. C. J. Meskers, J. C. Hummelen, R. A. J. Janssen, *J. Phys. Chem. A*, 2000, **104**, 5974.

8. N. Armaroli, F. Barigelletti, P. Ceroni, J.-F. Eckert, J.-F. Nicoud, J.-F. Nierengarten, *J. Chem. Soc., Chem. Commun*., 2000, 599.

9. E. Peters, P. A. van Hal, J. Knol, C. J. Brabec, N. S. Sariciftci, J. C. Hummelen, R. A. J. Janssen, *J. Phys. Chem. B*, 2000, **104**, 10174.

10. J. L. Segura, R. Gómez, N. Martín, C. Luo, D. M. Guldi, *J. Chem. Soc. Chem. Commun*. 2000, 701.

11. I. B. Martini, B. Ma, T. Da Ros, R. Helgeson, F. Wudl, B. Schwartz, *Chem. Phys. Lett*., 2000, **327**, 253.

12. P. A. van Hal, J. Knol, B. M. W. Langeveld-Voss, S. C. J. Meskers, J. C. Hummelen, R. A. J. Janssen, J. Phys. Chem. A, 2000, 104, 5974.

13. T. Martens, J. D'Haen, T. Munters, L. Goris, Z. Beelen, J. Manca, M. D'Olieslaeger, D. Vanderzande, L. De Schepper, R. Andriessen, *MRS Proc.*, in press.

14. R. J. O. M. Hoofman, M. P. de Haas, L. D. A. Siebbeles, J. M. Warman, *Nature*, 1998, **54**, 392.

15. J. Simonet, J. Rault Berthelot, *Prog. Solid State Chem*. 1991, **21**, 1.

16. J. Roncali, *J. Mater. Chem*., 1999, **9**, 1875, and references therein.

17. Reference 16, p. 1888.

18. European Commission, Joule III program for Molecular Plastic Solar Cells, Contract No. JOR3CT980206.

19. Kini, A. M.; Cowan, D. O.; Gerson, F.; Möckel, R.; *J. Am. Chem. Soc.* 1985, **107**, 556.

20. G. Zotti, *Handbook of Organic Conductive Molecules and Polymers*, H. S. Nalwa, Ed., Wiley, Chichester, 1997, Vol. 2, Chapter 4.

21. Smilowitz, L.; Sariciftci, N. S.; Wu, R.; Gettinger, C.; Heeger, A. J.; Wudl, F.; *Phys. Rev. B* 1993, **47**, 13835.

22. Janssen, R. A. J.; Moses, D.; Sariciftci, N. S.; J. Chem. Phys. 1996, **101**, 9519.

23. G. Dellepiane, C. Cuniberti, D. Comoretto, G. F. Musso, G. Figari, A. Piaggi, A. Borghesi, *Phys. Rev. B*, 1993, **48**, 7850.

24. C. Botta, S. Luzzati, R. Tubino, D. D. C. Bradley, R. H. Friend, *Phys. Rev. B*, 1993, **48**, 14809.

25. G. Zerza, M. C. Scharber, C. J. Brabec, N. S. Sariciftci, R. Gómez, J. L. Segura, N. Martín, V. I. Srdanov, *J. Phys. Chem. A* 2000, **104**, 8315.

26. Dyakonov, V.; Zorinaints, G.; Scharber, M.; Brabec, C. J.; Janssen, R. A. J.; Hummelen, J. C.; Sariciftci, N. S. *Phys. Rev. B* 1999, **59,** 8019.

27. Mizoguchi, K.; Kuroda, S.; in *Handbook of Conductive Molecules and Polymers*, ed. Nalwa, H. S. vol. 3, p251, John Wiley & Sons, **1997**.

28. C. J. Brabec, N. S. Sariciftci, J. C. Hummelen, *Adv. Funct. Mater*., 2001, **11**, 15, and references therein.

29. Österreichische Patentanmeldung No 15A 775/2002

30. N. Camaioni, L. Garlaschelli, A. Geri, M. Maggini, G. Possamai, G. Ridolfi, J. Mater. Chem., 2002, **12**, 2065.

31. D. Gebeheyu, F. Padinger, T. Fromherz, J. C. Hummelen, N. S. Sariciftci, *Int. J. Photoenergy*, 1999, **1**, 95.

32. T. Benincori, E. Brenna, F. Sannicoló, L. Trimarco, G. Zotti, *Angew. Chem. Int. Ed. Engl*. 1996, **35**, 648

33. J. P. Ferraris, A. Yassar, D. Loveday, M. Hmyene, *Optical Materials* (Amsterdam), 1998, **9**, 34.

34. L. Echegoyen, L. E. Echegoyen, *Acc. Chem. Res*., 1998, **31**, 593.

35. B. Horovitz, *Solid State Commun*. 1982, **41**, 729.

36. Ehrenfreund, E.; Vardeny, Z. V.; Brafman, O.; Horowitz, B. *Phys.Rev. B* **1987**, *36*, 1535.

37. See for instance, Del Zoppo, M.; Castiglioni, C.; Zuliani, P.; Zerbi, G. In *Handbook of Conducting Polymers*, 2nd ed.; Skotheim, T. A.; Elsenbaumer, R. L.; Reynolds, J. R., Eds.; Marcel Dekker: New York, 1988; Chapter 28, and references therein.

38. Castiglioni, C.; Gussoni, M.; Lopez Navarrete, J. T.; Zerbi, G. *Solid State Comm*. **1988**, *36*, 1535.

39. Neugebauer, H.; Neckel, A.; Brinda-Konopik, N. In *Electronic Properties of Polymers and Related Compounds*; Kuzmany, H.; Mehring, M.; Roth, S.; Eds.; Solid State Sci. 63, Springer; Heidelberg, 1985; p.227.

40. Agosti, E.; Rivola, M.; Hernandez, V.; Del Zoppo, M.; Zerbi, G. *Synth. Met*. **1999**, *100*, 101.

41. Allemand, P. M.; Srdanov, G.; Koch, A.; Khemani, K.; Wudl, F.; Rubin, Y.; Diederich, F.; Alvarez, M. M., Anz, S. J.; Whetten, R. L. *J. Am. Chem. Soc*., **1992**, *114*, 6446.

42. Brabec C. J., Padinger F., Dyakonov V., Hummelen J. C., Janssen R. A. J., Sariciftci N. S. (1998). In: Electronic Properties of Novel Materials - Progress in Molecular Nanostructures, World Scientific Co, Singapore, p. 519.

CHAPTER 5. CONCLUSIONS AND PERSPECTIVES

5.1. POSITIVE AND NEGATIVE CHARGE CARRIERS IN CONJUGATED POLYMERS

The results obtained by *in situ* spectroelectrochemical techniques during *p*- and *n*-doping on the same conjugated polymer show that charge carriers with opposite sign can display different spectroscopic features. This effect, for which the theoretical models developed so far do not account,[1] indicates the different structure and delocalisation of positive and negative charge carriers. In PDTTs this behaviour can be explained by the complicated structure of the repeating unit. In fact, the spectral patterns are strongly affected by the different aromatic moieties fused to the thiophene rings forming the polythiophene-like chain. In particular, as the aromaticity of the fused moiety increases and thus the polymer band-gap decreases, modes located within the fused moiety are more coupled to the delocalised electron system along the polythiophene backbone. However, preliminary results suggest that differences between the spectra of a conjugated polymer in its *p*- and *n*-doped state are possible in simpler systems too.[2]

In pristine PDTTs, the Raman modes mostly contributing to the ECC do undergo intensity redistribution as well as frequency dispersion. Moreover, modes with carbon-carbon double bond character undergo softening as the polymer band-gap decreases, while modes with carbon-carbon single bond character show the opposite behaviour. These effects can be taken as vibrational signature of the enhanced quinoid character of polythiophene-like chains as their band-gap decreases.

5.2. *DOUBLE-CABLE* POLYMERS

Preparation and properties of a novel class of functional materials such as *double-cable* polymers have been reported. These materials consist of a hole conducting,

conjugated backbone (*p-cable*) with covalently bound electron acceptor moieties (*n-cable*) such as TCAQ-type or fullerene derivatives. By the choice of the proper covalent linkage, the donor and the acceptor moieties can be electronically "isolated" to exclude ground-state electronic interactions. Thus, *double-cable* polymers are attractive for all organic electronic applications in which ambipolar transport is desired. Photoexcitation spectroscopic investigations have shown that *double-cable* polymers in their solid state undergo photoinduced electron transfer, leading to long-lived, mobile charge carriers as observed earlier in conjugated polymer:fullerene composites. Since in *double-cable* polymers phase separation cannot occur, these materials are indeed appealing as a viable way to control both electronic and morphological properties within the photoactive layer of plastic solar cells. Based on these results, the synthesis of *double-cable* polymers and their implementation to optoelectronic devices is proceeding worldwide. The progresses made on developing this novel class of materials are the subject of a recent review.[3] The very important technological issue is processability, which is certainly the major challenge towards practical application of *double-cable* polymers in thin film devices. With the few soluble *double-cable* polymers prepared so far, the fabrication of prototype photodiodes and solar cells has been demonstrated. However, in the *double-cable* approach a compromise between the fullerene loading (for the transport of electrons) and solubility has been made. With this respect:

- improving the design of the synthesis may allow the preparation of processable materials with acceptably high fullerene moieties percentage as well as acceptable solubility;

- fullerene loading as high as 14% -mol (24.2% -w) has been obtained in a soluble random copolymer, and a loading of 31.5% -w has been already obtained even in a polymer with well-defined backbone;[3]

- Balberg et al. have reported bipolar transport in a poly(3-hexylthiophene):C_{60} composite with a fullerene fraction of 10% mol.[4] Indeed, it can be considered that the volume fraction occupied by the fullerene moieties could be enhanced if the

volume occupied by the solubilising but electrically inactive chains would be minimised;

- the *double-cable* concept may lead to bipolar transport properties even in guest-host systems where the *double-cable* polymer is embedded within processable polymers as matrices;

- synthetic strategies toward fullerene derivatives able to self-assemble with suitably designed conjugated polymers shall be considered as an alternative to covalently bound *double-cables*, too. To this end, self-assembly strategies based on electrostatic or other key/lock interactions shall be possible.[5-7]

Finally, we would like to mention self-organization also as an interesting possibility to control the morphology of the photoactive film. In this respect, covalently linked *double-cable* polymers could be further functionalised, for example with amphiphilic substituents, to gain additional control of the final morphology by their tertiary structure.[5-8]

5.3. REFERENCES

1. P. B. Miranda, D. Moses, A. J. Heeger, *Phys. Rev. B*, **2001**, *64*, 81201-1.

2. D. Mühlbacher, *Diploma* Thesis, Linz, 2002.

3. A. Cravino, N. S. Sariciftci, *J. Chem. Mater*., **2002**, *12*, 1931.

4. I. Balberg, R. Naidis, M.-K. Lee, J. Shinar, L. F. Fonseca, *Appl. Phys. Lett.*, **2001**, *79*, 197.

5. M. T. Rispens, L. Sánchez, J. Knool, J. C. Hummelen, *J. Chem. Soc., Chem. Commun.*, **2001**, 161.

6. J. J. González, S. González, E. M. Prego, C. Luo, D. M. Guldi, J. de Mendoza, N. Martín, *J. Chem. Soc., Chem. Commun.*, 2001, 163.

7. S. Mizyed, P. E. Georghiou, M. Barcu, B. Cuadra, A. K. Rai, P. Cheng, L. T. Scott, *J. Am. Chem. Soc.*, 2001, **123**, 12770.

8. S. A. Jenekhe, X. L. Chen, *Science*, 1998, **279**, 1903.

APPENDIX

Curriculum vitae

Antonio Cravino

Nationality:	Italian
11th of February 1968:	Born in Genoa, Italy
July 1998 - November 2002:	PhD studies in Chemistry at the Johannes Kepler University Linz, Physical Chemistry
May 1998:	Qualified as chemist (State qualification)
December 1997:	Diploma thesis at the University of Genoa, Mathematical, Physical and Natural Sciences Faculty, summa cum laude.
September 1995 - September 1996:	Military Service 28° Bersaglieri Battalion "Oslavia", then Genoa Military District Headquarter.
1989 - 1999:	Studies in Chemistry at University of Genoa, Mathematical, Physical and Natural Sciences Faculty, Chemistry and Industrial Chemistry Department.
June 1989:	Graduated *Perito Chinico Industriale*, I.T.I.S. *"G. Ferraris"*, Savona, Italy.

Refereed publications

30) A. Cravino, G. Zerza, M. Maggini, S. Bucella, M. Svensson, M. R. Andersson, H. Neugebauer, C. J. Brabec, N. S. Sariciftci

"A Soluble Donor-acceptor Double-cable Polymer: Polythiophene with Pendant Fullerenes"

Monatsch. Chemie, Chem. Monthly, in press.

29) A. Cravino, N. S. Sariciftci

"Double-cable Polymers for Fullerene Based Organic Optoelectronic Applications"

J. Mater. Chem. 12 (2002) 1931.

(28) H. Neugebauer, C. J. Brabec, A. Cravino, Y. Teketel, P. Denk, S. Luzzati, M. Catellani, N. S. Sariciftci

"Infrared Spectroscopic Investigations of Organic Polymeric Photovoltaics Systems"

Organic Photovoltaics II, Z. H. Kafafi, Ed., Proceedings of SPIE Vol. 4465 (2002).

(27) A. Cravino, H. Neugebauer, S. Luzzati, M. Catellani, A. Petr, L. Dunsch, N. S. Sariciftci

"Positive and Negative Charge Carriers in Doped or Photoexcited Polydithienothiophenes: a Comparative Study Using Raman, Infrared and Electron Spin Resonance Spectroscopy"

J. Phys. Chem. B, 106 (2002) 3583.

(26) C. Pozo-Gonzalo, T. Khan, J. J. W. McDouall, P. J. Skabara, D. M. Roberts, M. E. Light, S. J. Coles, M. B. Hursthouse, H. Neugebauer, A. Cravino, N. S. Sariciftci

"Synthesis and Electropolymerisation of 3',4'-Bis(alkylsulfanyl)terthiophenes and the Significance of the Fused Dithiin Ring in 2,5-Dithienyl-3,4-ethylenedithiophene (DT-EDTT)"

J. Mater. Chem. 12 (2002) 500.

(25) A. Cravino, G. Zerza, H. Neugebauer, M. Maggini, S. Bucella, E. Menna, M. Svensson, M. R. Andersson, C. J. Brabec, N. S. Sariciftci

"Electrochemical and Photophysical Properties of a Novel Polythiophene with Pendant Fulleropyrrolidine Moieties: Toward "Double Cable" Polymers for Optoelectronic Devices"

J. Phys. Chem. B 106 (2002) 70.

(24) C. J. Brabec, A. Cravino, D. Meissner, N. S. Sariciftci, M. T. Rispens, L. Sanchez, J. C. Hummelen, T. Fromherz

"The Influence of Materials Work Function on the Open Circuit Voltage of Plastic Solar Cells"

Thin Solid Films 403-404 (2002) 368.

(23) C. J. Brabec, A. Cravino, D. Meissner, N. S. Sariciftci, T. Fromherz, M. T. Rispens, L. Sanchez, J. C. Hummelen

"On the Origin of the Open Circuit Voltage of Plastic Solar Cells"

Adv. Funct. Mat. 11 (2001) 374.

(22) G. Zerza, A. Cravino, R. Goméz, J. L. Segura, M. Svensson, M. R. Andersson, N. Martín, H. Neugebauer, N. S. Sariciftci

"Photoinduced Charge Carriers in a Donor-acceptor Double-cable Polythiophene with Covalently Bound Tetracyanoanthraquinodimethane Moieties"

Mat. Res. Soc. Symp. Proc., Vol. 660, S. C. Moss, Ed., MRS, Warrendale, 2001, p. JJ8.11.1.

(21) A. Cravino, G. Zerza, H. Neugebauer, S. Bucella, M. Maggini, E. Menna, G. Scorrano, M. Svensson, M. R. Andersson, N. S. Sariciftci

"Electropolymerization and Spectroscopic Properties of a Novel Double-cable Polythiophene with Pendant Fullerene for Photovoltaic Applications"

Synth. Met. 121 (2001) 1555.

(20) R. Muellner, A. Cravino, J. Williams, F. Stelzer, G. Jakopic, G. Leising

"Poly(2-hexyl-9,10-anthrylene vinylene) - A Class of Soluble Poly(anthrylenevinylene)s"

Synth. Met. 119 (2001) 193.

(19) G. Zerza, A. Cravino, H. Neugebauer, N. S. Sariciftci, R. Gómez, J. L. Segura, N. Martín, M. Svensson, M. R. Andersson

"Photoinduced Electron Transfer in Donor/Acceptor Double Cable Polymers: Polythiophene Bearing Tetracyanoanthraquinodimethane Moieties"

J. Phys. Chem. A 105 (2001) 4172.

(18) P. J. Skabara, I. M. Serebryakov, I. F. Perepichka, N. S. Sariciftci, H. Neugebauer, A. Cravino

"Towards Controlled Donor-Acceptor Interactions in Non-composite Polymeric Materials - Synthesis and Characterisation of a Novel Polythiophene Incorporating p-Conjugated 1,3-Dithiol-2-ylidenefluorene Units as Strong D-A Components"

Macromolecules 34 (2001) 2232.

(17) M. Alloisio, A. Cravino, I. Moggio, D. Comoretto, S. Bernocco, C. Cuniberti, C. Dell'Erba, G. Dellepiane

"Solution Spectroscopic Properties of PolyDCHD-HS: a Novel Highly Soluble Polydiacetylene"

J. Chem. Soc., Perkin Trans. 2 (2001) 146.

(16) C. J. Brabec, A. Cravino, G. Zerza, N. S. Sariciftci, R. Kieboms, D. Vanderzande, J. C. Hummelen

"Photoactive Blends of Poly(para-phenylene vinylene) from a Novel Precursor Polymer and Methanofullerene: Photophysics and Device Performance"

J. Phys. Chem. B 105 (2001), 1528.

(15) A. Cravino, H. Neugebauer, S. Luzzati, M. Catellani, N. S. Sariciftci

"Vibrational Spectroscopy on pDTT3 - a Low Band Gap Polymer Based on Dithienothiophene"

J. Phys. Chem. B 105 (2001) 46.

(14) A. Cravino, G. Zerza, M. Maggini, S. Bucella, M. Svensson, M. R. Andersson, H. Neugebauer, N. S. Sariciftci

"A Novel Polythiophene with Pendant Fullerenes: Toward Donor/Acceptor Double-Cable Polymers"

J. Chem. Soc., Chem. Commun. (2000) 2487.

(13) S. Sottini, G. Margheri, E. Giorgetti, F. Gelli, A. Cravino, D. Comoretto, C. Cuniberti, C. Dell'Erba, I. Moggio, G. Dellepiane

"Thin Films of a Novel Polydiacethylene for Applications to All-Optical Signal Processing"

Nonlinear Optics 25 (2000) 385.

(12) E. Giorgetti, G. Margheri, F. Gelli, S. Sottini, D. Comoretto, A. Cravino, C. Cuniberti, C. Dell'Erba, G. Dellepiane

"Optical Properties of Films of Polycarbazolyldiacethylene PDCHD-HS for Photonic Applications"

Synth. Met. 116 (2000) 129.

(11) H. Neugebauer, C. Kvarnstroem, A. Cravino, Y. Teketel, N. S. Sariciftci

"Photoexcited Spectroscopy and In-situ Electrochemical Spectroscopy in Conjugated Polymers: a Comparative Study"

Synth. Met. 116 (2000) 115.

(10) E. Giorgetti, G. Margheri, S. Sottini, X. Chen., A. Cravino, D. Comoretto, C. Cuniberti, C. Dell'Erba, G. Dellepiane

"Linear and Non Linear Characterization of PolyDCHD-HS Films"

Synth. Met. 115 (2000) 257.

(9) A. Cravino, H. Neugebauer, N. S. Sarciftci, M. Catellani, S. Luzzati

"Electrochemically- and Photo-induced IR Absorption of Low Band-Gap Polydithienothiophenes: a Comparative Study"

Mat. Res. Soc. Symp. Proc., Vol. 598, S. P. Ermer, J. R. Reynolds, J. W. Perry, A.K-Y. Jen, Z. Bao Ed.s, MRS, Warrendale, 2000; p. BB3.74.1.

(8) C. J. Brabec, A. Cravino, G. Zerza, F. Padinger, N. S. Sariciftci, R. Kiebooms, D. Vanderzande, J. C. Hummelen

"Investigation of Photoinduced Charge Transfer in Composites of a Novel Precursor PPV Polymer and Fullerenes"

Mat. Res. Soc. Symp. Proc., Vol. 598, S. P. Ermer, J. R. Reynolds, J. W. Perry, A.K-Y. Jen, Z. Bao Ed.s, MRS, Warrendale, 2000; p. BB3.25.1.

(7) A. Cravino, I. Moggio, C. Dell'Erba, D. Comoretto, C. Cuniberti, G. Dellepiane, E. Giorgetti, D. Grando, G. Margheri, S. Sottini

"Films of a Novel Polydiacetylene for Photonic Studies"

Synth. Met. 115 (2000) 275.

(6) E. Giorgetti, G. Margheri, S. Sottini, D. Comoretto, A. Cravino, C. Cuniberti, C. Dell'Erba, G. Dellepiane

"Films of PolyDCHD-HS for Photonic Applications: Linear and Non-linear Characterization"

Proceedings of the International Conference on LASERS '99, V. J. Corcoran, T. A. Corcoran, Ed.s, STS Press, McLean, VA., 2000, pp. 529-535.

(5) C. J. Brabec, H. Johansson, A. Cravino, N. S. Sariciftci, D. Comoretto, I. Moggio, G. Dellepiane

"The Spin Signature of Charged Photoexcitations in Carbazolyl Subsituted Polydiacetylene"

J. Chem. Phys. 111, 22 (1999) 10354.

(4) B. Gallot, A. Cravino, I. Moggio, D. Comoretto, C. Cuniberti, C. Dell'Erba, G. Dellepiane

"Supramolecolar Organization in the Solid State of a Novel Soluble Polydiacetylene"

Liquid Crystals 26, 10 (1999) 1437.

(3) A. Cravino, I. Moggio, C. Dell'Erba, D. Comoretto, C. Cuniberti, G. Dellepiane, E. Giorgetti, D. Grando, S. Sottini

"A Novel Processable Polydiacetylene for Photonic Studies"

Synth. Met. 102 (1999) 943.

(2) C. J. Brabec, M. C. Scharber, H. Johansson, D. Comoretto, G. Dellepiane, I. Moggio, A. Cravino, J. C. Hummelen, N. S. Sariciftci

"Photoexcitations in Carbazolyl Substituted Polydiacetilene/Fullerene Composites"
Synth. Met. 101 (1999) 298.

(1) I. Moggio, M. Alloisio, A. Cravino, D. Comoretto, P. Piaggio, G. F. Musso, G. Garbarino, C. Cuniberti, C. Dell'Erba, G. Dellepiane
"Vibrational Properties of Novel Diacetylenic Monomers"
J. Chem. Soc., Perkin Trans. 2 (1998) 2249.

Other publications

F. Gelli, E. Giorgetti, D. Grando, G. Margheri, S. Sottini, A. Cravino, I. Moggio, C. Dell'Erba, D. Comoretto, C. Cuniberti, G. Dellepiane
"Films of a Novel Polydiacethylene for Photonic Studies"
IROE Technical Report n. TR/IRM/3.98, June 1998.

D. Comoretto, I. Moggio, G. F. Musso, M. Ottonelli, G. Dellepiane, C. J. Brabec, H. Joansson, A. Cravino, N. S. Sariciftfci
"On the Nature of the Photoexcited States in Polydiacethylenes"
INFM 4th National Meeting, 2000, published in Genoa, Italy.

A. Cravino, G. Zerza, H. Neugebauer, M. Maggini, S. Bucella, M. Svensson, M. R. Andersson, N. S. Sariciftci
"Photoinduced electron transfer in Donor/Acceptor Double-Cable Polymers"
Proceeding of the 199th ECS Meeting, 25-29 March, 2001, Washington, D.C.

H. Neugebauer, A. Cravino, G. Zerza, M. Maggini, S. Bucella, G. Scorrano, M. Svensson, M. R. Andersson, N. S. Sariciftci
"Fullerenes as Functional Moieties in Conjugated Polymers: Towards Donor-Acceptor Double Cable Polymeric Materials"
AIP Conf. Proc. 591 Electronic Properties of Molecular Nanostructures 2001, p. 511.

A. Cravino, N. S. Sariciftci
"Conjugated Polymer/Fullerene Based Plastic Solar Cells"
Proceedings of the European Meeting on High Efficiency Plastic Solar Cells, 15-16 November, 2001, Ispra, Italy.

Participation to Conferences

Talks

(17) (Cravino) A. Cravino, H. Neugebauer, S. Luzzati, M. Catellani, A. Petr, L. Dunsch, N. S. Sariciftci

"Positive and Negative Charged States in Doped and Photoexcited Low Band-Gap Polydithienothiophenes: a Spectroscopic Study Using Raman, Infrared and ESR Spectroscopy"

81.Bunsen-Kolloquium, 21-23 September, 2002, Dresden, Germany.

(16) (Cravino) A. Cravino, H. Neugebauer, N. S. Sariciftci

"Design of Novel Donor-acceptor Structures for Plastic Photovoltaics"

ICSM 2002, 29 June-5 July, 2002, Shanghai, China.

(15) (Cravino) A. Cravino, M. A. Loi, D. Mühlbacher, M. C. Scharber, C. Winder, H. Neugebauer, N. S. Sariciftci, H. Meng, Y. Chen, F. Wudl

"A Novel Processable Low Band-gap Polymer: Spectroscopic and Photovoltaic Properties of PEDOTEHIITN"

IV International Conference on "Electronic Processes in Organic Materials (ICEPOM-4)", 3-8 June, 2002, L'viv, Ukraine.

(14) (Mühlbacher) D. Mühlbacher, H. Neugebauer, A. Cravino, N. S. Sariciftci, K. J. van Duren, A. Dhanabalan, P. A. van Hal, R. A. J. Janssen, J. C. Hummelen

"Comparison of Spectroscopic and Electrochemical Data of the Low Band-gap Polymer PTPTB"

IV International Conference on "Electronic Processes in Organic Materials (ICEPOM-4)", 3-8 June, 2002, L'viv, Ukraine.

(13) (Matt) G. J. Matt, T. Fromherz, A. Cravino, C. Winder, D. Meissner, J. C. Hummelen, N. S. Sariciftci, C. J. Brabec

"Device Characterization of Conjugated Polymer / Methanofullerene Bulk-heterojunction Solar Cells"

IV International Conference on "Electronic Processes in Organic Materials (ICEPOM-4)", 3-8 June, 2002, L'viv, Ukraine.

(12) Invited A. Cravino

"Politiofeni con Sostituenti Elettron-accettori: Verso Materiali Non-compositi per Applicazioni in Dispositivi Fotovoltaici ed Optoelettronici"

IV Convegno Nazionale Materiali Molecolari Avanzati per Fotonica ed Elettronica, 20-22 September, 2001, Calaserena, Geremeas (CA), Italy.

(11) Invited (Sariciftci) A. Cravino, G. Zerza, H. Neugebauer, N. S. Sariciftci, S. Bucella, M. Maggini, M. Svensson, M. R. Andersson

"Photoinduced Electron Transfer in Donor/Acceptor Double-Cable Polymers and Application to Plastic Solar Cells"

UPS'01 10th International Conference on Unconventional Photoactive Systems, 4-8 September, 2001, Les Diablerets, Switzerland.

(10) Invited (Meissner) D. Meissner, C. J. Brabec, A. Cravino, T. Fromherz, J. C. Hummelen, M. T. Rispens, J. Rostalski, L. Sanchez, N. S. Sariciftci

"Modeling Organic Solar Cells"

SPIE 46th Annual Meeting, Organic Photovoltaics II, 29 July-3 August, 2001, San Diego, CA.

(9) Invited (Cravino) A. Cravino, G. Zerza, H. Neugebauer, N. S. Sariciftci, S. Bucella, M. Maggini, M. Svensson, M. R. Andersson

"Photoinduced Electron Transfer in Donor/Acceptor Double-cable Polymers"

ECS 199th Meeting, Symposium Q: Fullerenes, Nanotubes and Carbon Nanoclusters; Q2: Electrochemistry and ESR, March 25-30, 2001, Washington, D.C.

(8) (Neugebauer) H. Neugebauer, A. Cravino, G. Zerza, S. Bucella, M. Maggini, G. Scorrano, R. Gómez, J. L. Segura, N. Martín, M. Svensson, M. R. Andersson, N.

S. Sariciftci

"Donor-acceptor Double Cable Polymer Films Prepared by Electrochemical Polymerization. Investigation of the Photoinduced Charge Transfer as the Basic Process for Optoelectronic Devices"

13th International Workshop on Quantum Solar Energy Conversion, March 10-17, 2001, Kirchberg, Austria.

(7) (Cravino) C. J. Brabec, A. Cravino, N. S. Sariciftci, J. Meyer, V. Dyakonov, J. Parisi, M. T. Rispens, J. C. Hummelen

"Investigation of the Open Circuit Voltage in Plastic Solar Cells - Pinning of the Fermi Energy"

MRS 2000 Fall Meeting, Cluster 8: Organics and Biomaterials; Symposium JJ: Organic Electronic and Photonic Materials and Devices, November 2000, Boston, MA.

(6) (Neugebauer) A. Cravino, G. Zerza, H. Neugebauer, N. S. Sariciftci, M. Maggini, S. Bucella, G. Scorrano, M. Andersson, M. Svensson

"Photoinduced Charge Carriers in a Donor-acceptor Double-cable Polythiophene with Covalently Bound Fullerene Moieties"

MRS 2000 Fall Meeting, Cluster 8: Organics and Biomaterials; Symposium JJ: Organic Electronic and Photonic Materials and Devices, November 2000, Boston, MA.

(5) (Giorgetti) E. Giorgetti, G. Margheri, F. Gelli, S. Sottini, A. Cravino, D. Comoretto, C. Cuniberti, C. Dell'Erba, I. Moggio, G. Dellepiane

"Films of PolyDCHD-HS for Photonic Applications: Linear and Non Linear Characterization"

OP 2000, February 2000, Salt Lake City, Utah.

(4) (Neugebauer) H. Neugebauer, A. Cravino, Y. Teketel, N. S. Sariciftci

"Photoexcited Spectroscopy and In-Situ Electrochemical Spectroscopy in Conjugated Polymers: a Comparative Study"

OP 2000, February 2000, Salt Lake City, Utah.

(3) (Cravino) A. Cravino, H. Neugebauer, N. S. Sariciftci, M. Catellani, S. Luzzati

"Studio Spettroscopico di Polimeri a Basso Energy-Gap: Poliditienotiofeni"

XVI Convegno G. N. S. R. 1999, November 1999, Milano, Italy.

(2) (Comoretto) A. Cravino, I. Moggio, D. Comoretto, C. Dell'Erba, C. Cuniberti, G. F. Musso, G. Dellepiane

"Electronic Properties of Solutions and Thin Films of a Novel Polydiacetylene for Non Linear Optics"

Europhysics Conference on Macromolecules Physics: Electrooptical Properties of Polymers and Related Materials, September 1998, Varenna, Italy.

(1) (Moggio) A. Cravino, I. Moggio, C. Dell'Erba, D. Comoretto, C. Cuniberti, G. Dellepiane, D. Grando, S. Sottini

"Films of a Novel Polydiacetylene for Photonic Studies"

EMRS 1998, June 1998, Strasbourg, France.

Posters

(20) (Rispens) J. C. Hummelen, M. T. Rispens, C. J. Brabec, A. Cravino, D. Meissner, N. S. Sariciftci, T. Fromherz, F. B. Kooistra, J. Knol, L. Sánchez, W. Verhees, M. Vienk, J. M. Kroon

"On the Origin of the Open Circuit Voltage of "Plastic" Solar Cells"

ICSM 2002, June 29-July 5, 2002, Shanghai, China.

(19) (Cravino) A. Cravino, M. A. Loi, M. C. Scharber, C. Winder, P. Denk, H. Neugebauer, H. Meng, Y. Chen, F. Wudl, N. S. Sariciftci

"Spectroscopic Properties of PEDOTEHIITN, a Novel Soluble Low Band-gap Polymer"

ICSM 2002, June 29-July 5, 2002, Shanghai, China.

(18) (Cravino) D. Mühlbacher, H. Neugebauer, A. Cravino, N. S. Sariciftci

"Comparison of the Electrochemical and Optical Band-gap Data of Low Band-gap Polymers"

ICSM 2002, June 29-July 5, 2002, Shanghai, China.

(17) (Cravino) C. Winder, M. A. Loi, A. Cravino, C. J. Brabec, H. Neugebauer, N. S. Sariciftci, I F. Perepichka, J. Roncali

"A Soluble PEDOT Derivative for Plastic Solar Cells"

ICSM 2002, June 29-July 5, 2002, Shanghai, China.

(16) (Brabec) C. J. Brabec, A. Cravino, D. Meissner, N. S. Sariciftci, M. T. Rispens, L. Sanchez, J. C. Hummelen, T. Fromherz

"On the Open Circuit Voltage of Bulk-heterojunction Plastic Solar Cells"

EMRS 2001, June 2001, Strasbourg, France.

(15) (Neugebauer) H. Neugebauer, A. Cravino, G. Zerza, S. Bucella, M. Maggini, G. Scorrano, M. Svensson, M. R. Andersson, N. S. Sariciftci

"Fullerenes as Functional Moieties in Conjugated Polymers: Towards Donor-acceptor Double-cable Polymeric Materials"

IWEPNM 2001, March 4-9, 2001, Kirchberg, Austria.

(14) (Cravino) A. Cravino, C. J. Brabec, A. Y. Andreev, E. Peeters, R. A. J. Janssen, J. Knol, J. C. Hummelen, N. S. Sariciftci

"Oligo(para-phenylene vinylene)-Fullerene Dyads as Acceptors in MDMO-PPV Based Bulk Heterojunction Solar Cells"

SPIE, Optoelectronics 2001, 20-26 January, 2001, San José, CA.

(13) (Cravino) G. Zerza, A. Cravino, H. Neugebauer, N. S. Sariciftci, R. Gómez, J. L. Segura, N. Martín, M. Svensson, M. R. Andersson

"Photoinduced Charge Carriers in a Donor-acceptor Double-cable Polythiophene with Covalently Bound Tetracyanoanthraquinodimethane Moieties"

MRS 2000 Fall Meeting, Cluster 8: Organics and Biomaterials; Symposium JJ: Organic Electronic and Photonic Materials and Devices, November 2000, Boston, MA.

(12) (Cravino) A. Cravino, C. J. Brabec, A. Y. Andreev, R. Rittberger, N. S. Sariciftci, E. Peeters, R. A. J. Janssen, J. Knol, J. C. Hummelen

"Oligo(p-phenylene vinylene) - Fullerene Dyads Incorporated in Conjugated Polymer Plastic Solar Cells"

MRS 2000 Fall Meeting, Cluster 8: Organics and Biomaterials; Symposium JJ: Organic Electronic and Photonic Materials and Devices, November 2000, Boston, MA.

(11) (Muellner) R. Muellner, A. Cravino, J. Williams, F. Stelzer, G. Leising

"Poly(2-hexyl-9,10-anthrylene vinylene) - A New Class of Soluble Poly(arylene vinylene)s"

ICSM 2000, July 2000, Gastein, Austria.

(10) (Cravino) A. Cravino, G. Zerza, H. Neugebauer, S. Bucella, M. Maggini, E. Menna, G. F. Scorrano, M. Svensson, M. R. Andersson, N. S. Sariciftci

"Electropolymerization and Spectroscopic Properties of a Novel Double-Cable Polythiophene with Pendant Fullerenes for Photovoltaic Applications"

ICSM 2000, July 2000, Gastein, Austria.

(9) (Comoretto) D. Comoretto, I. Moggio, G. F. Musso, M. Ottonelli, G. Dellepiane, C. J. Brabec, H. Johansson, A. Cravino, N. S. Sariciftci

"On the Nature of the Photoexcited States in Polydiacetylenes"

INFM 4th National Meeting, June 2000, Genova, Italy.

(8) (Sottini) S. Sottini, G. Margheri, E. Giorgetti, F. Gelli, A. Cravino, D. Comoretto, C. Cuniberti, I. Moggio, G. Dellepiane

"Thin Films of a Novel Polydiacetylene for Applications to All-Optical Signal Processing"

ICONO's 2000, March 2000, Davos, Switzerland.

(7) (Brabec) C. J. Brabec, A. Cravino, G. Zerza, F. Padinger, N. S. Sariciftci, R. Kieboms, D. Vanderzande, J. C. Hummelen

"Investigation of Photoinduced Charge Transfer in Composites of a Novel Precursor PPV Polymer and Fullerenes"

MRS 1999 Fall Meeting, November-December 1999, Boston, MA.

(6) (Cravino) A. Cravino, H. Neugebauer, N. S. Sariciftci, M. Catellani, S. Luzzati

"Electrochemically- and Photo-induced IR Absorption of Low Band-Gap Polydithienothiophenes: a Comparative Study"

MRS 1999 Fall Meeting, November-December 1999, Boston, MA.

(5) (Giorgetti) E. Giorgetti, G. Margheri, S. Sottini, A. Cravino, D. Comoretto, C. Cuniberti, C. Dell'Erba, G. Dellepiane

"Films of PolyDCHD-HS for Photonic Applications: Linear and Non Linear Characterization"

Laser 1999, December 1999, Quebec City, Canada.

(4) (Sottini) E. Giorgetti, G. Margheri, F. Gelli, S. Sottini, A. Cravino, D. Comoretto, C. Cuniberti, C. Dell'Erba, I. Moggio, G. Dellepiane

"Linear and Non Linear Characterization of polyDCHD-HS Films"
INFM Workshop on Applications of Nonlinear Optical Phenomena and Related Industrial Perspectives, October 1999, Amalfi, Italy.

(3) (Giorgetti) E. Giorgetti, G. Margheri, S. Sottini, C. Xianfeng, A. Cravino; D. Comoretto, C. Cuniberti, C. Dell'Erba, G. Dellepiane
"Linear and Non Linear Characterization of PolyDCHD-HS Films"
EMRS 1999, June 1999, Strasbourg, France.

(2) (Brabec) C. J. Brabec, M. C. Scharber, H. Johansson, D. Comoretto, G. Dellepiane, I. Moggio, A. Cravino, J. C. Hummelen, N. S. Sariciftci
"Photoexcitations in Carbazolyl Substituted Polydiacetylene/Fullerene Composites"
ICSM 1998, July 1998, Montpellier, France.

(1) (Cravino) A. Cravino, I. Moggio, C. Dell'Erba, D. Comoretto, C. Cuniberti, G. Dellepiane, E. Giorgetti, D. Grando, S. Sottini
"A Novel Processable Polydiacetylene for Photonic Studies"
ICSM 1998, July 1998, Montpellier, France.

Schools

August 1998: *European Summer School on Quantum Solar Energy Conversion*, Hirschegg, Austria.

March 2002: *Alan J. Heeger Lectures on Physics and Chemistry of Organic Semiconductors*, Kirchberg, Austria.

Affiliations

Societá Chimica Italiana, Organic Chemistry

Electrochemical Society

Eidesstattliche Erklärung

Ich erkläre an Eides statt, dass ich die vorliegende Dissertation selbstständig und ohne fremde Hilfe verfasst, andere als die angegebenen Quellen und Hilfsmittel nicht benutzt bzw. die wörtlich oder sinngemäß entnommenen Stellen als solche kenntlich gemacht habe.

Linz, Novenber 2002 Mag. Antonio Cravino

Die vorliegende Dissertation entstand zwischen July 1998 und Nobember 2002 am Forschunginstitut für Organische Solarzellen und Abteilung Physikalische Chemie der Technisch-Naturwissenschaftlichen Fakultät der Johannes Kepler Universität Linz unter Betreuung von o. Univ. Prof. Mag. Dr. N. S. Sariciftci.